DOCKET NO: A-98-49
II-B1-16

TECHNICAL SUPPORT DOCUMENT FOR SECTION 194.23

REVIEW OF THE 2004 COMPLIANCE RECERTIFICATION PERFORMANCE ASSESSMENT BASELINE CALCULATION

U. S. ENVIRONMENTAL PROTECTION AGENCY
Office of Radiation and Indoor Air
Center for the Waste Isolation Pilot Plant
1310 L St., NW
Washington, DC 20005

March 2006

TABLE OF CONTENTS

LIST OF TABLES

LIST OF FIGURES

LIST OF APPENDICES

ACRONYM LIST

AMWTF	Advanced Mixed-Waste Treatment Facility
CCA	Compliance Certification Application
CDF	Cumulative distribution function
CCDF	Complementary cumulative density function
CH	Contact handled
CPR	Cellulosics, plastics, and rubber
CRA	Compliance Recertification Application
D	Difference between log values of measured and calculated solubilities
DBR	Direct brine release
DOE	U.S. Department of Energy
DRZ	Disturbed Rock Zone
EDTA	Ethylenediaminetetraacetic acid
EPA	U.S. Environmental Protection Agency
FEPs	Features, events, and processes
FGE	Fissile gram equivalents
FMT	Fracture Matrix Transport
GWB	Generic Weep Brine
LCL	Lower confidence limit
LWB	Land Withdrawal Boundary
kPa	Kilopascal
m	Molal (moles/kg)
M	Molar (moles/liter)
MB	Marker Bed
MPa	Megapascal
PA	Performance assessment
Pa	Pascal
PABC	Performance Assessment Baseline Calculation
PAPDB	Performance Assessment Parameter Database
PAVT	Performance Assessment Verification Testing
RFETS	Rocky Flats Environmental Technology Site
RH	Remote handled

RMSE	Root mean squared error
S_M	Measured solubility
SNL	Sandia National Laboratories
S_P	Predicted solubility
SSE	Sum of squared errors
T	Transmissivity
TBM	Technical Baseline Migration
TDOP	Ten-drum overpack
TWBID	Transuranic Waste Baseline Inventory Database
TWBIR	Transuranic Waste Baseline Inventory Report
UCL	Upper confidence limit
WIPP	Waste Isolation Pilot Plant
WTWBIR	WIPP Transuranic Waste Baseline Inventory Report
WWIS	WIPP Waste Information System

EXECUTIVE SUMMARY

The U.S. Department of Energy (DOE) operates the Waste Isolation Pilot Plant (WIPP), for the disposal of defense-related transuranic (TRU) waste. DOE submitted the Compliance Certification Application (CCA) to the U.S. Environmental Protection Agency (EPA or the Agency) in 1996. As required by 40 CFR 194.34, the CCA included the results of a performance assessment (the CCA PA) carried out to predict the ability of the repository to meet the containment requirements. After review of the CCA documentation and the CCA PA results, the Agency required that DOE perform a revised PA, referred to as the Performance Assessment Verification Testing (PAVT). The results of the PAVT and review of the CCA and supplemental information formed the basis of the Agency's certification that DOE had met regulatory requirements. WIPP began accepting waste in March 1999.

DOE is required to submit a Compliance Recertification Application (CRA) every 5 years after the date waste was first received at WIPP; the first CRA was submitted in March 2004 (DOE 2004b). The CRA was based on a PA that included revisions since the PAVT. After review of the CRA and additional information provided by DOE, the Agency found that changes would be required to the CRA PA (EPA 2005a). Consequently, DOE carried out a new PA, referred to as the Performance Assessment Baseline Calculations (PABC). The PABC assumptions, parameters, calculations, and results have been reviewed by the Agency. Because the Agency did not find the initial CRA PA to be adequate, the PABC results were compared to those of the PAVT. However, information the Agency obtained from the review of the CRA PA was considered during review of the PABC. This report represents EPA's assessment and evaluation of the PABC results.

Section 1.0 of this report provides a brief introduction to WIPP and the CRA.

In Section 2.0, the features, events, and processes (FEPs) identified and included in the CCA (DOE 1996b) were reassessed for the PABC. A review carried out of the FEPs assessment for the CRA PA indicated that two new FEPs were added, four FEPs were deleted or combined with other FEPs, and seven FEPs had changed Screening Decisions since the PAVT. However, all of these latter FEPs remained "Screened out" of the CRA PA. For the PABC, DOE evaluated whether the specified PA changes would have an impact on the included FEPs. DOE's FEPs impact assessment did not identify any inconsistencies or omissions to the current FEPs baseline list as a result of the changes incorporated in the PABC. The Agency reviewed this information and found this conclusion to be reasonable.

Section 3.0 describes the inventory used in the PABC. The PABC inventory was created by taking the CCA/PAVT inventory, adjusting it for the changes made in the CRA, and finally revising the CRA inventory to that used in the PABC. During its review of the CRA inventory, DOE uncovered several discrepancies and changed situations regarding the baseline inventory. Concurrent with the DOE review of the CRA inventory, EPA was conducting an independent review. EPA raised questions regarding completeness and technical adequacy of the CRA inventory in comment letters to DOE, and DOE provided responses to each comment. Based on its review, EPA required that the baseline inventory be revised for the PABC. Major changes to the inventory between the CRA and the PABC include the following:

- Removal of double-counted waste streams at Hanford-RL
- Inclusion of pre-1970 buried waste streams from INEEL
- Adjustment of the volume and fissile grams equivalents of an important LANL waste stream
- Correction of all other errors detected in DOE and EPA audits of CRA inventory

In addition, EPA required that emplacement materials be added to the quantities of cellulosics, plastics, and rubber in the baseline inventory. EPA verified that all changes to inventory parameters used in the PABC were correctly implemented. Based on its review of the process by which the CRA and PABC inventories were developed and implementation of EPA's required changes for the PABC inventory, the Agency concluded that the PABC baseline inventory was adequate for use in PA.

DOE must demonstrate that PA software is in compliance with regulatory requirements of 40 CFR 194.23. Section 4.0 describes the Agency's review of DOE's testing of the PA computer codes to show that they perform properly on the updated hardware and software implemented since the PAVT. Based on this review, the Agency concluded that the PA codes are approved for use in compliance calculations.

Section 5.0 describes the Agency's review of changes in the WIPP parameter database since the PAVT. These parameter database changes occurred in three stages: (1) changes associated with the Technical Baseline Migration (TBM) in which the PAVT parameters were transferred to a new platform and new software, and renamed the Performance Assessment Parameter Database (PAPDB); (2) parameter changes for the CRA PA; and (3) parameter changes for the PABC. The Agency reviewed the procedural adequacy of changes made to the database for the PABC as well as the technical adequacy of all database changes made since the TBM. The results of this review indicated that the parameters used in the PABC were technically acceptable and appropriately documented.

Microbial degradation of cellulosics, plastics, and rubber (CPR) may influence WIPP repository performance because of its effects on repository chemistry and gas generation. As a result of the Agency's review of the CRA, DOE changed the modeling of microbial degradation processes for the PABC. Section 6.0 describes the results of the Agency's review of these changes. Because of additional information developed since the PAVT related to microbial presence in diverse environments and microbial viability, the Agency found that the probability of significant microbial degradation of cellulosics should be increased in PA. The Agency therefore specified and DOE implemented a change in the microbial degradation probability for CPR materials from the probability of 0.5 used in the PAVT to 1.0 in the PABC. For the PABC, there was a 0.75 probability of degradation of cellulosics alone, with a 0.25 probability of degradation of plastics and rubber materials, as well as cellulosics. Consequently, microbial degradation of cellulosics was assumed to occur in all vectors in the PABC. Because of the presence of abundant sulfates in brine and solid phases [anhydrite, $CaSO_4(s)$] in the Salado Formation, the Agency also specified that the PABC should include the assumption that excess sulfate in the repository would prevent the microbial degradation of CPR via the reaction that produces methane

(methanogenesis). Therefore, for the PABC, all CPR degradation was assumed to take place via denitrification and sulfate reduction reactions, which resulted in the production of one mole of carbon dioxide (CO_2) for each mole of organic carbon consumed. During EPA's review of the CRA PA, DOE indicated that additional experimental data were available since the PAVT related to microbial gas generation rates that were not included in the CRA PA. When EPA required DOE to provide a new PA for recertification, DOE requested to update the gas generation rate. DOE used the additional data to revise the gas generation rates. The revised approach assumed rapid initial gas generation followed by much slower, long-term rates. The Agency reviewed DOE's evaluation of the microbial gas generation rates and implementation of the revised microbial degradation probability and gas generation rates and found them to be appropriately implemented in the PABC. The Agency also verified that methanogenesis was not included in the PABC – an assumption unchanged since the PAVT. As a result of these changes in microbial gas generation probability and rates, modeled repository pressures were lower for the PABC than for the PAVT. These lower repository pressures caused decreased spallings releases. However, direct brine releases (DBR) increased in the PABC relative to the PAVT due to changes in solubility discussed below and because lower gas pressures allowed for higher brine saturations in the repository

Actinide solubility calculations and the development of uncertainty distributions for actinide solubilities are reviewed in Section 7.0. The approach for modeling +III, +IV, and +V actinide solubilities using the Fracture-Matrix Transport (FMT) code remains unchanged since the PAVT. However, the thermodynamic database used by FMT was updated, including data for actinide solid phases and aqueous species and inclusion of data necessary for calculating the effects of organic ligands on actinide solubilities. The concentrations of organic ligands used in the solubility calculations were based on estimated inventory amounts of acetate, citrate, EDTA and oxalate and the minimum amount of brine required for DBR. Since the PAVT, the Salado Brine formulation used in the solubility calculations changed from Brine A to GWB. Based on published data available since the PAVT, the Agency specified use of an increased fixed uranium(VI) concentration in the PABC (10^{-3} M) instead of the lower concentration (8.8×10^{-6} M) plus an estimated uncertainty range used in the PAVT. At the Agency's direction, DOE used the revised FMT thermodynamic database and available measured solubilities to develop new uncertainty ranges for the +III, +IV, and +V actinide solubility calculations for the PABC. These changes were reviewed by the Agency and found to be adequately documented and technically acceptable. The new data regarding complexation of actinides by organic ligands indicated that organic ligands could significantly affect the solubilities of the +III actinides. Because of the increased solubilities and associated uncertainties predicted for the PABC, DBR replaced spallings as the second-most important release mechanism at higher probabilities, behind cuttings and cavings. At low probabilities for the PABC, DBR became the most important release mechanism.

Section 8.0 describes the Agency's review of the Culebra flow and transport modeling. In the PAVT, CRA, and PABC, the Culebra member of the Rustler Formation is conceptualized as a horizontal, confined aquifer of uniform density. For fluid flow, the Culebra is assumed to be a heterogeneous porous medium with spatially varying transmissivity (T). A heterogeneous velocity field is used for radionuclide transport, but all other rock properties are conceptualized as constant (homogeneous) across the model area. The Culebra is assumed to have two types of porosity; a portion of the porosity is associated with high-permeability features where transport

occurs by advection, and the rest of the porosity is associated with low-permeability features where flow does not occur and retardation occurs by physical processes (diffusion) and chemical processes (sorption). This type of conceptual model is commonly referred to as double-porosity.

The key factors controlling fluid flow in the Culebra are the hydraulic gradient, transmissivity distribution, and porosity. In the Culebra conceptual model, the spatial distribution of transmissivity is important. In its review of the CRA, EPA determined that the approach taken by DOE to modify the transmissivity fields to include the effects of mining was not acceptable and required a revised approach for the PABC. In developing transmissivity fields for the CRA, DOE had assumed a one-mile exclusion zone from potash mining around existing oil and gas wells. In the PABC, the potash mining area was assumed to involve all mined and unmined potash resources regardless of proximity to oil or gas wells.

The increase in transmissivity due to mining increases the relative flow rate through the mining zones, with a corresponding decrease in flow through the non-mining zones. This decrease in flow through the non-mining zones produces longer travel times for the mining scenarios. Comparing the full-mining scenarios of the PABC analysis to the CCA and CRA calculations, the median travel times are approximately 2.53 and 1.14 times longer, respectively. By eliminating the exclusion zone around the existing oil and gas wells, DOE has addressed the Agency's concern regarding the mining scenario. EPA has determined that this change has been properly implemented in the PABC.

Section 9.0 describes the Agency's review of the Salado flow and transport modeling. Flow in the Salado is computed by the BRAGFLO code, which simulates brine and gas flow in and around the repository. BRAGFLO includes the effects of processes such as gas generation and creep closure. Outputs from the BRAGFLO simulations describe the conditions (pressure, brine saturation, porosity) and flow patterns (brine flow up an intrusion borehole and out anhydrite marker beds to the accessible environment) that are used by other software to predict radionuclide releases. EPA noted a number of technical changes and corrections to the CRA that it deemed necessary. Additionally, EPA stated that a number of modeling assumptions used in CRA have not been sufficiently justified and that alternative modeling assumptions must be used. The issues and changes for the PABC that affect the BRAGFLO\NUTS portion of WIPP PA include:

(1) Inventory information was updated

(2) Parameters describing the bulk compressibility and residual gas saturation for the marker bed materials were changed to constants

(3) Changes to the parameter describing the probability of microbial gas generation in the repository were made

(4) Methanogenesis is no longer assumed to be the primary microbial gas generation reaction

(5) Microbial gas generation rates were revised to be consistent with, long-term laboratory experimental results

(6) The LHS software was revised

Section 3 provides additional discussion of Item 1 above, while Items 3, 4, and 5 are discussed in Section 6. The Agency has concluded that changes to the computer codes for modeling Salado Formation flow and transport have been properly implemented as have changes in conceptual models and model parameters. The Agency finds that the approach taken by DOE for the modeling the Salado is acceptable.

In Section 10.0, the PABC direct-release calculations are reviewed and the results compared to those obtained for the PAVT. Direct releases are defined as solid and liquid materials removed from the repository and carried to the ground surface through intrusion boreholes at the time of drilling. Direct releases occur in WIPP PA through cuttings and cavings releases, DBR, and spallings releases. Cuttings and cavings are the solid materials removed from the repository and carried to the ground surface by drilling fluid during the process of drilling a borehole that intersects the repository. Cuttings are the materials removed directly by the drill bit, and cavings are the materials eroded from the borehole walls by shear stresses from the circulating drill fluid. The contribution of mean cuttings and cavings releases to total mean radionuclide releases for the PABC remained essentially unchanged from the PABC. Direct brine releases occur when contaminated brine originating in the repository is driven up an intrusion borehole to the ground surface by repository gas pressure. Because of the increased actinide solubilities and associated uncertainties described in Section 7.0 and higher brine saturations caused by lower gas generation rates (Section 6.0), the contribution of DBR to total mean direct radionuclide releases for the PABC was greater than for the PAVT. Spallings releases occur when solid waste is ejected through an intrusion borehole by repository gas pressures that exceed the estimated 8 MPa hydrostatic pressure of the drilling fluid. Spallings releases calculated for the PABC were lower than those calculated for the PAVT. This reduction in calculated spallings releases was caused in part by revisions to the spallings model. In addition, lower long-term microbial gas generation rates described in Section 6.0, resulted in lower PABC spallings releases because of the prediction of lower repository pressures than the PAVT.

Section 11.0 describes the Agency's review of the results of the PABC, including releases through both undisturbed and disturbed pathways. Normalized releases calculated for the PABC are summarized and the sensitivity analyses of the results are reviewed. Total normalized releases are calculated by totaling the releases from each pathway and primarily consist of cuttings and cavings releases, DBRs, spallings releases, and releases from the Culebra. There were no releases from transport up the shaft in the PABC and no disturbed releases through the anhydrite interbeds. Undisturbed releases through the anhydrite interbeds in the PABC were as much as 11 orders of magnitude smaller than the typical disturbed releases, and were therefore not significant contributors to total normalized releases.

Because cuttings, cavings, direct brine, and spallings releases account for an overwhelming majority of the total releases, the calculated total releases are most sensitive to uncertainties in the parameters governing these release mechanisms. In both the PAVT and the PABC analyses, total normalized releases were most sensitive to uncertainty in waste shear strength (WTAUFAIL), which is a key parameter governing cavings volumes. In the PABC, direct brine releases supplant spallings as the second-most important contributor to total releases and even surpass cuttings and cavings at low probabilities. The second most important variable in the

PABC analysis is WSOLVAR3, a solubility multiplier added to the PABC analysis to represent uncertainty in solubilities for all actinides in the +3 oxidation state.

Section 12.0 provides a summary and the conclusions of the Agency's review of the PABC. Based on the information presented in this report, EPA believes that the revised performance assessment (PABC) contains all of changes requested by the Agency. These changes are transparent, traceable against prior PAs, consistent with EPA direction, and appear to be properly implemented. The PABC results described in Section 11 show that the WIPP continues to comply with the containment requirements of 40 CFR 191.13.

1.0 INTRODUCTION

The U.S. Department of Energy (DOE) operates the Waste Isolation Pilot Plant (WIPP), for the disposal of defense-related transuranic (TRU) waste. DOE submitted the Compliance Certification Application (CCA) to the U.S. Environmental Protection Agency (EPA or the Agency) in 1996. As required by 40 CFR 194.34, the CCA included the results of a performance assessment (the CCA PA) carried out to predict the ability of the repository to meet the containment requirements. After review of the CCA documentation and the CCA PA results, the Agency required that DOE perform a revised PA, referred to as the Performance Assessment Verification Testing (PAVT). The results of the PAVT and review of the CCA and supplemental information formed the basis of the Agency's certification that DOE had met regulatory requirements. WIPP began accepting waste in March 1999.

DOE is required to submit a Compliance Recertification Application (CRA) every 5 years after the date waste was received at WIPP; the first CRA was submitted in March 2004 (DOE 2004b). The CRA included the results of a PA that was revised since the PAVT. After review of the CRA and additional information provided by DOE, the Agency found that changes would be required to this CRA PA (EPA 2005a). Consequently, DOE carried out a new PA,[1] referred to as the Performance Assessment Baseline Calculation (PABC). The PABC assumptions, parameters, calculations, and results have been reviewed by the Agency. Because the Agency did not find the initial CRA PA to be adequate, the PABC results were compared to those of the PAVT. However, information the Agency obtained from the review of the CRA PA was considered during review of the PABC. This report represents EPA's assessment and evaluation of the PABC results.

In Section 2.0 of this report, the features, events, and processes (FEPs) identified and included in the CCA (DOE 1996b) are reassessed for the PABC. Section 3.0 describes the inventory used in the PABC. Section 4.0 describes the Agency's review of DOE's testing of the PA computer codes to show that they perform properly on the updated hardware and software implemented since the PAVT. Section 5.0 describes the Agency's review of changes in the WIPP parameter database since the PAVT.

Section 6.0 describes the results of the Agency's review of the effects of microbial degradation of cellulosics, plastics, and rubber on repository chemistry and gas generation. Actinide solubility calculations and the development of uncertainty distributions for actinide solubilities are reviewed in Section 7.0. Section 8.0 describes the Agency's review of the Culebra flow and transport modeling, while Section 9.0 describes a related review of the Salado flow and transport modeling.

In Section 10.0, the PABC direct-release calculations are reviewed and the results compared to those obtained for the PAVT. Section 11.0 describes the Agency's review of the results of the PABC, including releases through undisturbed pathways and disturbed pathways. Finally, Section 12 summarizes the Agency's conclusions regarding the acceptability of the PABC in determining continuing compliance with 40 CFR Part 194.34.

[1] DOE documents refer to the PABC as the CRA-2004 PABC. For simplicity and clarity, EPA has chosen the shorter description used here.

This report summarizes EPA's review of the major elements used to develop the inputs to the PABC and the results of the performance assessment. This review provides the basis for EPA conclusions regarding the acceptability of the PABC as one of the bases for compliance recertification.

2.0 FEPS REVIEW

The features, events, and processes (FEPs) that were identified and included in the CCA (DOE 1996b) were reassessed for the CRA (DOE 2004b, Appendix PA, Attachment SCR). This reassessment was required by 40 CFR §194.15(a). The CRA FEPs reassessment process, documented in Wagner et al. 2003, focused primarily on updating screening arguments and Screening Decisions as a result of new or different information provided since the CCA. The key changes in the list of FEPs developed for the CRA were (EPA 2005c):

- Two new FEPs addressing solution mining (H58, *Solution mining for potash* and H59, *Solution mining for other resources*) were added to the database. In its review of the CCA, the Agency had noted the omission of solution (brine) mining and had requested additional information.

- Four FEPs were either deleted or combined logically with other related FEPs.

- Seven FEPs (W50, Galvanic coupling; W68, Organic complexation; W69, Organic ligands; H27, Liquid waste disposal; H28 Enhanced oil and gas production; H29, Hydrocarbon storage; and H41, Surface disruptions) had their Screening Decisions changed. However, these FEPs remained 'Screened out' of the CRA.

The above changes resulted in a total of 235 FEPs being included in the CRA compared with 237 FEPs for the CCA.

Following its technical review of the CRA, the Agency requested that various changes be made to the PA, resulting in the CRA PABC (Leigh et al. 2005a). The specific changes requested by the Agency were itemized in Kirkes 2005b:

(1) Updated waste inventory information
(2) Updated actinide solubility values
(3) Updated actinide solubility uncertainty ranges
(4) Updated microbial gas generation model
(5) Updated Culebra transmissivity field reflecting mining modifications
(6) Update of the LHS code
(7) Update of the CUTTING_S code
(8) Updates of the CCDFGF and PRECCDFGF codes
(9) Modifications to spallings calculations

The scenarios for the CRA and the CRA PABC were identical, however.

DOE's strategy for dealing with potential impacts of the above changes on FEPs to be included in the PABC was to perform a FEPs impact assessment, as described in Kirkes 2005b and 2005c. The general strategy involved an evaluation of the changes made to the PA since the CRA PA (DOE 2004b), in terms of the possible impacts of these changes on the current FEPs baseline. The FEPs included in the CRA PA were identified in Wagner and Kirkes 2003 and Appendix PA, Attachment SCR, of the CRA (DOE 2004b).

Specifically, the impact assessment process involved:

- Identification of the required changes made to the CRA PA and identification of all FEPs related to these changes
- Evaluation of whether any new FEPs were required as a result of these changes
- Evaluation of whether updates to screening arguments and/or Screening Decisions were necessary
- Identification of implications of any revised screening arguments and/or Screening Decisions
- Summary of potential impacts to the current FEPs baseline

As described in Kirkes 2005b, the FEPs associated with each of the topics contained in the above list (Items 1–9) were first identified. Because the last four topics (Items 6–9) deal with the logistics of PA calculations (codes, data input, data transfer) rather than the disposal concept, no FEPs are directly related to these topics.

Each of the FEPs associated with Items 1–5 was discussed in Kirkes 2005b. A total of 22 FEPs were identified for updated inventory information, the same 16 FEPs for both actinide solubility values and uncertainty, 12 FEPs for microbial gas generation, and only 2 FEPs concerning modifications to the Culebra transmissivity field as a result of mining activities. The major part of the FEPs impact assessment involved an evaluation of each of these identified FEPs that had previously been screened out from the CRA, to determine whether the Screening Decision remained valid. Screening arguments and Screening Decisions for screened-in FEPs did not change.

In summary, DOE's FEPs impact assessment did not identify any inconsistencies or omissions to the current FEPs baseline list as a result of the changes incorporated in the PABC. The Agency has reviewed the information and finds this conclusion to be reasonable. The new FEPs baseline list (no changes) is provided in Kirkes 2005a. This list and the Screening Decisions therein, are the same as those provided in Appendix PA, Attachment SCR of the CRA (DOE 2004b). DOE's evaluation, in terms of the FEPs impact assessment, and the conclusion that no revision to the baseline FEPs list is warranted, are technically valid.

3.0 BASELINE INVENTORY

This section describes and discusses the inventory used in the PABC. The PABC inventory was created by taking the CCA/PAVT inventory, adjusting it for the changes made in the CRA, and finally revising the CRA inventory to that used in the PABC. Thus, assessment of the PABC inventory involves tracking changes made to the CCA/PAVT inventory, which was one of the key elements in EPA's original approval of the WIPP site for operation. Additional detail on EPA's review of the WIPP baseline inventory is presented in *Technical Support Document for Section 194.24: Review of the Baseline Inventory Used in the Compliance Recertification Application and the Performance Assessment Baseline Calculation* (EPA 2006a).

3.1 EVOLUTION OF THE BASELINE INVENTORY

The first DOE attempt to describe all TRU waste at the waste stream level was documented in the *WIPP Transuranic Waste Baseline Inventory Report* (WTWBIR, Revision 0) issued in June 1994. A revised report (WTWBIR, Revision 1) was issued in February 1995. Revision 1 contained modifications based on site reviews and data quality checks. In Revision 2 of the December 1995 report (DOE 1995b), the title was changed to *Transuranic Waste Baseline Inventory Report* (TWBIR, Revision 2) to reflect the fact that the revision included information on TRU waste not intended for disposal at the WIPP. The June 1996 revision of this report (TWBIR, Revision 3), together with Revision 2, was used by DOE to prepare the CCA. Based on its review of the CCA as submitted by DOE, EPA required DOE to revise some of the parameters and assumptions used in the CCA performance assessment (PA) and rerun the PA. This revised performance assessment was designated the Performance Assessment Verification Test (PAVT). The PAVT was used by EPA to certify, in May 1998, that the WIPP meets the disposal standards set forth in 40 CFR Part 191 and the specific WIPP compliance criteria set forth in 40 CFR Part 194. The inventory used for the PAVT calculations was the same as for the CCA PA.

To prepare for its submittal of the CRA, DOE updated the inventory to be current as of September 30, 2002. This revised inventory was documented in Appendix DATA, Attachment F, of the CRA, also referred to by DOE as the *2003 Update Report*.[2] Based on its review of the completeness of the CRA, EPA determined that changes should be made to the PA. Many of these changes were based on errors in the CRA inventory and changes in assumptions that had occurred since September 30, 2002. This revised PA, designated the Performance Assessment Baseline Calculation (PABC), provides the basis for the EPA compliance recertification decision. The adjusted inventory used in the PABC is described by DOE in Leigh et al. 2005a, also referred to here as the *PABC Inventory Report*. The chronology of reports documenting the WIPP TRU inventory is presented in Table 3-1.

[2] As will be discussed subsequently in this report, inventory information is also located in other sections of the CRA.

Table 3-1. Chronology of Reports Documenting the Development of the WIPP Baseline Inventory

Inventory	Date	Reference	Comments
WTWBIR Rev. 0	June 1994	DOE 1994	First DOE attempt to report all TRU waste at waste stream level.
WTWBIR Rev. 1	February 1995	DOE 1995a	Included data changes based on site reviews and quality checks.
TWBIR Rev. 2	December 1995	DOE 1995b	Included WIPP and non-WIPP wastes and other information on characteristics.
TWBIR Rev. 3	June 1996	DOE 1996a	Included same waste stream data as TWBIR, Revision 2. Added information on waste components needed to support PA. Used for CCA and PAVT.
2003 Update Report	March 2004	CRA, Appendix DATA, Attachment F	Inventory updated to September 30, 2002. Used for CRA.
PABC Inventory Report	September 2005	Leigh et al. 2005a	Inventory updated to 2005. Used for PABC.

The data from which the information in these inventory reports was developed is contained in the Transuranic Waste Baseline Inventory Database (TWBID)—a qualified electronic database. A Microsoft Access 2.0 format database (TWBIR.mdb, dated January 29, 1996) was used to generate TWBIR Revision 3. After compliance certification, this database was converted to Microsoft Access 2000 format and was modified to incorporate new requirements (Appendix DATA, Attachment F, Section DATA-F-2.2.1). This database was named TWBID Revision 2.1. New site data reflective of the then-current TRU inventory status were incorporated into this database. TWBID Revision 2.1, Data Version 4.09 (Software Version 3.12) was used to develop the data for the *2003 Update Report*, while TWBID Revision 2.1, Data Version 4.16 (Software Version 3.13) was used for the *PABC Inventory Report*. A complete listing of the changes associated with each Data Version (D0.00 through D4.16) of TWBID Revision 2.1 is presented in Appendix A of Leigh et al. 2005a.

Several key input parameters in the WIPP PA involve waste-inventory-related values. Much of the inventory-related information for the CRA was derived from data summarized in the *2003 Update Report*, included in the CRA as Attachment F of Appendix DATA. Sites that generate or store transuranic waste provided their best estimates of waste-stream-specific stored and projected waste volumes, and associated radiological, chemical, and physical properties of each waste stream to DOE, and these estimates were included in Waste Stream Profiles presented in CRA Appendix Data, Attachment F, Annex J. DOE then summarized these data to obtain an estimate of the WIPP waste inventory, including the inventory that is expected to be shipped to WIPP in the future. In addition, DOE used information contained in the WIPP Waste Information System (WWIS) to determine the quantities of wastes (including radionuclide quantities, waste material parameter quantities, and packaging quantities) emplaced in the WIPP as of September 30, 2002. These data were summarized in Annex K of the *2003 Update Report*.

DOE indicated that the inventory estimates in the *2003 Update Report* reflect information obtained since the original baseline inventory report used in the CCA/PAVT. The CRA identifies the following as the more significant changes (as quoted from the Preface to Appendix DATA, Attachment F):

- This report accounts for the Idaho National Engineering and Environmental Laboratory (INEEL) Advanced Mixed Waste Treatment Facility process by which 55-gallon drums are compacted and put into 100-gallon drums and disregards those calculations related to future waste incineration described in the TWBIR Revision 3 (DOE 1996a) that never went into operation.

- This report includes 7,095 m^3 (250,595 ft^3) of stored Hanford tank waste that was added to the inventory in December 2002.

- This report also addresses the waste that has been emplaced since the WIPP opened in 1999.

3.2 DOE PROCESS TO DEVELOP CRA INVENTORY

To develop the inventory used for the CRA, DOE sent a data call to all TRU waste generator sites to update the waste stream data information used in the CCA/PAVT, as documented in TWBIR Revision 2. The sites were requested to provide updated data as of September 30, 2002.

During the data acquisition phase, Los Alamos National Laboratory - Carlsbad Operations (LANL-CO) personnel visited some sites to facilitate data collection and resolve issues. Following acquisition of site data, DOE, LANL-CO, and Sandia National Laboratories (SNL) representatives examined the information provided, going back to the sites for additional clarification if questions arose. Once issues were addressed, the waste stream profile information was validated by the DOE site manager responsible for TRU waste management. Data were then evaluated based upon screening criteria to determine whether the wastes were eligible for disposal at WIPP; wastes that were not eligible were not included in future data evaluations and roll-ups, although these wastes were included for informational purposes in Appendix DATA, Attachment F, Annex I. Data obtained from the sites were then decay-corrected to a common base year (2001), and packaging volume corrections were made. This information from individual waste streams was rolled up for use in PA, or was directly input into PA (i.e., cuttings and cavings). The information from this data call, which was used in the CRA, was designated TWBID Revision 2.1, Version 3.12, Data Version 4.09.

3.3 SUMMARY OF THE CRA INVENTORY

The inventory used for the CRA, as described in the *2003 Update Report* (CRA, Appendix DATA, Attachment F), was based on site inventories as of September 30, 2002. Principal changes that occurred in the 6 years since TWBIR Revision 3 was published include the following:

- Emplacement of 7,716 m^3 of CH waste at the WIPP

- Inclusion of waste from the INEEL Advanced Mixed Waste Treatment Facility where 55-gallon drums are compacted and put into 100-gallon drums

- Deletion of product from future waste thermal treatment at INEEL described in the TWBIR Revision 3, since the process was never implemented

- Inclusion of 7,095 m^3 (250,595 ft^3) of stored Hanford tank waste that was added to the inventory in December 2002

- Inclusion of updates to site Waste Stream Profiles that were reported in TWBIR Revision 2[3]

The total curies of transuranic, alpha-emitting radionuclides with half-lives greater than 20 years were 3.44×10^6 Ci in the CCA, 3.59×10^6 Ci in the PAVT, and had decreased to 2.48×10^6 Ci in the CRA.

The stored and anticipated CH TRU waste volume for the *2003 Update Report* (1.42×105 m^3) is 26.5% higher than in the TWBIR Revision 2. Increases in estimates of stored waste at INEEL, SRS, Hanford, and RFETS reflect new data and increased accessibility to the waste. At Hanford, tank wastes handled by the Office of River Protection (Hanford-RP) had been identified in the TWBIR Revision 2, but not included in the CCA/PAVT. Subsequently, these wastes were added to the CRA inventory. On the other hand, estimates of projected CH TRU wastes are lower in the CRA than in the CCA/PAVT. This change is consistent with progress in site clean-up and decommissioning activities, where projected wastes have been converted to stored wastes.

Stored RH TRU wastes increased from 3.61×10^3 m^3 in the CCA/PAVT to 5.31×10^3 m^3 in the CRA. Hanford increased the volume of wastes under the aegis of the Richland Operations Office (Hanford-RL) based on new information, and added the Hanford-RP wastes. ORNL moved all of its RH TRU waste from the stored category in the CCA/PAVT to the projected category in the CRA based on a decision to process all their RH waste using segregation, size reduction, and evaporative drying (Leigh et al. 2005b, Section 4.1.2.2). Projected RH TRU volumes decreased by 1.35×10^4 m^3 from the CCA/PAVT to the CRA. Most of this is based on a reassessment of projected wastes at Hanford-RL.

Changes in waste volume, per se, have no effect on PA, since the projected volumes are scaled to the statutory limits of 7.08×10^3 m^3 for RH and 1.68×10^5 m^3 for CH. However, changes in projected waste volumes can affect the radionuclide content of the scaled projected waste streams. As noted above, the anticipated volume of RH TRU wastes (1.57×10^4 m^3) exceeds the limit, so the volume of projected waste is scaled downward by a factor of 0.172 to meet the limit (Appendix DATA, Attachment F, Table DATA-F-8). Conversely, since the anticipated and

[3] Waste stream profiles were unchanged between TWBIR Revision 2 and Revision 3. Additional data on waste inventory components were compiled in Revision 3.

emplaced volume of CH waste, 1.42×10^5 m^3, is less than the limit, projected wastes are scaled upward by a factor of 2.11 to reach the limit.

Generally small changes occurred in the CH-TRU waste material densities between the CCA/PAVT and the CRA. Such changes are to be expected as more information is gathered on waste streams between the two inventories. Quantities of metals were smaller in the CRA, as were vitrified materials, cement, and soils. CPR materials, solidified organic and inorganic materials, and other inorganic materials increased in the CRA. The increase in CPR materials is attributable, in large measure, to a decision made by INEEL, after the CCA/PAVT inventory had been developed, not to thermally treat certain waste streams, but rather to supercompact them—a process that does not destroy the CPR materials. For RH TRU, the metals content, the CPR content, and the other materials content are all reduced in the CRA as compared to the CCA/PAVT.

3.4 EPA REVIEW OF THE CRA INVENTORY DEVELOPMENT PROCESS

The Agency reviewed the DOE's inventory data acquisition and data manipulation processes to determine whether (1) the processes were reasonable and well-documented, and (2) PA input parameters could be traced back through the CRA to confirm data origin. This review did not examine the actual data values received from the sites for technical adequacy. Rather, the review was performed to ensure that an adequate process was used to assemble and interpret inventory information, and to ensure that PA parameters can be reasonably traced to the initial site inventory information.

The Agency performed site visits to the ORNL, the Hanford Site, and SRS to examine the TRU waste data acquisition processes at these sites. Site reports for each visit are provided in EPA Docket A-98-49: Items II-B3-78, II-B3-86, and II-B3-87. In addition, the Agency met with DOE/SNL representatives in Albuquerque to further discuss the data acquisition and transfer process from sites, as well as the data manipulation and review process performed after data receipt. Through the course of these meetings, the Agency gained an understanding of the data assembly process at representative TRU waste generator sites, as well as how this information was examined, reviewed, modified, and manipulated by DOE for inclusion in the CRA and PABC. Through this analysis, the Agency attempted to verify that information contained in the CRA was consistent and traceable within the various chapters, appendices, attachments, and annexes. In addition, the Agency examined the paper trail documenting changes to selected waste streams to ascertain whether or not changes from the CCA/PAVT to the CRA were traceable and transparent

The data acquisition, review, documentation, and assembly process associated with the *2003 Inventory Update* is well-documented and appears to be adequate with respect to establishing a general protocol and methodology for acquiring the information. However, the paper trail is not always consistent or transparent. Implementation of new procedures put into place after the initial data calls should improve the system, but care must be taken to ensure that all inventory changes and manipulations are carefully documented and are readily traceable.

3.5 EPA REVIEW OF THE CRA INVENTORY DATA

In addition to determining that a reasonable process had been used to develop the CRA inventory, building upon the CCA/PAVT inventory previously judged to be acceptable, EPA also reviewed the data contained in the inventory. As described in Section 5 below and its supporting references, a comprehensive validation of parameter changes from the CRA/PAVT to the CRA was conducted. This involved many of the inventory parameters used in PA.

For example, in December 2004, EPA published a Technical Support Document (TSD)—*Technical Support Document For Section 194.23: Review of Changes to the WIPP Performance Assessment Parameters Since the Database Migration* (EPA 2004d)—describing changes to the parameter database that had occurred from the time the database migration had been completed until the CRA was issued in March 2004. EPA's conclusions are noted below:

> *There were 128 new parameters and 203 changes to parameter values in the PAPDB since the Technical Baseline Migration was conducted in 2002 and 2003 that support DOE's Compliance Recertification Application. Accuracy of the data entry process was checked and found to be satisfactory. There were no transcription errors between the parameter entry forms and the entry of data into the computer database. Our review of the parameter entry forms found them to be adequate although the practice of permitting data entry staff to make changes to the data entry forms may result in data entry errors or data values not intended by the data originator. Although current procedures do not explicitly prohibit this practice, procedures should be modified to prohibit this practice. All parameter values in the PAPDB as of July 2004 appear correct and traceable to documentation justifying their values.*

The TSD also documents (in Table 7 of that report) the verification of numerous parameters used in PA that are not included in the PAPDB.

In addition to the detailed checking of all the parameters in the PAPDB described above, EPA, as part of its review of the WIPP waste inventory, conducted numerous cross checks of the inventory data located in various places in the CRA including Chapter 4, Appendix PA, Attachment PAR; Appendix DATA, Attachment F; and Appendix TRU WASTE for consistency of data reporting in the various locations, and also spot-checked the rolled-up values to ensure that the summed data were consistent with the individual waste stream data. No discrepancies were discovered in this review.

Another check of the inventory data conducted by EPA involved assessing whether the ORIGEN2 Version 2.2 decay calculations were performed correctly. Since radioactivity measurements for individual waste streams as reported by the waste generator sites are not on a uniform basis, the measurements must be adjusted to a common starting point (the year 2001). Three waste streams were selected and were decayed independently by EPA using this code. Results of these decay calculations show that, on a spot-check basis, the ORIGEN2 values derived by DOE and used in EPAUNI were done correctly.

3.6 SUMMARY OF THE PABC INVENTORY

3.6.1 Basis for Inventory Changes

During its review of the CRA inventory, DOE uncovered several discrepancies and changed situations regarding the baseline inventory. DOE's documentation and review of these issues are described in Warren 2004, and Leigh and Crawford 2004. Concurrent with the DOE review of the CRA inventory, EPA was conducting an independent review. EPA raised questions regarding completeness and technical adequacy of the CRA inventory in comment letters to DOE, and DOE provided responses to each comment. EPA inventory questions were documented in Cotsworth 2004a, 2004b, 2004c, 2004d and Gitlin 2005. These items are included in Docket A-98-49 as Items II-B3-72, II-B3-73, II-B3-74, II-B3-78, and II-B3-79, respectively. DOE responses are documented in Detwiler 2004a, 2004b, 2004c, 2004d, 2004e, Piper 2004, Patterson 2005, and Triay 2005 (Docket A-98-49, Items II-B2-39, II-B2-38, II-B2-35, II-B2-34, II-B2-36, II-B2-37, II-B2-40, II-B2-47, and II-B2-41, respectively). This correspondence was supplemented by technical meetings involving DOE, EPA, and their contractors. EPA's comments and DOE's responses are summarized in Section 1.3 of Leigh et al. 2005b.

Based on EPA's review of the CRA and the supplementary information supplied by DOE, EPA requested that the CRA PA be rerun with certain modifications (Cotsworth 2005). As noted previously, the revised PA was designated the Performance Assessment Baseline Calculation (PABC). The inventory changes included in the PABC are discussed in Leigh et al. 2005b. Data for the PABC inventory are contained in TWBID Revision 2.1, Data Version 4.16.

Major changes to the inventory between the CRA and the PABC are described in the following paragraphs.

Hanford Wastes

After submittal of the CRA data, Hanford-RL discovered that some waste streams had been double counted. Correcting this resulted in removal of 9 waste streams (8350.0 m^3) of RH TRU and 3 waste streams (7362.6 m^3) of CH TRU for the PABC. In addition, a discrepancy in the Sr-90 and Ba-137m content of two waste streams was corrected. Correcting this discrepancy resulted in a reduction of about 50% in the values used for these radioisotopes in the PABC.

Idaho National Engineering and Environmental Laboratory Wastes[4]

Pre-1970 buried waste had been identified at INEEL, but had not been included in the inventory designated for WIPP. However, based on a court decision made after the CRA inventory data call, it was decided that the pre-1970 buried waste could be excavated, packaged, and shipped to the WIPP. INEEL identified five waste streams for inclusion in the PABC having a total volume of 17,997.6 m^3. In addition, data on the isotopic composition of waste stream IN-BN-510 was incorrectly reported in the CRA inventory, and this was corrected for the PABC. One other change involved the concentrations of radioisotopes in non-debris AMWTF waste based on the number and type of final form waste containers.

Los Alamos National Laboratory Wastes

Review of the data on LANL waste stream LA-TA-55-48 indicated that the fissile gram equivalents (FGE) were about 10 times greater than acceptable for shipment to the WIPP. Volume data and FGE for this waste stream were corrected.

Rocky Flats Environmental Technology Site

No substantive changes were made to the RFETS inventory for the PABC. A minor change designating some as "compressed" rather than supercompacted was made to more accurately reflect waste stream processing.

Other Sites

No substantive changes were made to the inventory for the other waste generator sites. However, the changes described above affect the scaled projected volumes for all sites.

Although none of the major issues with respect to inventory were thought by DOE to impact PA, procedure AP-113 (*Analysis Plan for Inventory Reconciliation: Compliance Recertification*) was written, based on the Leigh and Crawford 2004 improvement recommendations, that describes a process that will be followed for subsequent PA calculations. This process is designed to ensure that the issues identified pertaining to the inventory are rectified. Specifically, AP-113 states the following:

> *Specific recommendations made in Leigh and Crawford (2004) and its supporting documents will be implemented under this scope of work....when a systematic omission or inconsistency identified in Harvill (2004)*[5] *was substantiated in Leigh and Crawford (2004) and its supporting documents, queries of the ...(TWBID)...will be run to identify other possible instances of the systematic*

---

[4] On February 1, 2005, the Idaho National Engineering and Environmental Laboratory (INEEL) was combined with Argonne National Laboratory-West, and the new entity was designated the Idaho National Laboratory (INL).

[5] Harvill 2004 is the same as Warren 2004.

omission so that they all can be corrected, even when each omission was not separately identified...

Primary inventory areas that were addressed in this procedure include the following:

(1) Waste Stream Volumes—adequate reporting of final form volumes by viable payload containers

(2) Waste and Packaging Materials—revision of LANL packaging material densities and changes to assignments of packaging material densities where none were reported by a given TRU waste site

(3) Radionuclide Activities—correction of decay dates to a common start date on the waste profile forms; correcting Am-241 concentrations in INEEL, LANL, and SRS waste streams; addition of Sr-90 in ANL and ANL-E wastes; correction of Pu-241 under-reporting in INEEL AMWTP wastes; removal of "unimportant" daughter products from waste profile forms; correction of Cm-244 concentration in LANL waste streams; correction of site reporting error for LA-TA-55-48 FGE

(4) Waste Stream Descriptions—correction of waste stream name, description, waste material parameters, final waste forms, and other fields on waste profile forms

(5) EPA Codes—removal of redundant codes, correction of code identification errors

3.6.2 Description of PABC Inventory

The total curies of transuranic, alpha-emitting radionuclides with half-lives greater than 20 years decreased from 2.48×10^6 Ci in the CRA to 2.32×10^6 Ci in the PABC (Leigh et al. 2005b). The total radioactivity in the PABC is estimated to be 3.53×10^6 Ci decayed to the 2033 repository closure date (Leigh and Trone 2005).

The volumes in emplaced wastes were unchanged from the CRA to the PABC, remaining at 7.7×10^3 m^3. The stored inventory of CH TRU was also unchanged from the CRA to the PABC. Major changes in projected CH TRU waste inventory involved the addition of buried pre-1970 waste at INEEL and removal of three double-counted waste streams at Hanford-RL. For RH TRU waste, the stored waste is unchanged for the PABC and projected waste is decreased by 7.9×10^3 m^3, primarily due to the deletion of double-counted waste streams at Hanford-RL.

Since the volume of emplaced-plus-stored-plus-projected CH TRU waste was greater for the PABC ($7.7 \times 10^3 + 1.1 \times 10^5 + 3.5 \times 10^4 = 1.5 \times 10^5$ m^3) than for the CRA ($7.7 \times 10^3 + 1.1 \times 10^5 + 2.5 \times 10^4 = 1.4 \times 10^5$ m^3), the scaling factor for the projected waste in the PABC was adjusted downward to 1.48 from 2.11 used in the CRA. This scaling factor assures that allowable CH TRU waste capacity of 168,485 m^3 is fully accounted for in PA calculations. For RH TRU, the volume of stored-plus-projected waste for the PABC is 7.4×10^3 m^3, as compared to 1.5×10^4 m^3 in the CRA. There is no emplaced RH TRU to date. Based on the allowable repository limit of 7,079 m^3, the scaling factor for projected RH TRU in the PABC is 0.861, as compared to

0.172 in the CRA. The increase in the scaling factor is basically due to the reduction in projected RH TRU waste from Hanford-RL in the PABC.

In its completeness review of the CRA, EPA questioned the lack of inclusion of the emplacement materials in PA (Cotsworth 2004b, Comment G-2). In responding to the EPA comment, DOE noted that addition of emplacement materials would increase the CPR content of the waste by 12% over that used in the CRA and that this quantity of CPR would have a negligible impact on PA (Detwiler 2004d). Nevertheless, EPA specified that, in the interests of completeness and use of the most current information in PA, emplacement materials should be included in the PABC calculations. Consequently, 2.07×10^5 kg of cellulosics and 1.48×10^6 kg of plastics were added for the PABC (Leigh et al. 2005b). It should be noted that, in its 2004 response to Comment G-2, DOE stated that the quantities of cellulosics and plastics associated with emplacement materials would be 2×10^5 and 2.6×10^6, respectively. However, by the time the PABC inventory was developed in mid-2005, the estimated masses had been refined to the values quoted above in Leigh et al. 2005b.

3.6.3 Release Limits

As specified in 40 CFR 194.31- Application of Release Limits, "The release limits shall be calculated according to part 191, appendix A of this chapter, using the total activity in curies that exists in the disposal system at the time of disposal." For the PABC, DOE calculated the total activity in curies at the time of disposal (assumed to be 2033) using the ORIGEN2, Version 2.2 computer code (Leigh and Fox 2005c). As described in Attachment B of EPA 2005f (Docket No. A-98-49, II-B1-9), EPA checked a limited selection of DOE's decay calculations using a separately copy of ORIGEN2, Version 2.2 code and found the results to be identical with those of DOE.

According to Table1 (Note 1e) in Appendix A of 40 CFR Part 191, release limits for the radionuclides specified in the rule are based on "an amount of transuranic (TRU) waste containing one million curies of alpha-emitting transuranic radionuclides with half-lives greater than 20 years." To obtain release limits for use in PA, the release limits per 10^6 curies specified in Table 1 of Appendix A must be multiplied by a factor which defines the number of millions of TRU curies in the waste. For PA purposes, this factor, defined as the waste unit factor (WUF) or unit of waste, is expressed as:

$$f_w = \frac{\sum W_f}{10^6\ Ci}$$

where f_w is the waste unit factor and W_f is the inventory in curies of each alpha-emitting TRU radionuclide with a half-life of 20 years or more. DOE identified a total of 138 radionuclides expected to be present in the waste based on the PABC inventory. Of these, 17 meet the definition of TRU waste in Appendix A, Table 1 for calculating the waste unit factor. Table 2 of Leigh and Trone 2005 identifies these nuclides and determines that they contribute 2.32 x 10^6 Ci at closure resulting in a WUF of 2.32. The methodology for calculating the waste unit factor and release limits in the PABC is unchanged from that used in the CCA and the CRA and is appropriate and acceptable for PA.

3.7 EPA REVIEW OF PABC INVENTORY

As described in Section 5 of this report and its supporting references, a detailed verification of all parameter changes between the CRA and the PABC was made. No database problems were identified during the review. Transcription accuracy and technical adequacy were checked for the 13 new parameters and the 92 parameters that had been updated between the CRA and PABC analyses. All parameter distributions, values, and units were correctly entered into the PAPDB, and were technically adequate and appropriate. The rationale for dropping certain parameters from the CRA analysis was also evaluated and found to be acceptable.

A check of all supporting documents listed in the PAPDB was made for 27 selected parameters and 30 different documents. Based on this check, EPA concluded that the necessary documents are readily available to support the new and updated parameters. A database-code interface evaluation was performed for the same 27 parameters and the correct parameter values were retrieved from the PAPDB for each parameter (EPA 2005e).

4.0 MODELS AND CODES

DOE must demonstrate on an ongoing basis that PA computer software is in compliance with regulations outlined in 40 CFR 194.23 - Models and Computer Codes. Since the Agency's certification of the CCA, DOE has added computer hardware and upgraded the computer software. In order to maintain compliance with 40 CFR 194.22 and 40 CFR 194.23, DOE is required to conduct testing on the computer codes to ensure that they still function properly with new hardware and software. The Agency reviewed the testing performed by DOE to demonstrate continued compliance with the addition of computer hardware and upgraded software. In September 2004, the Agency completed their review with respect to the qualification of the computer codes on the Compaq ES40 and the Compaq Alpha 8400 (EPA 2004e). At that time, the Agency concluded that 38 (of 39) computer codes and three libraries migrated to the Compaq ES45 and 8400 using OpenVMS 7.3-1 were approved for use in compliance calculations for the WIPP PA.

EPA questioned the ability of SANTOS to accurately simulate creep closure and resultant porosity in rooms within the repository where rigid super-compacted waste had been emplaced. In the CCA, the porosity of the waste was combined with the porosity of the room into a collective porosity. This conceptualization was considered to be an appropriate simplification because the waste was assumed to be fully degraded and room closure tightly encapsulated the wastes within a few hundred years. In the case of super-compacted waste, however, the wastes have very low porosities and portions of the room may remain open. Consequently, EPA considered the conceptualization of a single porosity to describe both the room and the wastes to be inappropriate. However, the porosity surfaces developed by SANTOS are only used to simulate room-scale pore volumes during creep closure. While the combined, room-scale porosity and pore volume are used in BRAGFLO to calculate repository gas pressures, no direct use is made of the porosities of individual waste forms. EPA therefore concluded that, under the present configuration of the performance assessment codes, the conceptualization of a single porosity to describe both the room and the waste is reasonable (see Docket EPA 2004c for additional details).

In 2005, DOE made revisions to eight of the computer codes, including LHS, POSTLHS, CUTTINGS, DRSPALL, PANEL, SUMMARIZE, PRECCDFGF and CCDFGF. The Agency's findings with respect to the qualification of these eight computer codes on the Compaq ES40 and ES45 are described in detail in EPA 2006b. After reviewing the information summarized in EPA 2006b, the Agency concluded that the most recent versions of these eight codes are approved for use in compliance calculations on the Compaq ES40 and ES45 using OpenVMS 7.3-1.

5.0 PARAMETERS

Changes to the WIPP parameter database between the PAVT and the CRA-2004 PABC occurred in three stages and were the subject of three separate Agency reviews. The first of these reviews (EPA 2003a, Docket A-98-49, Item II-B3-51) evaluated changes occurring during the Technical Baseline Migration (TBM), in which the DOE's original CCA performance assessment database, as modified for the Agency's mandated PAVT, was transferred to a new platform and software, and renamed the Performance Assessment Parameter Database (PAPDB). The second review (EPA 2004d) evaluated changes made to the TBM database for the Department's first Compliance Recertification Application (CRA). The performance assessment supporting the CRA is identified in the PAPDB as the CRA1 analysis. The third review (EPA 2005e) evaluated the procedural adequacy of changes made to the CRA database for DOE's PABC, and also reviewed the technical adequacy of all database changes made since the TBM. The PABC is identified in the PAPDB as the CRA1BC analysis. The results of these reviews are summarized below.

All database issues that were identified in these reviews were quickly corrected by DOE and no Agency concerns related to the PA database remain outstanding. The database changes resulted from factors such as correction of errors, updated hydrogeologic conditions, updated Delaware Basin drilling and plugging practices, removal of hardwired parameters from codes, and code modifications. Other changes included correction of parameter units and updating of parameter-related metadata. Transcription accuracy and technical adequacy were checked for all new and updated parameter values and units. The rationale for dropping certain parameters from the PA codes was also evaluated and found to be acceptable. Representative samples of supporting documents listed in the PAPDB were checked for retrievability from the WIPP Records Center, maintained by Sandia National Laboratories (SNL) in Carlsbad, and no concerns were identified. Procedural changes made by SNL that were associated with the PAPDB were identified as part of the parameter reviews and upon further review by the Agency's Quality Assurance staff were found to be acceptable and consistent with the requirements of NQA Parts 1 and 2 for software, and with the requirements of the Agency's 40 CFR 194.23.

6.0 MICROBIAL DEGRADATION AND GAS GENERATION

Microbial degradation of cellulosics, plastics, and rubber (CPR) may influence WIPP repository performance because of its effects on repository chemistry and gas generation. The Agency reviewed the approach and assumptions used by DOE to model microbial degradation for the CRA PA (EPA 2005b). The Agency's review comments to DOE focused on the probability of significant microbial degradation, the nature of the microbial degradation reactions likely to occur in the repository, and microbial gas generation rates. As a result of the Agency's review and comments, DOE changed the modeling of microbial degradation processes for the PABC.

6.1 PROBABILITY OF SIGNIFICANT MICROBIAL DEGRADATION

The same assumptions regarding the probability of significant microbial degradation of CPR were used for the CCA, PAVT, and the CRA PA (DOE 1996b, EPA 1998a, and DOE 2004b). Significant microbial gas production was assumed to occur in only half the PA realizations because of uncertainties associated with microbial processes. These uncertainties included the presence and long-term viability of microbes capable of degrading CPR, the presence of adequate nutrients, and potential toxicity of waste components or repository conditions to microbes. In half of the realizations in which significant microbial consumption of CPR occurred (one quarter of all realizations), only cellulosics were assumed to be consumed by microbial activity. In the remaining half of the realizations with significant microbial consumption of CPR (one quarter of all realizations), all CPR materials, including plastics and rubber, were assumed to be consumed by microbial activity (DOE 2004b, Section 6.4.3.3).

6.1.1 Information Developed Since the Compliance Certification Application

During their review of the CRA PA, the Agency noted that additional information related to the probability of significant microbial degradation in the WIPP repository had become available since the time of the CCA PA and PAVT. The Agency therefore requested that DOE evaluate whether the assumed probability of significant microbial degradation of CPR should be increased based on the available information (EPA 2004a, Comment G-9). DOE responded to this request (DOE 2004a, Comment G9a) with information based on an analysis by Brush 2004. Brush 2004 identified factors that could affect the probability of significant microbial degradation of CPR in the WIPP repository. These factors included the presence and long-term survival of microorganisms in the repository and whether sufficient degradable substrates, water, and nutrients would be present. The Agency reviewed the information presented by Brush 2004 and other available information and concluded that new data regarding the potential existence and survival of microbes had increased the probability of significant microbial degradation of cellulosics (EPA 2005b). On the other hand, the Agency did not find significant information supporting an increase in the probability of microbial degradation of plastics and rubbers in the repository (EPA 2005b). Therefore, the Agency instructed DOE to assume that microbial degradation of CPR would occur in all PABC vectors (EPA 2005a).

6.1.2 Revised Microbial Degradation Probability

The parameter WAS_AREA:PROBDEG is a sampled function used by BRAGFLO to indicate whether microbial gas generation occurs and what type of material degrades (Nemer 2005c). DOE updated this parameter to reflect the increased probability (0.75) of microbial degradation of only cellulosics materials and the unchanged probability (0.25) of microbial degradation of all CPR materials. These changes to WAS_AREA:PROBDEG are consistent with the available data and are an adequate response to the Agency's request that significant microbial degradation should be assumed to occur in all PABC vectors.

6.1.3 Effects of Increased Microbial Degradation Probability on Performance Assessment

The Agency asked DOE to assess the potential effects of a higher probability of significant microbial degradation of CPR in the repository on microbial gas generation rates, as well as on microbial colloid formation and mobilization of actinides (EPA 2004a, Comment G-9). In their evaluation, DOE found that CRA PA gas generation rates and repository pressures at early times were larger for vectors with microbial degradation, and also found higher maximum cumulative gas generation and repository pressure over the 10,000-year regulatory period for vectors with significant microbial degradation of CPR (DOE 2004a, EPA 2005b).

DOE assessed the effects of the assumed probability of microbial CPR degradation on actinide mobilization in the CRA PA by comparing total radionuclide mobilization for microbial and nonmicrobial vectors, based on PANEL output for Scenarios S1 and S3 (DOE 2004a). Higher releases were observed in microbial vectors for direct brine releases and for spall releases. However, total releases were not significantly higher for microbial vectors than for nonmicrobial vectors because cuttings and cavings dominated total releases, and cuttings and cavings releases were not significantly affected by microbial activity (DOE 2004a, EPA 2005b).

6.2 MICROBIAL DEGRADATION REACTIONS

The same conceptual model for microbial degradation of CPR was used in the CCA PA, the PAVT, and CRA PA (DOE 1996b, DOE 2004b). DOE assumed that microbial degradation of CPR could occur in the repository and produce methane (CH_4) and carbon dioxide (CO_2). The major pathways for microbial degradation of CPR were predicted to include the following reactions:

$$C_6H_{10}O_5 + 4.8\ H^+ + 4.8\ NO_3^- \rightarrow 7.4\ H_2O + 6\ CO_2 + 2.4\ N_2 \qquad (1)$$

$$C_6H_{10}O_5 + 6\ H^+ + 3\ SO_4^{2-} \rightarrow 5\ H_2O + 6\ CO_2 + 3\ H_2S \qquad (2)$$

$$C_6H_{10}O_5 + H_2O \rightarrow 3\ CH_4 + 3\ CO_2 \qquad (3)$$

where $C_6H_{10}O_5$ is the chemical formula for cellulose. In reactions (1) and (2), referred to respectively as denitrification and sulfate reduction, one mole of carbon dioxide is produced for each mole of organic carbon consumed. However, methanogenesis (reaction 3) produces only 0.5 moles of carbon dioxide per mole of organic carbon consumed. Therefore, the predominant

microbial degradation reaction or reactions can affect gas physical properties, repository chemistry, and the required quantity of MgO backfill.

Reactions (1) to (3) were predicted to occur sequentially, according to the energy yield of the reactions (Wang and Brush 1996). DOE assumed that the denitrification and sulfate-reduction reactions would consume the limited amounts of nitrate and sulfate in the WIPP waste inventory. For both the CCA and the CRA, DOE predicted that methanogenesis (reaction 3) would be the dominant reaction pathway because of limited amounts of available sulfate and nitrate. Consequently, DOE predicted that approximately half the organic carbon consumed would be converted to carbon dioxide and approximately half would be converted to methane (DOE 1996b, Appendix SOTERM Section 8.2.2; DOE 2004b, Appendix PA Attachment SOTERM Section 2.2.2).

The Agency reviewed DOE's conceptual model of microbial degradation of CPR for the Advanced Mixed Waste Treatment Facility (AMWTF) and for the CRA (EPA 2004b, 2004c, and 2005a). The Agency observed that abundant sulfate was potentially available for sulfate reduction (reaction 2) because of the presence of anhydrite ($CaSO_4$) in the Salado Formation surrounding the repository. Therefore, the Agency found that assuming methanogenesis to be the dominant degradation reaction was not supported by the available data. The Agency consequently stated that DOE should assume that all CPR carbon in the WIPP repository could be converted to carbon dioxide via denitrification and sulfate reduction, unless new and convincing evidence was provided by DOE that methanogenesis would occur (EPA 2004b, Comment G-14). Because DOE did not provide additional evidence that methanogenesis would occur in the WIPP repository, the Agency specified that all CPR should be assumed to degrade via denitrification and sulfate reduction for the PABC (EPA 2005a).

DOE evaluated the likely effects of removing methanogenesis on the WIPP PA modeling of repository pressure, brine saturation, and brine outflow (Nemer and Zelinski 2005). The calculation of the maximum and minimum values for the stoichiometric factor y was originally described by Wang and Brush 1996. The stoichiometric factor y represents the moles of gas generated per mole of CPR carbon that is degraded. Gas generation was predicted to occur via reactions (1) through (3), however, for the CCA PA, PAVT and CRA PA, gas was predicted to be consumed by reaction with steel in the repository via the reactions:

$$Fe + CO_2(g) + H_2O \rightarrow FeCO_3 + H_2(g) \quad (4)$$

$$Fe + H_2S(g) \rightarrow FeS + H_2(g) \quad (5)$$

The maximum value of y was calculated assuming no reaction of carbon dioxide (CO_2) or hydrogen sulfide (H_2S) occurred with the steel, whereas the minimum value of y was calculated assuming the hydrogen sulfide gas reacted completely with the steel. The stoichiometric factor y was assumed to vary between these y_{max} and y_{min} values, and was determined by uniform sampling of the variable β, which varied from 0 to 1 (Wang and Brush 1996). However, Nemer and Zelinski 2005 noted that in reaction (5), one mole of hydrogen gas is produced for each mole of hydrogen sulfide gas consumed. Therefore, because reaction of iron with hydrogen sulfide would not decrease the amount of gas in the repository, y_{max} was set equal to y_{min} and both y and β were not sampled parameters for the PABC (Nemer and Zelinski 2005). Because only a

relatively small fraction of CPR degradation occurred by the sulfate reduction pathway in the CCA PA, PAVT, and CRA PA, the effects of sampling over y_{max} to y_{min} were likely to be small (Nemer and Zelinski 2005). The effects of the changes to the stoichiometric factor y were determined by comparing repository pressures calculated using the assumed microbial degradation probabilities used for the CCA PA, PAVT, and CRA PA and the original and revised stoichiometric factor y values (Nemer and Zelinski 2005). The changes in the stoichiometric factor y had only small effects on repository pressures, brine saturation, and cumulative brine outflow (Nemer and Zelinski 2005).

For the PABC, an excess of sulfate was assumed to be present and 4% of the CPR degradation occurred by denitrification (reaction 1) and 96% by sulfate reduction (reaction 2) (Leigh et al. 2005a). The implementation of gas generation without methanogenesis in BRAGFLO is described by Nemer and Stein 2005. DOE has therefore adequately responded to the Agency's request to remove methanogenesis from the gas generation model and to assess the effects of removing this reaction on PA results.

6.3 MICROBIAL GAS GENERATION RATES

DOE used the same microbial gas generation rates in humid and inundated conditions for the CRA PA as were used for the CCA PA (see Tables 6-1 and 6-2 below). These microbial gas generation rates were based on data from an experimental investigation of the microbial consumption of papers under inundated and humid conditions (Wang and Brush 1996). The gas generation rates were calculated from the initial linear portion of the experimental curve of carbon dioxide evolution as a function of time (Wang and Brush 1996; DOE 2004b, Appendix PA Attachment PAR). The experiments used by Wang and Brush (1996) to determine the maximum and minimum inundated and humid rates are listed in Table 6-3. The gas generation rate used in each CRA PA realization was determined in BRAGFLO from the humid and inundated rates based on the effective liquid saturation (DOE 2004b, Section 6.4.3.3).

During EPA's review of the CRA PA, DOE indicated that the microbial gas generation experiments had continued and additional information related to microbial gas generation rates in the WIPP repository had become available since the time of the CCA PA and the PAVT but had not been incorporated into the CRA PA. In their letter directing DOE to perform the PABC, the Agency allowed DOE to propose a new gas generation rate scheme based on the new experimental data (EPA 2005a). DOE's evaluation and implementation of new microbial gas generation rates are summarized by Leigh et al. 2005a, Nemer et al. 2005, Nemer and Stein 2005, and Stein and Nemer 2005.

6.3.1 Determination of PABC Microbial Gas Generation Rates

Nemer et al. 2005 describes the determination of the microbial gas generation rates used in the PABC. The microbial gas generation data used to determine the rates were obtained from experiments summarized by Gillow and Francis 2002, and Francis et al. 1997. These experiments were also described by Gillow and Francis 2003. The microbial production of carbon dioxide as a function of time in these experiments took place at relatively high rates at the beginning of the experiments, but carbon dioxide production typically slowed after about 1.5 years. The exact causes of these slowing rates are not known, as acknowledged by

Nemer et al. 2005. However, this type of bacterial growth curve is commonly encountered because of limitations on resources such as nutrients or readily-degradable substrate, or because of increasing concentrations of metabolites.

Because of the shape of the curve formed by carbon dioxide generated as a function of time, the degradation rates were modeled by obtaining a least-squares fit of two linear functions to the reported mean values for the carbon dioxide gas generation data. In this manner, both a short-term and a long-term rate were determined for each experimental data set. A minimum of three data points were included in each short-term or long-term fit to the data. The best fit was determined by choosing the model with the smallest residual between the observed and fitted values of carbon dioxide produced as a function of time (Nemer et al. 2005).

None of the data considered by Wang and Brush 1996 or Nemer et al. 2005 were from experiments that included bentonite. Bentonite was not included in the repository as backfill, although its use was under consideration at the time the microbial gas generation experiments began. Samples from initially aerobic experiments were also not considered in either analysis. Wang and Brush 1996 justified the use of data only from the initially anaerobic experiments by noting that the WIPP repository was expected to become anoxic shortly after closure.

6.3.1.1 Inundated Gas Generation Rates

Wang and Brush (1996) determined the maximum inundated rate from experiments with cellulosics that were inoculated and amended with nutrients and nitrates. The linear portion of the carbon dioxide generation data from 69 and 411 days was used to calculate a maximum carbon dioxide generation rate of 0.3 moles CO_2/kg cellulosics/year. The minimum inundated rate of 0.01 moles CO_2/kg cellulosics/year was calculated from experiments with cellulosics that were inoculated and unamended with nutrients or nitrate, using the carbon dioxide generation data from 0 and 1,034 days (Table 6-3).

The inundated experiments evaluated by Nemer et al. 2005 included those used by Wang and Brush (1996) (Table 6-3) as well as experiments that were amended with nutrients but without excess nitrate. Nemer et al. 2005 used the 95% upper confidence limit (UCL) and 95% lower confidence limit (LCL) about the mean slope values to determine the maximum and minimum possible rates. The Agency reproduced the calculations of these long-term rates using the same carbon dioxide data as Nemer et al. 2005 (Appendix C).

The data used by Nemer et al. 2005 omitted experimental results reported by Gillow and Francis 2003 at 3,929 days. Because of the tendency for slower carbon dioxide generation with time, inclusion of these last data points in the long-term rate determination would have resulted in lower maximum and minimum rates. However, methane production was detected in some samples from the inundated experiments (Table 6-4). Therefore, the reduced rate of carbon dioxide production at the end of these experiments may be partially attributable to methanogenesis. Methanogenesis may not occur in the WIPP repository because of the large quantities of sulfate present in the Salado anhydrite interbeds and brine (see Section 6.2). Therefore, the long-term rates obtained with data before methanogenesis was observed may be more representative of rates in the repository. These long-term rates were determined by linear regression of the data used by Nemer et al. 2005, excluding the data where methane production

was observed. The rates determined in the absence of methanogenesis (Table 6-5) were slightly higher than the rates determined by Nemer et al. 2005. However, the differences were relatively small compared to the uncertainties associated with extrapolating laboratory-determined microbial gas generation rates to the long-term WIPP repository. The inundated rates determined by Nemer et al. 2005 and used in the PABC therefore appear reasonable and are adequately supported by the available data.

6.3.1.2 Humid Gas Generation Rates

The data listed in Wang and Brush (1996) Appendix I for the calculation of the maximum humid cellulosics biodegradation rate are summarized in Table 6-3. The 415-day data are slightly different than the data reported by Francis et al. 1997 and Gillow and Francis 2003 for the same experiments (Table 6-6). Although the reason for this discrepancy is unknown, the calculated rates are not significantly different with either data set. Wang and Brush 1996 calculated the maximum humid gas generation rate (0.04 mole/kg/year) by averaging the amended and unamended carbon dioxide gas generation data at 6 and 415 days and calculating a linear rate between these average values.

Nemer et al. 2005 used data from the unamended experiments to determine the maximum long-term gas generation rate under humid conditions. The reasons for excluding data from the humid amended experiments were not stated. However, examination of the data reported by Gillow and Francis 2003 shows that the long-term rate for the humid amended experiments was essentially zero (Figure 6-1), and the lower limit for the humid gas generation rate was assumed to be zero by Nemer et al. 2005. The Agency successfully reproduced the calculation of the maximum long-term humid gas generation rate using the same carbon dioxide data as Nemer et al. 2005 (Appendix C). The assumption that the humid gas generation rate would range between this maximum rate and zero as observed in the amended humid experiments is consistent with the available experimental data.

6.3.2 Implementation of Microbial Gas Generation Rates

Nemer and Stein 2005 described the implementation of the revised microbial gas generation rates in BRAGFLO for the PABC. The two zero-order microbial gas generation rates for humid (WAS_AREA:GRATMICH) and inundated (WAS_AREA:GRATMICI) conditions were determined as described by Nemer et al. 2005, with units converted to those used by BRAGFLO (moles C/kg cellulose/sec) and accounting for the dissolution of carbon dioxide in water for the inundated rates. The rates used in the PABC are compared to those used in the CCA PA, PAVT and CRA in Tables 6-1 and 6-2. The revised inundated long-term microbial gas generation rate is more than an order of magnitude lower than the previously determined rate. However, the revised humid long-term microbial gas generation rate is only slightly lower than the previously determined humid rate.

The reported mean, median, and maximum rates for microbial gas generation were higher under humid conditions than under inundated conditions (Tables 6-1 and 6-2). Nemer and Stein 2005 indicated that this was "physically unrealistic" but do not provide any evidence to support this assertion. Because DOE believed the humid rate should be lower than the inundated rate, the sampled humid and inundated rates were compared within BRAGFLO; if the sampled humid

rate exceeded the sampled inundated rate, the humid rate was set equal to the inundated rate. Stein and Nemer 2005 did not provide information on the likely effects of assuming that the humid rate would always be lower than the inundated rate. However, because the mean, median, and high values of the rates differ by only about a factor of 2 (Tables 6-1 and 6-2), it is likely that the humid rates used in BRAGFLO were not significantly reduced by this assumption.

The revised microbial gas generation rates were based on long-term experimental data. Therefore, gas generation during the early stages of the repository was accounted for in BRAGFLO by assuming a fixed amount of gas was present in the repository at the beginning of the calculations (Nemer et al. 2005). The amount of gas in the repository was assumed to be equal to the amount of gas generated per gram of cellulose at the point where the relatively rapid short-term rate changed to the slower long-term rate in the nutrient and nitrate-amended inundated experiments; these experiments were used to evaluate the maximum long-term rate. This amount of gas initially present in the repository because of rapid early microbial gas generation rates equaled 181 μmole/g cellulose (Nemer et al. 2005). This value was converted to the total moles of gas in the repository based on the equivalent amounts of cellulose in the repository inventory and the microbial gas generation model of Wang and Brush (1996). This amount of gas was then converted to a pressure value of 26.714 kPa using the ideal gas equation and the volume and temperature of the repository. This additional pressure was assumed to be generated immediately upon closure, resulting in an initial total repository pressure of 128,039 kPa (Nemer et al. 2005, Stein and Nemer 2005).

At the Agency's direction, DOE changed the probability of microbial degradation to account for new evidence regarding the presence and viability of microbes capable of degrading CPR in the WIPP repository. The revised probability parameters resulted in microbial degradation in all vectors for the PABC (Section 6.1). However, DOE asserted that uncertainties remained regarding the viability of microbes in the repository because of different conditions in the repository compared to the conditions in the experiments (Nemer et al. 2005). DOE therefore introduced an additional sampled parameter, BIOGENFC. This parameter, which had a uniform distribution from 0 to 1, was multiplied by the microbial gas generation rates to effectively reduce the humid and inundated microbial gas generation rates from the experimentally determined long-term rates.

The uncertainties listed by DOE as justification for this rate reduction were:

- Whether microbes will survive for a significant fraction of the 10,000-year regulatory period
- Whether sufficient water will be present
- Whether sufficient quantities of biodegradable substrate will be present
- Whether sufficient electron acceptors will be present and available
- Whether enough nutrients will be present and available

The Agency questioned these justifications (EPA 2005b) and this was a factor in the Agency's

direction to DOE to change the probability of microbial degradation so that significant microbial gas generation occurred in all PABC vectors (EPA 2005a). Because of the inherent uncertainties associated with extrapolating experimentally measured microbial gas generation rates to repository conditions, it is reasonable to add an uncertainty factor to these rates.

6.4 EFFECTS OF MICROBIAL GAS GENERATION RATES AND PROBABILITY CHANGES ON PABC RESULTS

Nemer et al. 2005 evaluated the effects of the revised probability of microbial degradation and the revised microbial gas generation rates by comparing the results obtained with the revised assumptions with the results of the CRA PA. Nemer et al. 2005 observed that these changes tended to have offsetting effects: increased microbial degradation probability tended to increase repository pressure and decrease brine saturation, whereas lower microbial gas generation rates tended to decrease repository pressure and increase brine saturation. Nemer et al. 2005 compared repository pressures and brine saturations for the undisturbed repository (BRAGFLO scenario S1) and the repository with a drilling intrusion into a pressurized Castile brine pocket at 350 years (BRAGFLO scenario S2).

For scenario S1, average and maximum pressures tended to increase more slowly because of lower microbial gas generation rates; minimum pressures were higher because microbial gas generation occurred in all vectors. The slower increase in pressure resulted in slightly higher brine saturation (Nemer et al. 2005). For the PABC calculations, brine saturation increased more quickly and pressure increased more slowly than for the CRA PA calculations because of the lower microbial gas generation rates used in the calculations (Leigh et al. 2005a). The relationship between pressure and brine saturation was found to be dependent on pressure. At low pressure, increased brine saturation resulted in increased gas generation and pressure. However, at higher pressures, increasing pressure impeded brine inflow and decreased brine saturation (Leigh et al. 2005a). Cumulative brine outflow for the S1 scenario was slightly increased for the PABC calculations compared to the CRA PA calculations (Leigh et al. 2005a).

For the S2 scenario, little difference in maximum or average pressure was observed between the revised microbial gas generation assumptions and the CRA PA assumptions (Nemer et al. 2005). However, because of the assumption of microbial degradation in all vectors, the minimum pressure was higher for the revised assumptions than for the CRA PA assumptions. The average and minimum brine saturation for the S2 scenario was higher for the revised microbial gas generation assumptions than for the CRA PA. However, no effects were observed on maximum brine saturation for either set of assumptions because complete saturation was predicted for both sets of assumptions after the drilling intrusion (Nemer et al. 2005).

DOE's inclusion of the BIOGENFC parameter resulted in the use of microbial gas generation rates that were equal to or less than experimentally measured values. In addition, the inclusion of data from time periods when methanogenesis occurred may have lowered the rates calculated from the experimental data. However, because of the relatively large uncertainties in the rates over the regulatory time period, the microbial gas generation rates used in the PABC calculations are likely to provide a reasonable approximation of expected values. The results of the calculations reported by Nemer et al. 2005 and the PABC results reported by Leigh et al. 2005a indicate that the lower microbial gas generation rates tended to increase brine saturation. Higher

brine saturation may lead to increased flow up the borehole and direct brine release (DBR) of radionuclides. Therefore, the use of lower microbial gas generation rates may have had some previously unanticipated effects, in that the likelihood of DBR of radionuclides was increased. However, the frequency and volume of spallings releases were decreased in the PABC compared to the CRA PA because of the lower gas pressures (Leigh et al. 2005a). Because the releases from the repository are controlled by cuttings and cavings, except at low probability (Leigh et al. 2005a), these differences in spallings and DBR are unlikely to significantly affect overall repository performance.

Table 6-1. Inundated Cellulose Biodegradation Rates (GRATMICI) used in PA
(moles C/kg cellulose/sec)

Property	Performance Assessment		
	CCA/PAVT	CRA	PABC
Mean and Median	4.915×10^{-9}	4.92×10^{-9}	2.939×10^{-10}
High	9.5129×10^{-9}	9.51×10^{-9}	5.569×10^{-10}
Low	3.171×10^{-10}	3.17×10^{-10}	3.083×10^{-11}
Standard Deviation	0.00	2.65×10^{-9}	1.519×10^{-10}
Reference	DOE 1996b	DOE 2004b	Nemer 2005b

Table 6-2. Humid Cellulose Biodegradation Rates (GRATMICH) used in PA
(moles C/kg cellulose/sec)

Property	Performance Assessment		
	CCA/PAVT	CRA	PABC
Mean and Median	6.342×10^{-10}	6.34×10^{-10}	5.136×10^{-10}
High	1.2684×10^{-9}	1.27×10^{-9}	1.027×10^{-9}
Low	0.00	0.00	0.00
Standard Deviation	0.00	3.66×10^{-10}	2.965×10^{-10}
Reference	DOE 1996b	DOE 2004b	Nemer 2005a

Table 6-3. Experiments and Data Used to Determine Microbial Gas Generation Rates
All experiments were carried out with cellulosics, were initially anaerobic, and were inoculated.

Rate	CCA PA, PAVT and CRA PA Experiments and Data (Wang and Brush 1996)	PABC Experiments and Data (Nemer et al. 2005)
Maximum Inundated	Added nutrients, nitrate-amended; 69-day and 411-day data	Added nutrients, nitrate-amended; 481-day to 3,464-day data
Minimum Inundated	No nutrients or nitrate added; 0-day and 1,034-day data	Added nutrients; 411-day to 3,464-day data
Maximum Humid	Added nutrients, nitrate-amended; 6-day and 415-day data	No nutrients or nitrate added; 415-day to 2,945-day data
Minimum Humid	Assumed rate to be zero	Assumed rate to be zero

Table 6-4. Initially Anaerobic Experiments with Reported Methane
(Gillow and Francis 2003)

Conditions	Data Range (days)
Inundated unamended	2,718 and 3,462
Inundated, nutrient-amended	2,718 and 3,462
Inundated, nutrient-amended, excess nitrate	3,462

Table 6-5. Long-term Inundated Microbial Gas Generation Rates Calculated by Nemer et al. 2005

Data Set	Conditions	Data Range (days)	95% UCL Rate (μmole CO_2/g/day)	95% LCL Rate (μmole CO_2/g/day)
Nemer et al. 2005	Inundated unamended	481 to 3,464	0.00634	0.00481
Nemer et al. 2005	Inundated, nutrient-amended	411 to 3,464	0.00908	0.00171 (minimum)
Nemer et al. 2005	Inundated, nutrient-amended, excess nitrate	481 to 3,464	0.03087 (maximum)	0.00944
Without Methanogenesis	Inundated unamended	481 to 1,228	0.00952	0.00237
Without Methanogenesis	Inundated, nutrient-amended	411 to 1,228	0.01772	0.00188 (minimum)
Without Methanogenesis	Inundated, nutrient-amended, excess nitrate	481 to 2,723	0.04289 (maximum)	0.01449
Nemer et al. 2005	Humid, unamended	415 to 2,945	0.08881	-0.04403

Table 6-6. Anaerobic and Inoculated Humid Cellulosics Microbial Gas Generation Data Used by Wang and Brush 1996, and Reported by Francis et al. 1997 and Gillow and Francis 2003

Conditions	Time (days)	Wang and Brush 1996 (μmoles/g)	Francis et al. 1997 and Gillow and Francis 2003 (μmoles/g)
Unamended	6	7.7	7.7
Amended	6	13.3	13.3
Unamended	415	83.1	72.6
Amended	415	28.8	18.3

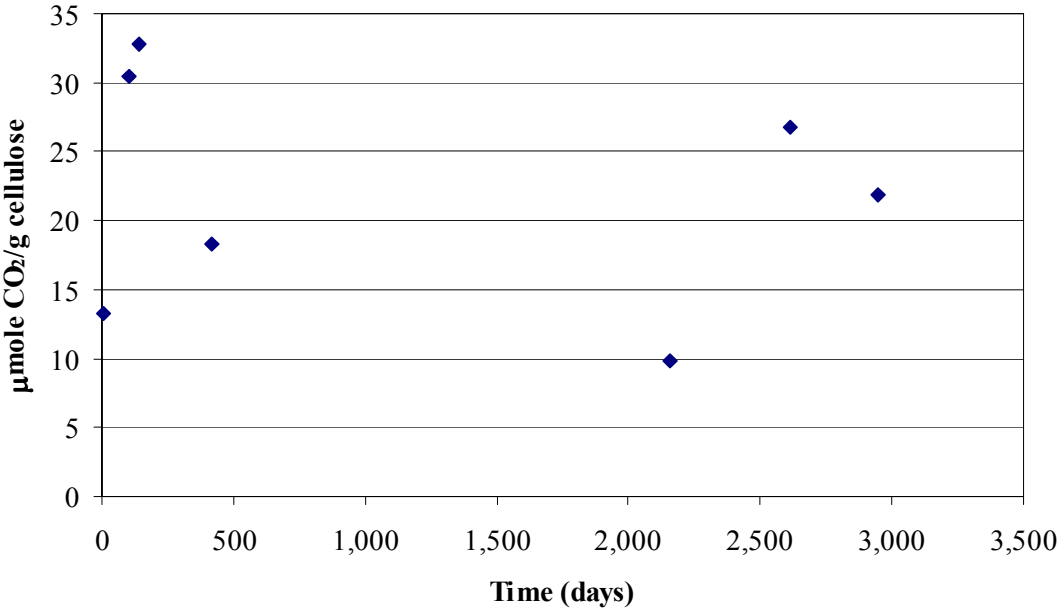

Figure 6-1. Initially Anaerobic, Amended Humid Experiments
(Gillow and Francis 2003)

7.0 ACTINIDE SOLUBILITY

The Fracture Matrix Transport (FMT) code was used to model actinide solubilities in WIPP brines for the CCA PA, PAVT, CRA PA, and PABC. The FMT code was used to calculate actinide concentrations in WIPP brines based on aqueous speciation and solubility equilibria using the Pitzer activity coefficient model. A number of solubility-related assumptions remained unchanged since the PAVT, including use of end-member Salado and Castile brines to represent the range of brine compositions in the repository, the assumption that brine is well-mixed with waste in the repository, dissolved radionuclide concentrations are assumed to be controlled by the solubility of solid phases, and repository brines are assumed to be in equilibrium with Salado minerals such as halite and anhydrite. The oxidation-state analogy was used in both the PAVT and PABC. Based on this analogy, americium(III), thorium(IV), and neptunium(V) solubilities were used to approximate the solubilities of other actinides in these oxidation states, e.g., plutonium(III) solubility was approximated by the solubility of americium(III). Because no new evidence has been identified that challenges these assumptions, the Agency has found that they remained appropriate for use in the PABC calculations.

For both the PAVT and PABC actinide solubility calculations, it was assumed that reducing conditions would be established in the repository shortly after closure. Americium(III), curium(III), and thorium(IV) were assumed to be the only oxidation states present in the actinide solubility calculations. Because of these reducing conditions, plutonium was assumed to be present only in the +III and +IV oxidation states and neptunium was assumed present only in the +IV and +V oxidation states. However, it was assumed that uranium could be present in either the +IV or +VI oxidation states. These oxidation-state assumptions remain unchanged since the PAVT. The Agency reviewed additional evidence regarding actinide oxidation state assumptions, particularly regarding the possible presence of plutonium(V) in the long-term repository (EPA 2005b). The Agency found that the available evidence indicated that the oxidation states assumed by DOE for the PAVT and PABC were appropriate.

The Agency reviewed the changes since the PAVT in the calculation of actinide solubilities for the CRA PA (EPA 2005b). As a result of this review, DOE incorporated a number of additional changes in the calculation of actinide solubilities and the estimation of the actinide solubility uncertainties for the PABC. Changes since the CRA were made to the FMT database and to the estimated concentrations of organic ligands used in the calculation of actinide solubilities for the PABC. The review of these changes is summarized below, with an evaluation of the selection of the Salado brine formulation used in the PABC. The results of the PABC actinide solubility calculations and the revised actinide solubility uncertainties were evaluated. For the CRA PA, DOE had revised the colloidal source term used in the CCA PA and PAVT. However, based on the increased probability of microbial activity and comments received from the Agency (EPA 2005b), the colloidal source term used in the PABC was unchanged from the PAVT.

7.1 FMT DATABASE

FMT Version 2.4 was used for both the CRA PA and PABC actinide solubility calculations (Brush and Xiong 2003a, Brush and Xiong 2005a). The FMT database versions used by DOE since the PAVT are summarized in Table 7-1. The FMT database FMT_021120.CHEMDAT

was used for the actinide solubility calculations for the CRA PA (DOE 2004b). Revisions were made to the FMT database since the PAVT to produce FMT_021120.CHEMDAT; these changes included the addition of new aqueous actinide species to the database and revisions to existing species data because of the availability of new experimental data. The Agency reviewed these changes and found that they were technically adequate and appropriately documented (EPA 2005b).

After the CRA PA, the FMT database was revised several times, ultimately to version FMT_050405.CHEMDAT (Table 7-1); this database was used for the PABC actinide solubility calculations (Brush and Xiong 2005a, Brush 2005). The database changes included revision of the thermodynamic data for one thorium aqueous species, addition of a calcium oxalate solid phase, and changes in the neptunium(V)-acetate complex thermodynamic data.

7.1.1 Thorium Data

Only minor revisions were made to the thorium(IV) aqueous species and thermodynamic data in the PAVT database prior to the CRA PA. These changes included a minor revision to the thermodynamic data for $Th(OH)_4(aq)$[6] and changes to the ternary interaction parameters (θ and ψ) describing the interaction of $Th(CO_3)_3^{6-}$ with Cl^- and Na^+ (Giambalvo 2002a). During their review of the actinide solubility calculations performed for the CRA PA and DOE's responses to the Agency's requests for additional information, the Agency noted that the actinide solubility model used during the CRA PA significantly underpredicted +IV actinide solubilities compared to experimentally measured values (EPA 2005b). DOE also noted this bias in the modeled data and investigated the likely cause of these differences (Nowak 2005, Brush 2005).

Nowak 2005 identified the thermodynamic data for $Th(OH)_4(aq)$ as the likely source of the discrepancies between the experimentally measured solubilities and the solubilities modeled with FMT. The $Th(OH)_4(aq)$ species is the principal aqueous thorium species above approximately pH 6, and thermodynamic data from a critically reviewed compilation by Neck and Kim 2001 and Neck et al. 2002 were used to modify the thermodynamic data for this species. Nowak 2005 derived the dimensionless standard free energy of formation (μ^0/RT) using the logarithm of the hydrolysis constant for $Th(OH)_4(aq)$ reported by Neck et al. 2002 and μ^0/RT data already in the FMT database for Th^{4+}, H_2O, and H^+. This calculated μ^0/RT was -626.5853, compared to the previous value in the FMT database of -622.4700. A revised μ^0/RT for $Th(OH)_4(aq)$ of -626.5853 was incorporated into FMT_050405.CHEMDAT (Xiong 2005). A comparison of the solubilities calculated with the revised database and experimental data indicated that solubilities calculated with the revised thermodynamic data for $Th(OH)_4(aq)$ are more consistent with the available solubility data (see Section 7.5).

A typographical error was made in Nowak 2005 when copying the $ThO_2(am)$[7] dissolution reaction from Giambalvo 2002a; this error appeared in the text and in equation (7) of Nowak 2005. The correct equation is:

[6] (aq) indicates an aqueous species

[7] The following notation was used to designate the crystallinity of the solid phases: (am) for an amorphous phase, (c) a crystalline phase, and (s) for a solid phase of unspecified crystallinity.

$$ThO_2(am) + 2H_2O = Th^{4+} + 4OH^-$$

These errors were typographical only and had no effect on the correct calculation of the $Th(OH)_4(aq)$ thermodynamic data. Nowak 2005 stated that the log solubility product at zero ionic strength (log K_{sp}^0) selected by the critical reviews of Neck and Kim 2001 and Neck et al. 2002 was -47.0. Although this value was selected during the critical review carried out by Neck and Kim 2001, the log K_{sp} value determined in the later study was -47.8 on the basis of additional evaluation of the available solubility data (see page 492 of Neck et al. 2002).

The log K_{sp}^0 of −45.5 for $Th(OH))_4(am)$ included in the FMT database was based on an investigation by Ryan and Rai (1987) and calculated by Felmy et al. 1991 (Giambalvo 2002a). This value is similar to a log K_{sp}^0 of -44.9 ± 0.5 reported by Rai et al. 2000. Neck et al. 2002 re-evaluated the experimental data at pH < 5 of Ryan and Rai 1987 and Rai et al. 2000, using the hydrolysis constants and SIT coefficients of Neck and Kim 2001; the re-evaluated log K_{sp}^0 values were -47.3 using the Ryan and Rai 1987 data and -46.2 using the Rai et al. 2000 data. Thus, the log K_{sp}^0 included in the thermodynamic database is higher than the values derived from the two studies (Ryan and Rai 1987; Rai et al. 2000) and is also higher than the value of -47.8 recommended by Neck et al. 2002. The higher log K_{sp}^0 included in the FMT database would be likely to conservatively overpredict thorium(IV) solubilities, and this value is therefore acceptable for use in PA.

7.1.2 Oxalate and Calcium Oxalate Data

Xiong 2004b described the correction of the molecular weight of oxalate ($C_2O_4^{2-}$) from the value listed in FMT_021120.CHEMDAT to the correct value of 88.0196 grams. The error in the oxalate molecular weight resulted from an input error during database development. The revised molecular weight is correct, and Xiong 2004b indicated that the error is unlikely to have affected previous solubility calculations.

Xiong 2004b also recommended inclusion of calcium oxalate solids in the thermodynamic database. The FMT_021120.CHEMDAT database version did not contain calcium oxalate solids data, even though these phases are relatively insoluble and likely to set upper limits on oxalate concentrations in solution. Xiong 2004b reviewed the available data on calcium oxalate solids and identified calcium oxalate monohydrate (whewellite, $CaC_2O_4 \cdot H_2O$) as the most stable calcium oxalate solid compared to calcium oxalate dihydrate ($CaC_2O_4 \cdot 2H_2O$) or calcium oxalate trihydrate ($CaC_2O_4 \cdot 3H_2O$). Based on the average of whewellite solubility products reported in three studies (Nancollas and Gardner 1974, Tomažič and Nancollas 1979, Streit et al. 1998), Xiong 2004b derived a μ^0/RT value of -326.0981 for whewellite. These calculations were reviewed and found to be accurate.

The changes in the oxalate and calcium oxalate data were incorporated in FMT_040628.CHEMDAT (Xiong 2004d); these data were also incorporated in the later version of the database, FMT_050405.CHEMDAT, used in the PABC. Including whewellite as a solid phase in the thermodynamic database is justified, because this phase has been shown to readily precipitate from low-temperature sodium chloride solutions. The precipitation of whewellite is likely to only affect the solubility of neptunium(V), because sensitivity calculations carried out

for WIPP conditions have shown that only the +V actinide solubility is sensitive to oxalate concentrations (EPA 2005b).

7.1.3 Neptunium(V)-Acetate Data

Xiong 2004c indicated that the μ^0/RT value for NpO_2Acetate(aq) in the FMT_021120.CHEMDAT database (-519.615) should be revised to -526.061, as recommended by Giambalvo 2002c. This change was incorporated into FMT_041116.CHEMDAT (Xiong 2004c). However, Xiong 2004a later rescinded this correction because of a poor fit to the experimental data of Choppin et al. 2001 previously identified by Giambalvo 2003. Giambalvo 2003 had rejected this value and recommended use of the μ^0/RT value for NpO_2Acetate(aq) of -519.615. The database used to evaluate the sensitivity of actinide solubilities to organic ligands concentrations (FMT_041210.CHEMDAT) included the appropriate μ^0/RT value for NpO_2Acetate(aq) of -519.615, as did the later database used in the PABC (FMT_050405.CHEMDAT).

7.1.4 Evaluation of FMT_050405.CHEMDAT

The changes and corrections noted above for the μ^0/RT values for $Th(OH)_4$(aq), whewellite, and NpO_2Acetate(aq), and for the molecular weight of oxalate were checked in FMT_050405.CHEMDAT. All of these changes were correctly incorporated in the database.

Nowak 2005 recommended revising the μ^0/RT value for $Th(OH)_4$(aq) based on the hydrolysis constant for $Th(OH)_4$(aq) selected by Neck et al. 2002. This revised value is likely to more reliably predict thorium(IV) solubilities under WIPP repository conditions, because it is based on the results of a critical review of the available thermodynamic data.

7.2 ORGANIC LIGANDS

The concentrations of organic ligands were re-evaluated for the PABC actinide solubility calculations based on a revised estimate of the minimum amount of brine that could lead to a release from the repository. In addition, new data regarding the possible complexation of +IV actinides by EDTA were identified; these data were evaluated to determine its potential significance to the actinide solubility calculations for WIPP repository conditions.

7.2.1 Organic Ligand Concentrations Used in the PABC Actinide Solubility Calculations

Sensitivity analyses of actinide solubility calculations performed at the Agency's request have demonstrated that organic ligands in the WIPP waste inventory could increase actinide solubilities (Brush and Xiong 2004). For the actinide solubility calculations, DOE has estimated organic ligand concentrations by assuming that the entire organic ligand inventory is dissolved in the minimum volume of brine required to be in the repository for a brine release to occur. The brine volume used for the CCA PA, the PAVT, and the CRA PA was based on an estimate developed prior to the CCA PA (Larson 1996, Stein 2005).

7.2.1.1 Brine Volume Used to Calculate Organic Ligands Concentrations

Stein 2005 re-evaluated the minimum amount of brine that could lead to a brine release from the WIPP repository for the PABC. Stein 2005 found that additional review was necessary for a number of reasons. The amount of brine had not previously been revised to account for the modified calculation of void volume in the current PA. The previous calculations relied on structural simulations that only lasted 2,000 years and did not include any gas generation. Errors were also discovered in the original excavated volume calculations made for the CCA that could result in the underestimation of the waste-filled portion of the repository. In addition, the original estimation that a minimum brine saturation of 0.75 was required for brine release is inconsistent with the current direct brine release conceptual model (Stein 2005).

Because all PABC realizations include gas generation, the void volume corresponding to the lowest gas pressure at 10,000 years was selected, which is the lowest void volume predicted in PA. The void volume in an individual room that corresponds to this pressure was interpolated from SANTOS results to be 301.5 m^3. Stein 2005 calculated the equivalent number of rooms in the repository to be 120.3, which is equal to the total repository volume divided by the volume of a single room. Stein also assumed that the minimum brine saturation necessary for brine release was 0.276, which was the median sampled residual brine saturation for the waste. Therefore, the minimum volume of brine required for a release was calculated to be:

$$301.5\ m^3 \times 120.3 \times 0.276 = 10{,}011\ m^3$$

For these calculations, Stein 2005 assumed that brine release occurred from the entire repository. However, this approach may not be entirely accurate. It is likely that the waste panels will respond independently to a drilling intrusion due to the robust seals that will be in place, and it is likely that different panels will have different brine saturations. An alternative and possibly more realistic approach would be to calculate the minimum brine release volume based on releases from a single panel instead of the entire repository. Because there are 10 panels, and not all panels will be of equal volume, the resulting minimum brine volume would be approximately $1/10^{th}$ of the volume calculated by Stein 2005, or about 1,000 m^3 of brine.

7.2.1.2 Organic Ligands Inventory and Concentration Calculations

The masses of organic ligands used to calculate concentrations for the CRA PA were later found to be overestimates of the amounts likely to be in the repository (Brush and Xiong 2003b). However, because these higher concentrations would overestimate releases from the repository, the actinide solubilities calculated using these higher organic ligand masses were used in the CRA PA (DOE 2004b). For the PABC, the corrected masses of organic ligands reported by Crawford and Leigh 2003 were used to calculate ligand concentrations (Brush and Xiong 2005b). Leigh 2005 found that none of the revisions to the WIPP inventory for the PABC had resulted in changes to the total masses of organic ligands expected in the WIPP inventory; therefore, Leigh 2005 recommended the use of the ligand inventories listed in Leigh 2003, which are the same as those listed in Crawford and Leigh 2003. These masses were converted to moles and divided by the minimum amount of brine (10,011 m^3 from Stein 2005) to yield the organic ligand concentrations used in the actinide solubility calculations. The resulting organic ligand

concentrations used for the PABC solubility calculations are compared to the PAVT organic ligands concentrations in Table 7-2.

The volume of brine used to dissolve the ligands may not be the minimum value that could be released from a single panel. It is also possible that the majority of ligands will be placed in a single panel because most ligands are in a limited number of waste streams. The assumption that all ligands are in the same panel and that these ligands would be mobilized by the minimum brine volume released from a single panel would be the most-conservative scenario for calculating ligands concentrations. However, the probability of a randomly located borehole encountering such a panel, if it existed in the repository, would be correspondingly reduced. The individual PA vectors would be influenced if modeling could be done on a panel-by-panel basis, but the influence on the mean concentrations would probably be small. Therefore, the use of the minimum amount of brine that could be released from the entire repository and assuming that all ligands are dissolved in this amount of brine is likely to be a reasonable approximation for calculating ligands concentrations and the resulting actinide solubilities.

7.2.2 Effects of EDTA Concentrations on +IV Actinide Solubilities

During its technical review of the CRA, the Agency identified a published study related to the solubility of ThO_2(am) in the presence of EDTA (Xia et al. 2003). The results of this study indicated that, in some circumstances, EDTA complexation of the +IV actinides could be significant. Therefore, the Agency asked DOE to evaluate the potential importance of this study to the WIPP actinide solubility modeling results.

In their response, DOE noted that the experimental results of Xia et al. 2003 could not be compared to predicted values generated with the current FMT database, because the experiments were conducted in concentrated nitrate (NO_3^-) solutions, and the FMT database does not include nitrate (DOE 2005). However, qualitative examination of the Xia et al. 2003 experimental results indicated that significant effects of EDTA complexation on total thorium(IV) concentrations in 0.5 M $NaNO_3$ solutions were not observed below an EDTA concentration of approximately 10^{-4} M. Because the EDTA concentrations predicted for the WIPP brines are approximately an order of magnitude lower (8.14×10^{-6}), the data of Xia et al. 2003 do not indicate that EDTA will significantly affect +IV actinide solubilities. This conclusion is consistent with the results of actinide solubility modeling carried out for the PABC, which found $Th(OH)_4$(aq) and $Th(OH)_3CO_3^-$ were the only significant aqueous thorium(IV) species in the ERDA-6 and GWB brines (Section 7.4.1).

7.3 SALADO BRINE FORMULATION

Two Salado Brine formulations, Brine A and GWB (Generic Weep Brine), have been used in PA calculations of actinide solubilities.[8] Brine A was used in the CCA PA and PAVT calculations. However, GWB is believed by DOE to more closely resemble the average composition of intergranular Salado brines at the repository horizon (Brush and Xiong 2005a). Therefore, DOE used the GWB composition for calculating actinide solubilities in Salado brine for the CRA PA (DOE 2004b Appendix PA Attachment SOTERM).

[8] Brine A and GWB compositions are compared in Table 3-1 of EPA (2005b).

Although DOE used actinide solubility calculation results for GWB in the CRA PA, actinide solubility calculations were also carried out with Brine A to permit comparison of the results obtained with the different brines. The Agency reviewed the documentation provided by DOE on the GWB and Brine A formulations and compared the results of solubility calculations with the two brines (EPA 2005b). The Agency found that the choice of brine formulation (GWB or Brine A) had relatively minor effects on the actinide solubility results. Brine A is representative of brines that have interacted with potassium and magnesium minerals, for example, brines that may enter the WIPP horizon by percolation through an overlying potash zone (Molecke 1983). Because the GWB formulation is reported to more closely match the composition of Salado intergranular brines, the Agency found that use of GWB brine in place of Brine A for the CRA PA actinide solubility calculations was appropriate.

DOE used the GWB formulation to calculate actinide solubilities in Salado brines for the PABC (Brush 2005, Brush and Xiong 2005a). However, for comparison purposes, DOE also reported the results of actinide solubility calculations using the Brine A formulation (Brush 2005, Table 5). Results were reported for calculations with organics present and hydromagnesite as Run 3 (Brine A) and Run 7 (GWB). Comparison of the results reported for these two simulations indicate that the differences in the +III, +IV, and +V actinide solubilities are relatively small (Table 7-3). The pH values and carbon dioxide fugacities were unaffected by the brine formulation. Because the GWB formulation is more representative of the Salado intergranular brine composition, the use of GWB in the PABC actinide solubility calculations is appropriate.

7.4 ACTINIDE SOLUBILITIES

The concentrations of the +III, +IV, and +V actinides used in the CCA PA, PAVT, CRA PA, and PABC were based on solubilities calculated using FMT. However, because DOE has not developed a solubility model for the +VI actinides, an assumed value for the +VI actinide solubility has been used in PA.

7.4.1 Calculated Actinide Solubilities

Many of the assumptions made for actinide solubility calculations for the PAVT and CRA PA remained unchanged for the PABC calculations (Brush 2005, Brush and Xiong 2005a). DOE assumed for the PABC actinide solubility calculations that instantaneous, reversible equilibria between WIPP brines, major Salado minerals, and MgO hydration and carbonation products will control pH, carbon dioxide fugacities, and brine composition. Salado minerals assumed to be present included halite (NaCl) and anhydrite ($CaSO_4$). If calculations indicated saturation with respect to glauberite [$Na_2Ca(SO_4)_2$] or $Mg_2Cl(OH)_3 \cdot 4H_2O$, these phases were allowed to precipitate.

The MgO hydration and carbonation phases assumed to be present in solubility calculations with Salado (GWB) brine were brucite [$Mg(OH)_2$], $Mg_2Cl(OH)_3 \cdot 4H_2O$, and hydromagnesite [$Mg_5(CO_3)_4(OH)_2 \bullet 4H_2O(s)$]. For actinide solubility calculations with Castile (ERDA-6) brine, brucite and hydromagnesite were assumed to be present. These MgO hydration and carbonation phases were the same as those assumed to control pH and carbon dioxide fugacity for the CRA

PA calculations that included significant microbial activity (DOE 2004b, EPA 2005b). The Agency reviewed the results of MgO hydration and carbonation experiments carried out by DOE and agreed that these phases are the most likely to control pH and carbon dioxide fugacities in the WIPP repository brines during the 10,000 year regulatory period (EPA 2005b). For CRA PA vectors without significant microbial activity, DOE had assumed that the brucite-calcite reaction would control carbon dioxide fugacity (DOE 2004b Appendix PA Attachment SOTERM). The Agency determined that DOE had not adequately supported the assumption that the brucite-calcite reaction would control carbon dioxide fugacities in the absence of significant microbial activity (EPA 2005b). However, because the microbial degradation probability was changed for the PABC so all vectors included microbial activity, it was appropriate to use the brucite-hydromagnesite reaction to buffer carbon dioxide fugacity in all actinide solubility calculations for the PABC (Brush 2005, Brush and Xiong 2005a).

The PABC FMT input and output files were reviewed to identify important actinide solid phases and aqueous speciation, and to ensure that the appropriate assumptions were included in the models. The results of the PABC solubility calculations with and without organic ligands for GWB and ERDA-6 brine are summarized in Table 7-4. Including organic ligands in the calculations resulted in the precipitation of whewellite and increased the predicted +III and +V actinide solubilities. The predicted thorium(IV) solubility did not change significantly in the presence of organic ligands because $Th(OH)_4(aq)$ and $Th(OH)_3CO_3^-$ were the only significant aqueous thorium species in the calculations with organic ligands for both GWB and ERDA-6 brine.

Significant americium(III) aqueous species included the hydrolysis species $AmOH^+$ and $Am(OH)_2^+$ and $AmEDTA^-$. The $AmEDTA^-$ species comprised a significant percentage of the dissolved americium(III) in both the GWB (45%) and ERDA-6 (64%) brine solubility calculations. Therefore, the presence of EDTA in the repository inventory has the potential to affect radionuclide releases, because it could affect the solubility of both plutonium(III) and americium(III), and radionuclide releases are predicted to be dominated by plutonium and americium (DOE 2004b, Appendix TRU WASTE).

Significant neptunium speciation in the two brines included carbonate complexes [$NpO_2CO_3^-$ and $NpO_2(CO_3)_2^{3-}$], the uncomplexed neptunium ion (NpO_2^+), the first hydrolysis species ($NpO_2OH(aq)$), and complexes with organic ligands ($NpO_2Ac(aq)$ and NpO_2Ox^-). The organic ligand complexes with neptunium constituted 33% of the aqueous neptunium calculated in the GWB solubility calculations and 27% of the aqueous neptunium in the ERDA-6 solubility calculations. However, because of the relatively small amounts of neptunium-237 in the repository, neptunium releases are not expected to significantly affect repository performance (EPA 2005b, DOE 2004b).

The actinide solubilities used in the CCA PA, PAVT, CRA PA and PABC are compared in Table 7-5. For calculations carried out with either the Salado and Castile brines, the modeled solubilities of the +III, +IV, and +V actinides were slightly higher for the PABC than for the PAVT. However, these differences in the calculated PAVT and PABC actinide solubilities are likely to be relatively unimportant because of the comparatively large uncertainties assigned to the actinide solubilities (see Section 7.5).

7.4.2 Uranium(VI) Solubility

Uranium is the only +VI actinide expected to be present in significant quantities in solution at equilibrium in the WIPP repository. For the CRA PA (DOE 2004b), DOE used the same estimated +VI actinide concentration that was used in the CCA PA and PAVT (Table 7-5). The Agency noted in their review of the CRA that DOE did not re-evaluate the +VI actinide solubility used in the CRA PA based on data that had become available since the CCA. The Agency requested additional information from DOE regarding relevant actinide solubility data developed outside the WIPP program since the CCA (EPA 2004b, Comment C-23-14). In their response, DOE cited data that were included in the FMT database for the +III, +IV, and +V actinides, but did not address the +VI actinides (DOE 2004d).

Because DOE did not address potential new information related to the solubility of the +VI actinides, the Agency reviewed the available literature to determine whether the assumed +VI actinide solubility should be revised (EPA 2005b). The Agency took into consideration the presence of low, but significant carbonate ion concentrations in the presence of the brucite-hydromagnesite buffer, as well as the uranium(VI) aqueous species and solid phases likely to form under WIPP repository conditions. Based on the results of this review, the Agency specified the use of a fixed upper-limit value of 10^{-3} M for the uranium(VI) concentration in the PABC (EPA 2005a and 2005b).

DOE stated that they have not developed a speciation and solubility model for calculating the solubility of uranium(VI) in the WIPP repository because of the complexity of uranium(VI) hydrolysis (DOE 2004b, Appendix PA Attachment SOTERM). However, DOE has apparently not considered the probability that carbonate complexes of uranium(VI) will dominate its aqueous speciation under expected WIPP chemical conditions. In addition, a study that provided estimated Pitzer parameters for uranium(VI) has been published since the PAVT (Plyasunov et al. 1998). DOE did not address whether these estimated Pitzer coefficients are sufficient for the development of an FMT solubility model or whether this type of approach could be used to develop a model for predicting uranium(VI) solubilities under WIPP conditions.

The uranium(VI) concentration specified as a fixed, upper-limit value for the PABC is higher than the upper limit of the uncertainty for the +VI actinide solubility used in the CCA PA, PAVT, and CRA PA. This conservative, higher upper limit was necessary because of the additional experimental data available in the literature since the PAVT and DOE's decision not to develop a solubility model for the +VI actinides. The Agency chose to specify a conservative, fixed value for uranium(VI) solubility of 10^{-3} M because it is difficult to provide a technical basis for an uncertainty range for a "reasonable" solubility estimate without additional data.

7.5 ACTINIDE SOLUBILITY UNCERTAINTIES

The uncertainty distribution assigned to the actinide solubilities and sampled in the CRA PA calculations was the same as the distribution developed for and used in the CCA PA and PAVT calculations (DOE 2004b). However, because the available solubility data and the FMT thermodynamic database had changed since the CCA PA and PAVT, the Agency requested that DOE re-evaluate the uncertainties associated with the actinide solubilities using the currently available information (EPA 2004b, Comment C-23-16). Xiong et al. 2004 evaluated the

uncertainties associated with the calculated actinide solubilities by comparing solubilities modeled with the FMT database FMT_040628.CHEMDAT and measured solubilities from published literature studies.

Xiong et al. 2004 and the Agency (EPA 2005b) noted that the available model and database significantly under-predicted the measured solubilities of the +IV actinides.

Consequently, Nowak 2005 re-evaluated the thermodynamic data for thorium(IV), which is used as an analogue for predicting the solubilities of all +IV actinides likely to be present in significant quantities in the WIPP inventory (see Section 7.1.1). Xiong et al. 2005 then updated the previous +IV actinide solubility uncertainty analysis using the thermodynamic database FMT_050405.CHEMDAT, which was the database version used for the PABC actinide solubility calculations (Table 7-1). The uncertainty analysis presented by Xiong et al. 2004 remained unchanged for the +III and +V actinides (Xiong et al. 2005).

7.5.1 Development and Implementation of Actinide Solubility Uncertainty Distributions

A single distribution was developed to represent the +III, +IV, and +V actinide solubility uncertainties for the CCA PA and PAVT (Bynum 1996, EPA 1998a). This distribution was developed by comparing measured actinide solubilities to curves fitted to the data using the code NONLIN, and a more limited number of comparisons of measured solubilities to solubilities calculated with FMT. Because of the limited available data, most of the data used in the determination were from studies of +III actinides and neodymium, with a smaller amount of +V data.

The revised approach taken by Xiong et al. 2004 and 2005 included the development of separate uncertainty distributions for the +III, +IV and +V actinide solubilities. Documented sources of measured solubilities were identified and data were selected for inclusion in the uncertainty analysis based on a set of criteria established by DOE (see Section 7.5.2). Solubilities were calculated using FMT for the conditions of the experiments. The differences (D) between the log values of the measured (S_M) and calculated (S_P) solubilities were determined using the equation:

$$D = \log_{10}(S_M) - \log_{10}(S_P)$$

A positive D value would indicate that the model-predicted solubility was less than the measured solubility, i.e., the model under-predicted the measured solubility. A negative D value would indicate that the model-predicted solubility was greater than the measured solubility, i.e., the model over-predicted the measured solubility.

The difference values were assembled into histograms within Microsoft® Excel spreadsheets, using an interval size of 0.15 for the accumulated D values. These histograms were then used to develop a cumulative distribution function (CDF), which describes the probability that a value of D is less than or equal to a specified interval value (Brush et al. 2005). The ranges established for each CDF are summarized in Table 7-6. For the PABC, only the CDFs for the +III and +IV actinide solubilities were sampled. The use of a single, fixed uranium(VI) value was specified by the Agency (see Section 7.4.2), so an uncertainty estimate was not needed. Neptunium is the only actinide expected to be present in the +V oxidation state at equilibrium in the WIPP

repository, and there will be insufficient neptunium present in the repository to affect performance regardless of its solubility. Therefore, the CDF for the +V actinides was not sampled for the PABC (Brush et al. 2005, Garner and Leigh 2005).

The +III and +IV actinide solubilities calculated using FMT for Salado or Castile brine (Table 7-5) were multiplied by the antilog of the corresponding sampled uncertainty value. For sampled values greater than 0, the calculated solubility would be increased; for sampled values less than 0, the calculated solubility would be decreased.

7.5.2 Data Selection Criteria for Actinide Solubility Uncertainty Analysis

During their review of the Xiong et al. 2004 revised uncertainty estimates, the Agency did not find a clear explanation of how available experimental data were identified and then either included or excluded from the uncertainty analysis. Clarification was therefore requested from DOE regarding the process used to select data for the actinide solubility uncertainty analysis (EPA 2005d). The Agency also identified several studies available in the open literature that were not included in the analysis (e.g., Altmaier et al. 2004, Rai et al. 1997) and requested the reasoning behind their exclusion.

In response to the Agency's request, DOE provided information regarding the data selection process for the actinide solubility uncertainty distribution (DOE 2005). The approach included:

- Data from open literature sources and unpublished reports were considered.

- Measured solubilities used to establish the range and distribution of actinide solubility uncertainties for the CCA PA were included in the analysis. Some of these data were used to generate the FMT database for the CCA PA.

- Data used in the CCA PA uncertainty analysis were not included if a comparison with the NONLIN fits used to obtain the Pitzer ion-interaction parameters was used to establish an uncertainty value. DOE noted that this constituted a significant fraction of the comparisons used to establish an uncertainty range and distribution for actinide solubilities for the CCA PA.

- Reported experimental solubility data available since the CCA PA were included if the existing FMT database can be used to model the experimental conditions.

- Measured solubility data that were used to develop or revise the FMT +III, +IV, and +V actinide solubility models were excluded, except for the data used to develop the CCA PA uncertainty ranges and distributions. This exclusion was meant to provide a more rigorous test of the model against independent data.

The decision to exclude data used to develop the FMT database seems appropriate based on DOE's stated goal, which was to provide a more rigorous test of the model against independent data. This decision would seem likely to maximize the number of values at the extremes of the uncertainties ranges for the PABC actinide solubilities.

7.5.3 Review of Data Selection Process for Uncertainty Evaluation

DOE's implementation of the selection criteria in Section 7.5.2 was reviewed by the Agency. Xiong et al. 2004 and 2005 provided a list of the solubility data sources used in the uncertainty analysis and histograms of the frequency distributions of the differences between the measured and modeled solubilities. However, the actual measured and modeled solubilities used in the analysis were not provided. The Agency requested this information as well as the relevant FMT input and output files from DOE (EPA 2005d). In response, DOE provided the Microsoft® Excel files used in the analyses by Xiong et al. 2004 and 2005, the FMT input files, and the FMT output files from DOE (DOE 2005). The Excel files included the measured and predicted actinide solubilities used in the evaluations as well as the histograms developed from the data.

The experimental studies used in the actinide solubility uncertainty evaluation are listed in Table 7-7. Xiong et al. 2005 indicated in their Table 2 that the data from Rao et al. 1999 and Al Mahamid et al. 1998 were included in the Bynum 1996 uncertainty evaluation. Because of the publication dates, it must be assumed that these data were available in unpublished form at the time of the Bynum 1996 evaluation.

According to DOE's criteria for data selection, studies used to develop the FMT database that were not included in the CCA determination of actinide solubility uncertainty should not have been used in the current evaluation. However, data from the Felmy et al. 1991 and Novak et al. 1997 investigations were included in the current evaluation, which is an apparent contradiction of DOE's stated criteria. Inclusion of the Felmy et al. 1991 solubility data for ThO_2(am) was difficult to avoid because of the limited high-ionic-strength solubility data identified by DOE for the +IV actinides. There is no obvious explanation for the inclusion of the Novak et al. 1997 data in the evaluation. However, because these data only affected the +V solubility uncertainty distribution and this distribution was not sampled for the PABC, its inclusion had no effect on the PA results.

Xiong et al. 2005 excluded data used to develop the FMT database because they believed that comparing predicted solubilities to independent measured solubilities would result in a more rigorous test. The underlying assumption is that data used to develop the FMT database would closely correspond to the predicted values and result in uncertainty distributions that were weighted toward difference values (D) of 0. One way in which this assumption can be evaluated is by examining the D values calculated for studies used in FMT database development (FMT_050405.CHEMDAT) and also included in the uncertainty evaluation. These studies are Felmy et al. 1991, Al Mahamid et al. 1998, and Novak et al. 1997.

For example, the distribution of D values for the Felmy et al. 1991 ThO_2(am) data is illustrated in Figure 7-1. Even though the thermodynamic data for ThO_2(am) in FMT_050405.CHEMDAT were derived from this study, the range of difference values was relatively large, with D values that ranged from -1.75 to 2.39. The distribution is weighted somewhat toward positive D values, indicating that the model tended to more often underpredict measured solubilities. This example indicates that using data included in the development of the thermodynamic database may not result in a solubility uncertainty distribution that is closely grouped or symmetric around D values of zero. Therefore, in future determinations of actinide solubility uncertainty distributions, it would be advisable to include all available data, even if it was used to develop

the FMT thermodynamic database. However, the distributions developed by DOE for the PABC appear to be fairly broad and provide a wide range of variability about the +III and +IV actinide solubilities, which are the important actinide oxidation states for PA. Therefore, the exclusion of some of the available data from the uncertainty analysis is unlikely to have significantly affected the results.

The Agency requested information from DOE regarding the exclusion from the uncertainty evaluation of several published studies that appeared to include relevant solubility data (EPA 2005d). DOE (DOE 2005) responded that Rai et al. 1997 data were used in database development so were excluded on that basis. Thorium(IV) solubilities reported by Xia et al. 2003 for nitrate solutions with EDTA were not included because of the lack of necessary Pitzer parameters for nitrate aqueous species. Xiong et al. 2005 also did not include thorium(IV) solubility data from Rai et al. 2003 or americium(III) solubility data from Rai et al. 1992, because Pitzer parameters for all important phosphate aqueous species are not included in the FMT database. DOE (DOE 2005) compared predicted ThO_2(am) solubilities to solubilities measured by Altmaier et al. 2004 after ultracentrifugation of 5.0 M NaCl and 2.5 M $MgCl_2$ solutions containing thorium(IV) colloids; the results indicated that the predicted values always exceeded the measured values, resulting in negative D values. Therefore, omission of these data from the determination of +IV actinide solubility uncertainties likely resulted in the more frequent use of higher thorium(IV) concentrations in the PABC calculations.

Although not cited in the Agency's recent communications with DOE regarding the actinide solubility uncertainty determination (EPA 2005d), the Agency previously observed that $Pu(OH)_3$(am) solubility data for brines by Felmy et al. 1989 was omitted from the CCA PA actinide solubility uncertainty evaluation (EPA 1998a). This study was also omitted from the revised evaluation carried out by Xiong et al. 2005. Because of the limited available data for the uncertainty analysis, inclusion of these data probably should have been considered by DOE.

As a check on DOE's thoroughness in identifying relevant studies of actinide solubilities, a recent review of thermodynamic data for uranium, plutonium, americium, and thorium (NEA 2003) was examined for solubility data at high ionic strength. Potentially useful solubility data for $NaNpO_2CO_3 \bullet 3.5H_2O$ (Neck et al. 1994a and 1994b, Neck et al. 1995b, Runde et al. 1996) obtained in high-ionic-strength NaCl solutions were identified in this review. However, the FMT thermodynamic data for $NaNpO_2CO_3 \bullet 3.5H_2O$ is reported in Giambalvo 2002b to be from Neck et al. 1995a; this study has common authors with Neck et al. 1994a and 1994b, and Neck et al. 1995b, and is likely to be the same data. However, the data in Runde et al. 1996 may be relevant solubility data that were overlooked by DOE. Two studies (Rai et al. 1995 and Felmy et al. 1997) provide solubility data for thorium(IV) and uranium(IV) hydrous oxides under alkaline, high-ionic-strength conditions, but were not included in the Xiong et al. 2005 evaluation. Solubility data were also reported by Giffaut (1994) for $AmOHCO_3$(s), as reported by NEA 2003, but these data were not included in DOE's actinide solubility uncertainty evaluation. The data may have been excluded from the actinide solubility uncertainty analysis for valid reasons, but Xiong et al. 2005 did not provide an explanation for their omission. Because of the limited actinide solubility data available in high ionic strength solutions, future efforts to develop solubility uncertainty distributions should include all available data. Evaluation of data cited by NEA 2003 and any future updates would be useful in maximizing the amount of data used to develop future actinide solubility uncertainty distributions.

7.5.4 Effects of Ionic Strength on the Accuracy of ThO_2(am) Solubility Predictions

Xiong et al. 2005 used 3 M NaCl data from Felmy et al. 1991 to evaluate the uncertainty associated with the +IV actinide solubilities. Available solubility data at lower ionic strengths were omitted to avoid biasing the uncertainty range toward negative values, which would result in more frequent use of lower +IV actinide solubilities in PA. DOE attributed the discrepancies between the measured and predicted solubilities at low ionic strength to the use of only high-ionic-strength data in the development of Pitzer and other parameters in the solubility model. The Agency (EPA 2005d) asked whether the inaccuracy of the thermodynamic model at low ionic strength might indicate potential problems with predicting +IV actinide solubilities at the higher ionic strengths of the WIPP brines, which may range up to 8 m (DOE 2004b, Appendix PA Attachment SOTERM). DOE responded that thorium solubility data from ionic strengths greater than 3 M are available, including data from Altmaier et al. 2004 and Rai et al. 1997. DOE did not provide the predicted solubilities for the Rai et al. 1997 data. DOE did provide predicted solubilities for the data reported by Altmaier et al. 2004 that indicated that the +IV actinide solubility model consistently over-predicted the measured solubilities. Based on the available data, it appears that the current FMT model is reasonably reliable for predicting +IV actinide solubilities at the ionic strengths of WIPP brines. However, the consistent over-prediction of the measured +IV actinide solubilities indicates that the model could be improved for future PA calculations.

7.5.5 Summary of Revised Actinide Solubility Uncertainty Evaluation

The overall approach used in the PABC for estimating the uncertainties associated with the actinide solubilities is a substantial improvement over the approach used for the CCA PA and PAVT. The use of a larger data set and the determination of separate uncertainty distributions for the +III, +IV, and +V actinide solubilities in the PABC are more likely to provide reasonable estimates of the uncertainties than the approach taken for the CCA PA, PAVT, and CRA PA.

However, the approach of Xiong et al. 2004 and 2005 for selecting the data for the evaluation may not have included all available experimental data. In addition, a number of inconsistencies appear to have occurred because of the inclusion of data used to develop the FMT database in some cases and its exclusion in others. Comparison of the separate PABC uncertainty distributions developed for the three modeled actinide oxidation states (Figures 7-1, 7-3, and 7-4) with the single uncertainty distribution used in the CCA PA, PAVT, and CRA PA (Figure 7-2) shows that the revised ranges are generally wider, particularly on the upper end of the distributions. Therefore, it is likely that the changes to the actinide solubility uncertainty distributions will result in the more frequent use of actinide solubilities in PA that are higher than the solubilities calculated using the FMT model, because the distributions extend from 2 to 3 orders of magnitude above the model-calculated values (Figures 7-1, 7-3, and 7-4). The larger amount of experimental data used to develop the distributions, the development of uncertainty distributions for each of the modeled oxidation states, and the large ranges developed for the uncertainties indicate that these uncertainty distributions are reasonable and acceptable for use in the PABC.

7.6 COLLOIDAL SOURCE TERM

The PAVT included microbial colloid transport of actinides for all vectors. The CRA PA included different assumptions about the colloidal source term concentrations for microbial and non-microbial vectors, with no microbial colloid transport of actinides assumed for non-microbial vectors. However, for the PABC, it was assumed that all vectors included microbial activity. Therefore, DOE included microbial colloid transport of actinides for all PABC vectors (Brush 2005). This approach therefore was the same for the PAVT and PABC, and was consistent with the Agency's direction that all vectors include microbial activity.

7.7 EFFECTS OF ACTINIDE SOLUBILITY CHANGES ON PABC RESULTS

DOE used the revised calculated +III, +IV and +V concentrations and the revised estimated uranium(VI) concentration of 10^{-3} M in the PABC (Brush 2005, Leigh et al. 2005a). Leigh et al. 2005a compared the total radionuclide source term for the CRA PA and PABC, which includes both dissolved and colloidal radionuclides. The concentrations of mobilized radionuclides were higher for the PABC than for the CRA PA. These changes were attributed to increased actinide solubilities and solubility uncertainties used for the PABC. The mean CCDF for radionuclide releases through direct brine release (DBR) was greater for the PABC than for the CRA PA, probably as a consequence of higher actinide solubilities and solubility uncertainties for the PABC (Leigh et al. 2005a). Consequently for the PABC, DBR replaced spallings as the second-most important release mechanism at higher probabilities, behind cuttings and cavings (Leigh et al. 2005a). At low probabilities for the PABC, DBR became the most important release mechanism.

7.8 CONCLUSIONS REGARDING PABC ACTINIDE SOLUBILITIES

Changes and improvements incorporated into the calculation of actinide solubilities for the PABC that have been implemented since the PAVT include:

- Incorporation of organic ligand complexation data into the FMT thermodynamic database so the effects of organic ligands on +III, +IV, and +V actinide solubilities can be calculated directly
- Refinement of the thermodynamic database using new +III, +IV, and +V actinide data
- Use of GWB instead of Brine A as the Salado Brine formulation for actinide solubility calculations
- Correction of the minimum brine volume necessary for direct brine release
- Revision of the estimated uranium(VI) solubility to account for new data
- Recalculation of actinide solubility uncertainties based on a much larger number of solubility measurements, with separate distributions developed for the +III, +IV, and +V actinide solubilities instead of the single distribution used for the PAVT

As a result of these changes and improvements, the calculated +III, +IV, and +V actinide solubilities were slightly higher than the solubilities calculated for the PAVT (Table 7-5). The uncertainties associated with these solubilities were also greater than the single uncertainty distribution used in the PAVT. The results of the calculations also indicated that organic ligands could significantly affect actinide solubilities, particularly EDTA complexation of the +III actinides. As a consequence of the higher calculated solubilities and associated uncertainties, the importance of DBR to total releases was increased in the PABC compared to the CRA PA and the PAVT. However, cuttings and cavings releases continued to dominate total radionuclide releases, except at low probabilities (Leigh et al. 2005a).

Although the actinide solubility calculations carried out for the PABC were significantly improved over the calculations for the PAVT, some areas of uncertainty remain. The uranium(VI) solubility specified for use in the PABC was a relatively high, fixed value because of the limited solubility data available for WIPP-relevant conditions and because DOE has not developed a solubility model for the +VI actinides. DOE should obtain additional data related to the likely solubility of uranium(VI) in WIPP brines and should use these data to develop a thermodynamic solubility model. The relatively large uncertainty associated with +IV actinide solubilities, even though the uncertainty was determined using data used in the development of the FMT database, indicates that the +IV actinide solubility model could be improved for future PA calculations. Finally, a more thorough and systematic approach should be implemented for identifying and selecting data for development of the actinide solubility uncertainties for future WIPP PAs.

Table 7-1. FMT Database Versions

Database Version	Analysis
FMT_970407.CHEMDAT	PAVT (HMW_970407_HMAG5424.CHEMDAT in EPA 1998a)
FMT_021120.CHEMDAT	CRA PA (DOE 2004b)
FMT_040628.CHEMDAT	Actinide solubility uncertainty evaluation (Xiong et al. 2004)
FMT_041210.CHEMDAT	Ligands sensitivity evaluation (Brush and Xiong 2004)
FMT_050405.CHEMDAT	Revised actinide solubility uncertainty evaluation (Xiong et al. 2005) and PABC (Brush 2005)

Table 7-2. Organic Ligand Concentrations Predicted at the Time of the PAVT and the Concentrations Used in the CRA PA and PABC Actinide Solubility Calculations
(Brush and Xiong 2005b)

Organic Ligand	PAVT Concentration (M)	CRA PA Concentration (M)	PABC Concentration (M)
Acetate	1.1×10^{-3}	5.05×10^{-3}	1.06×10^{-2}
Citrate	7.4×10^{-3}	3.83×10^{-4}	8.06×10^{-4}
EDTA	4.2×10^{-6}	3.87×10^{-6}	8.14×10^{-6}
Oxalate	4.7×10^{-4}	2.16×10^{-2}	4.55×10^{-2}

Table 7-3. Actinide Solubilities with Organic Ligands Calculated for the PABC Using Salado Brine Formulations Brine A and GWB
(Brush 2005)

Brine	Brine A	GWB
Americium(III) (M)	5.459×10^{-7}	3.873×10^{-7}
Thorium(IV) (M)	5.579×10^{-8}	5.640×10^{-8}
Neptunium(V) (M)	1.822×10^{-7}	3.545×10^{-7}

Table 7-4. PABC Actinide Solubility Modeling Results With and Without Organic Ligands

Brine	GWB		ERDA-6	
	With Ligands	Without Ligands	With Ligands	Without Ligands
pH (standard units)	8.69	8.69	8.94	9.02
Ionic Strength	7.66	7.54	6.80	6.72
Carbon dioxide fugacity (atm)	3.135×10^{-6}	3.135×10^{-6}	3.135×10^{-6}	3.135×10^{-6}
Total Carbon (M)	3.497×10^{-4}	3.506×10^{-4}	4.275×10^{-4}	4.709×10^{-4}
Sulfate (M)	0.2285	0.1824	0.1788	0.1679
Chloride (M)	5.379	5.440	5.240	5.255
Sodium (M)	4.347	4.345	5.243	5.325
Calcium (M)	8.948×10^{-3}	0.01078	0.01073	0.01129
Magnesium (M)	0.5778	0.5535	0.1572	0.1060
Acetate (M)	0.01134	0.00	0.01050	0.00
Citrate (M)	8.622×10^{-4}	0.00	7.986×10^{-4}	0.00
EDTA (M)	8.708×10^{-6}	0.00	8.065×10^{-6}	0.00
Oxalate (M)	1.364×10^{-3}	0.00	2.964×10^{-4}	0.00
Americium(III) (M)	3.873×10^{-7}	2.264×10^{-7}	2.878×10^{-7}	8.667×10^{-8}
Thorium(IV) (M)	5.640×10^{-8}	5.659×10^{-8}	6.791×10^{-8}	7.196×10^{-8}
Neptunium(V) (M)	3.545×10^{-7}	2.357×10^{-7}	8.244×10^{-7}	5.379×10^{-7}
Solid Phases	Anhydrite, halite, brucite, $Mg_2Cl(OH)_3 \bullet 4H_2O$, ThO_2(am), $KNpO_2CO_3$(s), $Am(OH)_3$(s), hydromagnesite$_{5424}$, whewellite	Anhydrite, halite, brucite, $Mg_2Cl(OH)_3 \bullet 4H_2O$, ThO_2(am), $KNpO_2CO_3$(s), $Am(OH)_3$(s), hydromagnesite$_{5424}$	Anhydrite, halite, brucite, ThO_2(am), $KNpO_2CO_3$(s), $Am(OH)_3$(s), hydromagnesite$_{5424}$, whewellite, glauberite	Anhydrite, halite, brucite, ThO_2(am), $KNpO_2CO_3$(s), $Am(OH)_3$(s), hydromagnesite$_{5424}$
Output File Name	FMT_CRA1BC_007_GWB_HMAG_ORGS.OUT	FMT_CRA1BC_008_GWB_HMAG_NOORGS.OUT	FMT_CRA1BC_011_ER6_HMAG_ORGS.OUT	FMT_CRA1BC_012_ER6_HMAG_ORGS.OUT

Table 7-5. Results of FMT Modeling of Actinide Solubilities

Property or Actinide Oxidation State	PABC All Vectors, With Organic Ligands		CRA Microbial Vectors, With Organic Ligands		PAVT All Vectors, No Organic Ligands		CCA All Vectors, No Organic Ligands	
Brine	Salado (GWB)	Castile	Salado (GWB)	Castile	Salado (Brine A)	Castile	Salado (Brine A)	Castile
pH	8.69	8.94	8.69	9.02	8.69	9.24	8.69	9.24
pcH	9.39	9.64	9.40	9.72	--	--	--	--
Log carbon dioxide fugacity	-5.50	-5.50	-5.50	-5.50	-5.50	-5.50	-6.90	-6.90
Carbonate ion (M)	2.16×10^{-5}	5.18×10^{-5}	2.16×10^{-5}	6.88×10^{-5}	--	--	--	--
III (M)	3.87×10^{-7}	2.88×10^{-7}	3.07×10^{-7}	1.69×10^{-7}	1.2×10^{-7}	1.3×10^{-8}	5.82×10^{-7}	1.3×10^{-8}
IV (M)	5.64×10^{-8}	6.79×10^{-8}	1.19×10^{-8}	2.47×10^{-8}	1.3×10^{-8}	4.1×10^{-8}	4.4×10^{-6}	6.0×10^{-9}
V (M)	3.55×10^{-7}	8.24×10^{-7}	1.02×10^{-6}	5.08×10^{-6}	2.4×10^{-7}	4.8×10^{-7}	2.3×10^{-6}	2.2×10^{-6}
VI (M) [1]	10^{-3}	10^{-3}	8.7×10^{-6}	8.8×10^{-6}	8.7×10^{-6}	8.8×10^{-6}	8.7×10^{-6}	8.8×10^{-6}
Equilibrium Nonradioactive Solid Phases	anhydrite, halite, brucite, hydromagnesite, [2] whewellite, $Mg_2Cl(OH)_3 \bullet 4H_2O$	anhydrite, halite, brucite, hydromagnesite, whewellite, glauberite	anhydrite, halite, brucite, hydromagnesite, $Mg_2Cl(OH)_3 \bullet 4H_2O$	anhydrite, halite, brucite, hydromagnesite	anhydrite, halite, brucite, hydromagnesite, $Mg_2Cl(OH)_3 \bullet 4H_2O(s)$	anhydrite, halite, brucite, glauberite, hydromagnesite	anhydrite, halite, magnesite, brucite, $Mg_2Cl(OH)_3 \bullet 4H_2O$	anhydrite, halite, magnesite brucite, glauberite,
Equilibrium Radioactive Solid Phases	$Am(OH)_3(s)$, $ThO_2(am)$, $KNpO_2CO_3(s)$,		$Am(OH)_3(s)$, $ThO_2(am)$, $KNpO_2CO_3(s)$		$AmOHCO_3(s)$, $ThO_2(am)$, $KNpO_2CO_3(s)$		$Am(OH)_3(s)$, $ThO_2(am)$, $KNpO_2CO_3(s)$	

[1] DOE did not develop a solubility model for the +VI actinides. Therefore, for the CCA PA, PAVT, CRA PA, and PABC, a fixed concentration was assumed for uranium(VI), which is the only +VI actinide predicted to be present in the WIPP repository in significant concentrations.

[2] Hydromagnesite of composition $Mg_5(CO_3)_4(OH)_2 \bullet 4H_2O(s)$ was used in the PAVT, CRA PA, and PABC solubility calculations. This hydromagnesite composition was referred to by DOE 2004b as hydromagnesite$_{5424}$.

Table 7-6. CDF Ranges Established by the Revised Actinide Solubility Uncertainty Analysis
(Xiong et al. 2005)

Actinide Oxidation State	CDF Range
III	-3.00 to 2.85
IV	-1.80 to 2.40
V	-1.95 to 1.95

[1] At the lower end of the range, there is a zero probability that a D value is less than or equal to this number; at the upper end of the range, the probability is equal to one because all D values were less than or equal to this number (Brush et al. 2005).

Table 7-7. Studies Used in Actinide Solubility Uncertainty Determination

Oxidation State	Solid Phase	Study	Study Cited Within FMT_050405.CHEMDAT?	Used in CCA PA Uncertainty Determination? [1]
+III	$Nd(OH)_3(am)$	Khalili et al. 1994	No	No
+III	$NaNd(CO_3)_2 \cdot 6H_2O$	Rao et al. 1999	No	Yes
+III	$Am(OH)_3(c)$ or $NaAm(CO_3) \cdot xH_2O$	Runde and Kim 1995	No	Yes
+III	$Am(OH)_3(c)$	Silva 1982	No	Yes
+III	$Nd(OH)_3(c)$	Silva 1982	No	No
+IV	$ThO_2(am)$	Felmy et al. 1991	Yes	No
+V	$KNpO_2CO_3(c)$	Al Mahamid et al. 1998	Yes	Yes
+V	$KNpO_2CO_3(c)$	Novak et al. 1996	No	No
+V	$K_3NpO_2(CO_3)_2$	Novak et al. 1997	Yes	No
+V	$NaNpO_2CO_3 \cdot xH_2O(c)$	Runde and Kim 1995	No	No

[1] As indicated in Table 2 of Xiong et al. 2005.

[2] Studies used in the development of FMT_050405.CHEMDAT that were not used in the CCA PA uncertainty determination should not have been included in the PABC uncertainty determination, according to DOE's stated criteria, i.e., Felmy et al. 1991 and Novak et al. 1997.

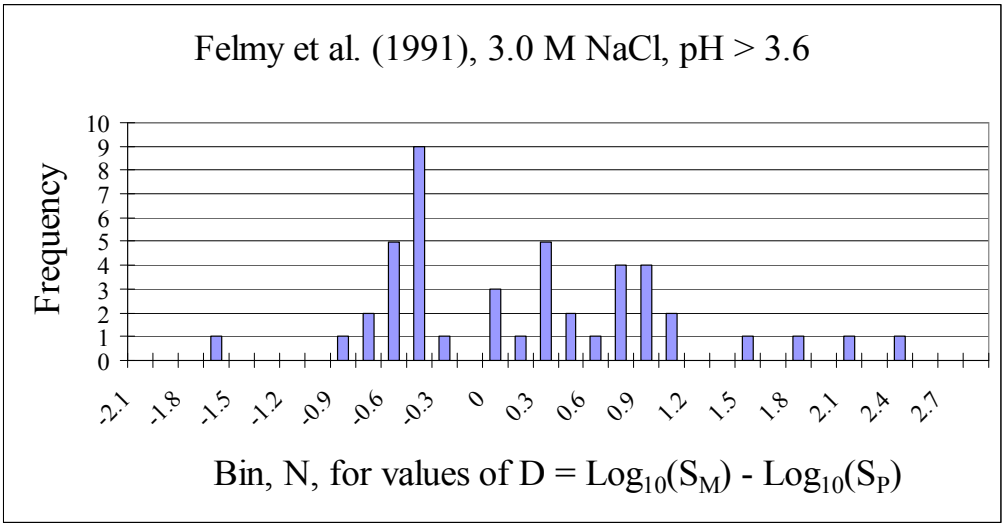

Figure 7-1. Felmy et al. 1991 ThO_2(am) Solubility Data Difference Value Histogram
(Source: ASTP.2005.04A_Xiong et al, An Sol Unc, Rev 1, Spreads, 2 of 2.xls)
This distribution was used to develop the +IV actinide solubility uncertainty for the PABC.

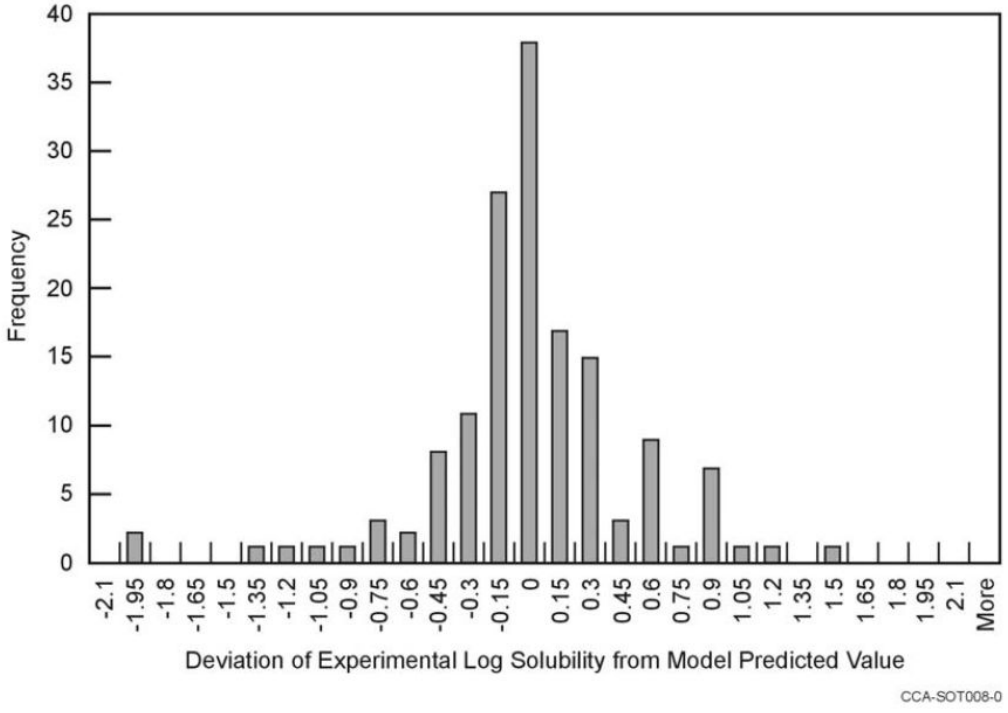

Figure 7-2. Uncertainty Distribution Used in the CCA PA and PAVT
(Source: DOE 2004b, Appendix PA, Attachment SOTERM)

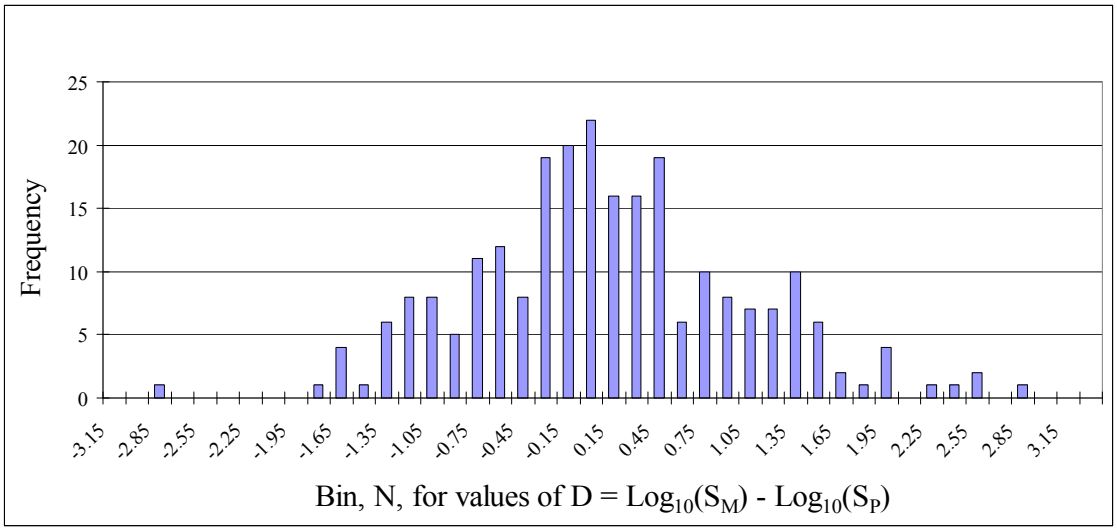

Figure 7-3. Uncertainty Distribution Developed for +III Actinide Solubilities
(Source: ASTP.2005.04A_Xiong et al, An Sol Unc, Rev 1, Spreads, 1 of 2.xls)

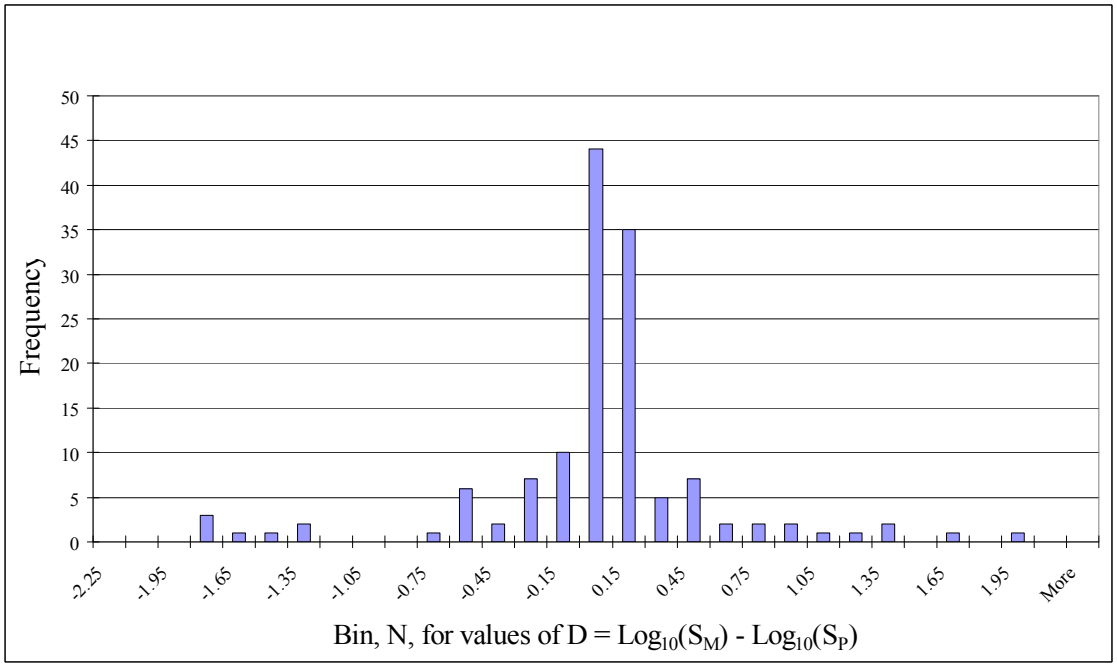

Figure 7-4. Uncertainty Distribution Developed for +V Actinide Solubilities
(Source: ASTP.2005.04A_Xiong et al, An Sol Unc, Rev 1, Spreads, 1 of 2.xls)

8.0 CULEBRA FLOW AND TRANSPORT

8.1 INTRODUCTION

In the PAVT, CRA and PABC the Culebra member of the Rustler Formation is conceptualized as a horizontal, confined aquifer of uniform density. For fluid flow, the Culebra is assumed to be a heterogeneous porous medium with spatially varying transmissivity (T). A heterogeneous velocity field is also assumed to be used for radionuclide transport, but all other rock properties are conceptualized as constant (homogeneous) across the model area. The Culebra is conceptualized as having two types of porosity; a portion of the porosity is associated with high-permeability features where transport occurs by advection, and the rest of the porosity is associated with low-permeability features where flow does not occur and retardation occurs by physical processes (diffusion) and chemical processes (sorption). This type of conceptual model is commonly referred to as double-porosity.

The key factors controlling fluid flow in the Culebra are the hydraulic gradient, transmissivity distribution, and porosity. In the Culebra conceptual model, the spatial distribution of transmissivity is important. The hydraulic gradient and transmissivities used in performance assessment are coupled because they are calibrated to observed conditions. It is possible that radionuclides might be introduced into the Culebra through brine leakage around shaft seals. However, the chief source of actinides in the Culebra is long-term releases from an inadvertent intrusion borehole that intersects the repository. If radionuclides are introduced into the Culebra, they may be transported from the point of introduction by groundwater flowing naturally through the Culebra.

In the PAVT, radionuclide transport in the Culebra was modeled by the following steps:

(1) Constructing conditioned geostatistical realizations of Culebra hydraulic transmissivity fields (T fields)

(2) Modifying the T fields to account for potential subsidence due to potash mining in formations beneath the Culebra

(3) Calculating steady state groundwater flow fields for each mining-modified T field

(4) Calculating radionuclide transport through the Culebra for each flow field

Culebra transport simulations calculate the cumulative discharge at the land withdrawal boundary over the 10,000-year regulatory period due to a source located at the center of the waste panel area. With the exception of several modifications made to SECOTP2D, as discussed in the next section, there have been essentially no changes made to the basic approach used for calculating transport through the Culebra since the PAVT. Furthermore, the Culebra transport conceptual model has not changed.

The transmissivity of the Culebra has been measured at a relatively large number of locations (Docket: A-93-02, II-G-1, Ref. #43 [SNL 1987]). Measured transmissivity values vary spatially

over several orders of magnitude, trending from lower values east of WIPP to higher values west of WIPP (*ibid.*). In the PAVT the spatial variations in transmissivity were implemented by numerically generating realizations conditioned on observed hydraulic head and transmissivity values using the pilot point technique (Docket: A-93-02, II-G-1, Ref. #390 [SNL 1992]). Multiple realizations were generated and sampled to address the uncertainty associated with the transmissivity field measurements. Except for the mining scenarios, transmissivity was assumed to be constant over time. A number of significant changes have been made since the PAVT with respect to the calculation of the transmissivity fields and are presented in the sections that follow.

8.2 MODIFICATIONS SINCE PAVT

8.2.1 Computer Codes

In the PAVT three computer codes were used to model flow and transport in the Culebra: GRASP_INV, SECOFL2D, and SECOTP2D (EPA 1998b). The mathematical model equations that comprise GRASP_INV are based on spatial correlations designed to predict the Culebra dolomite transmissivity fields (T fields) that impact the rates at which radionuclides migrate through this stratum (Docket: A-93-02, II-G-1, Volume XVII, Appendix TFIELD, Section TFIELD 3). For the PAVT, the results of the GRASP_INV calculations were used as input to the SECOFL2D computer code. The primary mathematical model equations incorporated into SECOFL2D describe advective (rock matrix) groundwater flow through the Culebra dolomite in two dimensions, using the releases predicted by the BRAGFLO, NUTS, and PANEL computer codes. SECOTP2D extends the mathematical model equations of SECOFL2D to calculate the transport of contaminants through the Culebra dolomite and to calculate radioactive decay, dispersion, and molecular diffusion.

Since the PAVT, the SECOFL2D code has been replaced with MODFLOW-2000. MODFLOW-2000 and SECOTP2D are now the computer codes used to simulate groundwater flow and radionuclide transport in the Culebra. Although the SECOTP2D code was used for the PAVT, CRA, and PABC analyses, it has undergone a series of revisions. SECOTP2D Version 1.30 was used in the WIPP PAVT. SECOTP2D 1.30 was validated in April 1996 on a DEC Alpha 2100 with the OpenVMS 6.1 operating system by demonstrating that the results of three test cases met the acceptance criteria defined in the RD/VVP for SECOTP2D 1.30. In 1997, SECOTP2D was revised to Version 1.41 and was validated on a DEC Alpha 2100 with OpenVMS 6.1 by demonstrating that the results of six new test cases met the acceptance criteria defined in the RD/VVP for SECOTP2D 1.4. Both SECOTP2D and MODFLOW-2000 have been evaluated by EPA and found to be acceptable (EPA 1998b, EPA 2004e).

8.2.2 Development of Transmissivity Fields

The starting point in the T field development process was to assemble information on geologic factors that might affect Culebra transmissivity. These factors include dissolution of the upper Salado Formation, the thickness of overburden above the Culebra, and the spatial distribution of halite in the Rustler Formation above and below the Culebra. DOE then applied a two-part "geologically based" approach to generate Culebra base T fields. In the first part, a conceptual model for geologic controls on Culebra T was formalized, and the hypothesized geologic

controls were regressed against Culebra T data to determine linear regression coefficients. The regression includes one continuously varying function, Culebra overburden thickness, and three indicator functions that assume values of 0 or 1 depending on the occurrence of open, interconnected fractures, Salado dissolution, and the presence or absence of halite in units bounding the Culebra.

In the second part, a method was developed for applying the linear regression model to predict Culebra T across the WIPP area. The regression model was combined with the maps of geologic factors to create 500 stochastically varying Culebra base T fields. Relevant aspects of these analyses are presented below.

Development of Geologic Model

Significant changes have been made to the T field development since the PAVT. In the PAVT the computer code GRASP_INV relied solely upon measured transmissivities and water levels to predict the T fields. DOE's most recent approach, however, incorporates geologic information that affects the transmissivity. These factors include dissolution of the upper Salado Formation, the thickness of overburden above the Culebra, and the spatial distribution of halite in the Rustler Formation above and below the Culebra. DOE obtained this geologic information from hundreds of oil and gas wells and potash exploration holes in the vicinity of the WIPP site.

DOE hypothesizes that Culebra transmissivity is inversely related to thickness of overburden because stress relief associated with erosion of overburden leads to fracturing and opening of preexisting fractures. Culebra transmissivity is observed to be high where dissolution of the upper Salado has occurred and the Culebra has subsided and fractured. Culebra transmissivity tends to be low where halite is present in overlying and/or underlying mudstones. DOE has assumed that high Culebra transmissivity leads to dissolution of nearby halite (if any). From this assumption, DOE concludes that the presence of halite in mudstones above and/or below the Culebra can be taken as an indicator for low Culebra transmissivity. Based upon the distribution of measured values of transmissivity in relation to overburden maps, the Agency believes that DOE's assumptions are reasonable.

In AP-088 (Beauheim 2002a), DOE developed maps for each of these factors using drillhole data of different types. The thickness of the overburden (Factor A) is represented by a contour map. The reduction in thickness of the upper Salado Formation by dissolution (Factor B) is depicted on a map as an approximate margin of the area beginning to be affected by the dissolution of the upper Salado. The spatial distribution of halite in the Rustler Formation below and above the Culebra (Factor C) is delineated on a map by lines that represent the boundary of the distribution of halite in the Los Medaños, Tamarisk, and Forty-niner Members of the Rustler Formation.

The general area for the geologic study comprised 12 townships, located in townships T21S to T24S, ranges R30-32E (the WIPP site lies in T22S, R31E). The original sources of geologic data for this analysis are mainly Powers and Holt 1995 and Holt and Powers 1988 and new information derived from drilling log interpretation by Powers 2003.

Relationship of Transmissivity to Geologic Properties

Holt and Powers (1988), Powers and Holt (1990), Beauheim and Holt (1990), and Holt (1997) have described the geology and geologic history of the Culebra. DOE developed several geologically based relationships from this work by assuming that variability in transmissivity is due strictly to post-depositional processes. The Agency has also reviewed this work and has concluded that the majority of the existing evidence (e.g., post-depositional precipitation of gypsum within the Culebra) supports DOE's conclusion.

As discussed above, DOE has assumed that the spatial distribution of transmissivity on a regional scale is a function of a series of deterministic geologic controls, including Culebra overburden thickness, dissolution of the upper Salado Formation, and the occurrence of halite in units above or below the Culebra. Geologic maps were developed to determine these controls at any location. In the region between the margin of upper Salado dissolution and the margin of halite occurrence above the Culebra, which includes the WIPP site, however, high-T regions occur that cannot be predicted using geologic data. This is because no geologic metric has yet been defined that allows prediction of where fractures are filled or open, and therefore knowledge of this indicator east of the Salado dissolution margin is limited to the test well locations. DOE treats these high transmissivity zones stochastically.

The second major step in the development of the T field involved regression of the three hypothesized geologic controls against Culebra transmissivity data to determine linear regression coefficients. The regression includes one continuously varying function, Culebra overburden thickness, and three indicator functions that assume values of 0 or 1 depending on the occurrence of open, interconnected fractures, Salado dissolution, and the presence or absence of halite in units bounding the Culebra.

The fracture interconnection relationship is based on a bi-modal assumption of Culebra transmissivity which is correlated to the degree that the fractures are filled with gypsum. The Agency believes that this assumption is reasonable based upon work conducted by Beauheim and Ruskauff 1998 and Holt 1997. Other major assumptions in DOE's regression analysis (e.g., an inverse relationship exists between Culebra overburden thickness and T) also appear to provide a reasonable means to establish correlations from which the transmissivity can be estimated.

Once the correlations were established, DOE developed a linear-regression model using the Windows-based program Mathcad 7 Professional. Although other variables are input, this model requires only $\log_{10}$ T data from tested wells, the depth of the Culebra at those wells, and an estimate of whether dissolution of the upper Salado has or has not occurred at each location. The fracture interconnectivity indicator is defined from the $\log_{10}$ T data, and a Salado dissolution indicator is defined using the Salado dissolution data. These data are then used in a standard linear regression algorithm to determine the regression coefficients. This aspect of DOE's effort is relatively standard with respect to regression analyses and the Agency is in agreement with the general approach.

Calculation of Base Transmissivity Fields and Seed Realizations

After DOE established the regression coefficients, a geostatistical approach was used to generate 500 equally probable realizations of zones with hydraulically significant fractures in the WIPP region. These simulations were parameterized using the frequency of occurrence of WIPP wells with hydraulically significant fractures and a fit to a variogram constructed using data from those same wells. The regression model was then applied to the entire WIPP area by:

(1) Overlaying the geologic map data for Culebra overburden thickness, Salado dissolution, and the presence or absence of halite in units bounding the Culebra with each of the 500 equally probable realizations of zones containing open, interconnected fractures.

(2) Sampling each grid point within the model domain to determine the overburden thickness and the indicator values for Salado dissolution, overlying or underlying halite, and fracture interconnectivity.

(3) Using the sampled data at each grid point with the regression model coefficients to estimate transmissivity.

When applied to the 500 equally probable realizations of zones containing open, interconnected fractures, this procedure generates 500 stochastically varying Culebra base T fields.

The base T fields rely on a regression model to estimate T at every location. By the nature of regression models, the estimated T values will not honor the measured T values at the measurement locations. Therefore, before using these base T fields in a flow model, they must be conditioned to the measured T values. DOE performs this conditioning with a Gaussian geostatistical simulation algorithm to generate a series of 500 spatially correlated residual fields where each field has a mean value of zero. These fields are conditional such that the residual value at each measurement location, when added to the value provided by the regression model (which is the same for all 500 fields), provides the known T value at that location. The result of adding the simulated residual field to the base T field is the "seed" realization.

Details about the creation of the base transmissivity fields are provided in Holt and Yarbrough 2002, 2003a, and 2003b. McKenna and Hart 2003b describe the creation of the "seed" fields. The Agency reviewed that information and concludes that, although there is uncertainty associated with DOE's approach (due to a limited amount of measured data), it does include greater amounts of actual data than were used in the development of the T fields for the PAVT (T fields were based solely on measurements from 46 well locations). It also provides a basis for the development of a conceptual model for the Culebra T fields, which was lacking in the PAVT.

Calibration to Steady-State and Transient Heads

This section presents details on the modeling approach used to calibrate the T fields to both the 2000 steady-state heads and 1,332 transient drawdown measurements. All of these steps outlined below can be considered as preprocessing aspects of the stochastic inverse calibration procedure also discussed later. The actual calibrations are done using an iterative coupling of the

MODFLOW-2000 and PEST codes. The details of this process are covered in McKenna and Hart 2003a and 2003b, and are briefly summarized in the sections that follow.

(1) Assumptions made in the modeling and the implications of these assumptions are provided. Major assumptions include:

- The boundary conditions along the model domain boundary are known and do not change over the time frame of the model.
- The fracture permeability of the Culebra can be adequately modeled as a continuum at the 100-m × 100-m grid block scale, and the measured T values used to condition the model are representative of the T in the 100-m × 100-m grid block in which the well test was performed.
- Variable fluid densities in the Culebra can be adequately represented by casting the numerical solution in terms of freshwater head. Davies 1989 investigated the effects of variable fluid density on the directions of flow calculated in the Culebra using a freshwater-head approach.

All of these assumptions were considered by the Agency during the CCA review and found to be acceptable (EPA 1998b). Of particular relevance is that, as will be discussed further below, on average, the grid blocks are considerably finer in the PABC than were used in the PAVT. Therefore, there is greater flexibility in the PABC to accommodate smaller spatial correlation lengths of fracture permeability and T.

(2) The initial heads used for each calibration are estimated at each location in the domain using the 37 heads measured in 2000 (Beauheim 2002b) in conjunction with kriging and accounting for the regional trend in the head values.

The Agency agrees that the 2000 potentiometric surface data should be used for initial conditions since earlier data sets are less complete and are not as representative of current conditions. The EPA also accepts kriging as a standard geostatistical method that is often used to contour (i.e., spatially correlate) hydrogeologic data.

(3) The initial heads are used to assign fixed-head boundaries to three sides of the model. The fourth side, the western edge, is set as a no-flow boundary for the model.

Conceptually, these boundary conditions follow the same basic principles that were accepted by the Agency during the CCA review (EPA 1998b), and remain appropriate for the modeling of the Culebra in the PABC.

(4) The transient head observations for each hydraulic test and each observation well are selected from the database. These heads are plotted as a function of time for each hydraulic test.

A major change in the calibration data set from the PAVT calculations is the exclusion of the hydraulic responses to the excavation of the exploratory (now salt) and ventilation (now waste)

shafts in the current calibration. DOE excluded the responses to the shaft excavations because the data covered a limited area (that was also covered in other well tests), was not particularly relevant to the transient calibration, and it was difficult to model both the flux and pressure changes accurately during the excavation of the shafts with MODFLOW-2000.

The Agency agrees with DOE's rationale for not including the responses to the water levels caused by the excavation of the shafts, particularly because their importance has diminished since the PAVT. The simulation of the long-term effects of the shafts on site-wide water levels were important for the CCA modeling because that modeling sought to replicate heads over time. In the current PABC calibration effort, however, shaft effects are not important because drawdowns resulting from specific hydraulic tests are used as the calibration targets and shaft effects can be considered as second-order compared to the effects of the hydraulic tests that are simulated.

(5) The spatial and temporal discretization of the model domain.

The flow model for the PABC was discretized into 68,768 regular, orthogonal cells each of which is 100 m × 100 m. The 100-m grid discretization was selected to make the finite-difference grid cell sizes considerably finer, on average, than those used in the CCA calculations, but still computationally tractable. In the CCA calculations, a telescoping finite-difference grid was used with the smallest cell being 100 m × 100 m near the center of the domain. The largest cells in the CCA flow model grid were 800 m × 800 m near the edges of the domain (Lavenue 1996).

In the PAVT, a constant Culebra thickness of 7.75 m was used (CCA Appendix TFIELD). This assumption was changed, however, in the PABC. The Culebra thickness was determined based upon elevations obtained from a digitized version of structure contour map of the top of the Culebra. Of the 68,768 cells (224 east-west by 307 north-south), 14,999 (21.8 percent) lie to the west of the no-flow boundary, so the total number of active cells in the PAVT model is 53,769. This number is nearly a factor of five larger than the 10,800 (108 × 100) cells used in the CCA calculations.

The Agency believes that the finer discretization used in the PABC is an improvement over the approach used in the PAVT. Not only can features be modeled at a finer scale, but the transport solutions will now be more accurate because the actual thickness of the Culebra can be used to calculate the hydraulic conductivity (transmissivity divided by thickness) required for the velocity calculations.

The time period assigned by DOE for the transient simulations lasted nearly 11 years and 2 months and began in October 15, 1985 and ended December 11, 1996. Additionally, a single steady-state calculation was run prior to the transient modeling. The length of this steady-state time period and the date at which it occurs were arbitrarily set to one day occurring from October 14, 1985, to October 15, 1985. These steady-state heads were measured in the year 2000 and were only set to these October dates to provide a steady-state solution prior to the start of any transient hydraulic events.

The method that DOE has used to initialize the transient simulations with steady state heads and to specify time periods are consistent with standard engineering practices and acceptable to the Agency.

(6) The transient head observations are given relative weights based on the inverse of the maximum observed drawdown in each hydraulic test.

DOE assigns weights to the observed data for each response to every transient hydraulic test to take into account the differences in the responses across the different tests. The weights are calculated as the inverse of the maximum observed drawdown for each hydraulic test. This weighting scheme applies relatively less weight to tests with large drawdowns and relatively more weight to tests with smaller responses. The Agency agrees with weighting of the data so that the overall calibration will not be dominated by trying to reduce the very large residuals that may occur at a few of the observation locations with very large drawdowns.

(7) The locations of the adjustable pilot points are determined using a combination of approaches.

A major development in the field of stochastic inverse modeling has occurred since the T fields were constructed for the CCA in 1996. Inverse techniques are now capable of simultaneously determining optimal T values at a large number of pilot points. In the T fields constructed for the CCA, pilot points were added one at a time and each point was calibrated prior to the addition of the next pilot point. Furthermore, the total number of pilot points was limited to less than or equal to the total number of T observations to avoid numerical instabilities in the solution of the inverse problem. With the techniques now available and implemented in the computer code PEST, it is possible to use many more pilot points than there are T observations and to calibrate these pilot points simultaneously.

Philosophically, the Agency believes that DOE should take advantage of advances in technology as they become available. The Agency is familiar with PEST applications on other EPA regulated sites and is satisfied with the fundamental principles of the code.

Stochastic Inverse Calibration

The stochastic inverse calibration process uses multiple pre- and post-processor codes in addition to PEST and MODFLOW-2000. The details of the overall numerical approach to the T field calibration are documented in McKenna and Hart 2003a and 2003b. In general, the calibration process is run iteratively until at least one of three conditions are met: (1) the number of iterations reaches the maximum allowable number of 15; (2) the objective function reaches a predefined minimum value of 1,000 m^2; or (3) the value of the objective function changes by less than one percent across three consecutive iterations.

At the end of the calibration process, a residual field is created that when added to the base T field reproduces the measured T values at the 43 measurement locations and provides a minimum sum of squared errors (SSE) between the observed and model-predicted heads/drawdowns.

T Field Acceptance Criteria

The calibration procedure was applied to 150 of the base T fields (the remaining 350 base fields were held in reserve, to be used only if necessary). Not all base T fields yielded a resulting calibrated T field. Four base T fields (d01r03, d01r09, d02r09, and d08r10) encountered numerical difficulties during the first iteration and did not calibrate at all. For each of the remaining 146 T fields, the calibration procedure stopped for one of three reasons:

(1) PEST completed the maximum allowed number of iterations (15)

(2) PEST was unable to improve the objective function (sum of squared errors of weighted residuals) for three successive iterations

(3) The optimization became numerically unstable

DOE notes that some of the T fields probably could have been calibrated better with more effort and adjustment of some of the PEST input parameters; however, DOE set these parameters to work for the largest number of fields possible.

Because the T field calibration procedure did not stop when some objective goodness-of-fit target was achieved, DOE established criteria to define what constitutes an acceptable calibration. Because the T fields were to ultimately be used for calculation of radionuclide transport, acceptance criteria were based on the travel times calculated in the T fields for a conservative particle released above the center of the WIPP waste panels (Ramsey et al. 1996) to reach the WIPP land-withdrawal boundary (LWB). That is, the sensitivity of the calculated travel-time distribution to potential acceptance criteria was used to identify those criteria that are important. Once the distribution of travel times showed no (remaining) sensitivity to continued refinement of the criteria applied (e.g., a reduction in some metric below a threshold value), DOE considered all T fields meeting those criteria to be acceptably calibrated.

DOE obtained the travel times using the streamline particle-tracking algorithm implemented in DTRKMF v. 1.0 (Rudeen 2003), assuming a single-porosity medium with a porosity of 0.16. DTRKMF calculates particle tracks in two or three dimensions for steady-state and time-dependent, variably saturated flow fields. The particles are tracked cell-by-cell using a semi-analytical solution. DTRKMF directly reads the cell-by-cell flow budget file from MODFLOW-2000 and uses those values to calculate the velocity field. For each calibrated T field, a final forward run of MODFLOW-2000 was done and the cell-by-cell fluxes from this run were used as input to DTRKMF to calculate the travel time. These travel times do not, however, represent the actual predicted travel times of solutes, conservative or non-conservative, through the Culebra. Culebra transport modeling treats the Culebra as a double-porosity medium with transport through advective porosity (e.g., fractures) retarded by diffusion into diffusive porosity (e.g., matrix porosity) and by sorption. The travel times are intended only to allow comparison among T fields. DTRKMF has been evaluated by EPA and found to be acceptable (EPA 2004).

Four factors were evaluated for their potential to provide T field acceptance criteria: the root mean squared error (RMSE) of the modeled fit to the measured steady-state heads, the agreement between the measured and modeled steady-state gradient/heads, the sum of squared weighted residuals (phi) for the transient data, and the agreement between the measured and modeled transient heads. These four criteria were applied to the calibrated Culebra T fields to determine if they allowed meaningful discrimination among the fields. Given that travel time is the performance measure of most concern, the four criteria were evaluated in terms of their effects on the calculated distribution of travel times from the T fields.

Of the criteria discussed above, the two related to the steady-state heads (RMSE and steady-state-fit slope) appeared to be more effective at identifying poorly calibrated T fields than the two related to transient heads (transient phi and number of failed well responses). The range and scatter of travel times appears to increase at RMSE values beyond 6 m (20 ft). Applying an RMSE cutoff of 6 m (20 ft) leaves 117 T fields, all with travel times less than 102,000 years except one (d01r06). This cutoff also excludes all T fields with steady-state-fit slopes less than 0.45. Steady-state-fit slopes less than approximately 0.5 appear to lead to significantly longer travel times, consistent with the low hydraulic gradients the low slopes imply. If a simple cutoff of a minimum steady-state-fit slope of 0.5 is applied, 116 T fields are left, again with travel times less than 102,000 years (except d01r06), and also with RMSE values less than 8.6 m (28.2 ft). Five T fields that meet the RMSE less than 6 m (20 ft) criterion fail the steady-state-fit slope greater than 0.5 criterion, while four T fields meeting the slope criterion fail the RMSE criterion. Thus, 112 T fields meet both criteria while 121 T fields meet at least one of the criteria.

Because only 100 T fields were needed, DOE refined the criteria to eliminate more T fields. Given that lower travel times provide a conservative (in terms of leading to increased solute transport) way to discriminate among sets of T fields, the 100 T fields with RMSE values <5 m (16 ft) and transient phi values <8,000 m^2 were selected for use in CRA-2004 calculations of radionuclide transport through the Culebra, because that set excluded the calibrated T field with the longest travel time.

The Agency believes that the approach adopted by DOE to develop and implement acceptance criteria provides a logical means to evaluate the modeling results.

Inverse Modeling Results

For comparison purposes, the CDF of travel times for the accepted 100 T fields is plotted in Figure 8-1 with the CDF of travel times for the 100 transient-calibrated T fields used in the CCA (Wallace 1996). In general, travel times are two to three times as long in the CRA fields as in the CCA fields.

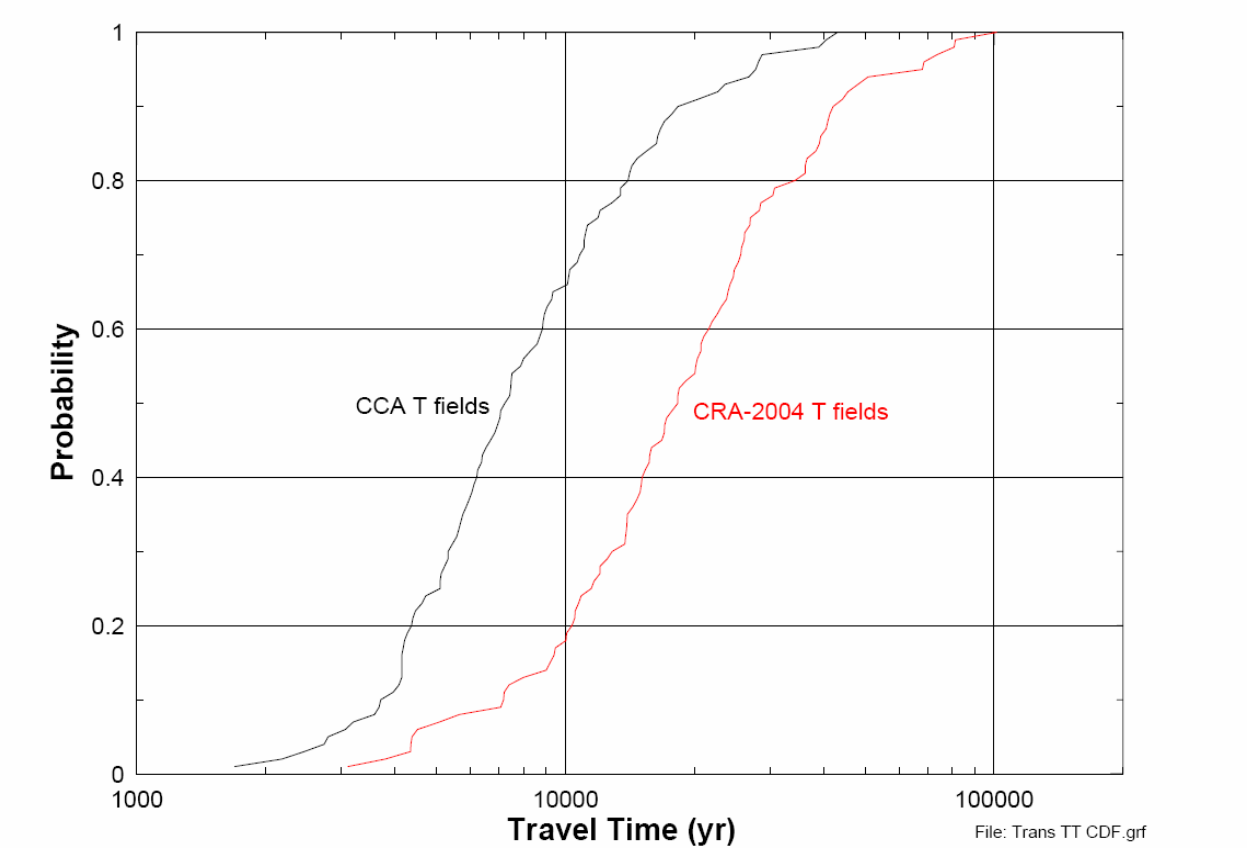

Figure 8-1. Travel-Time CDFs for CCA and CRA T Fields
(Source: DOE 2004b, Appendix PA, Attachment TFIELD)

The 121 T fields that were acceptably calibrated are combined into an ensemble average T field showing the average properties of the T fields. The average properties do not show a continuous north-south high-T zone exiting the southeastern portion of the WIPP site, as was present in the ensemble average T field provided in CCA (Appendix TFIELD, Figure 30). It also shows higher T values in the southwestern portion of the WIPP site than were present in the CCA ensemble average field. These differences explain why the travel paths in the CRA T fields take a more westerly course, on average, than those in the CCA T fields, and why the CRA travel times are longer than the CCA travel times (Figure 8-1). Furthermore, in the CCA T Fields, the high T observed at well H-11 continued to the south, eventually merging with the high T's in the southeastern arm of Nash Draw. In the CRA T fields, the high T at H-11 is a localized, isolated occurrence, with no connection to the area to the south (see CRA-2004 Figure TFIELD-63). Recent (August 2005) testing performed by DOE in newly drilled well SNL-14, approximately one mile south of H-11, has shown that high T does, in fact, extend to the south from H-1 as modeled in the CCA T fields. The apparent discrepancy in the T Fields resulted, in the CRA-2004 model, in a slight shift to the west of flow from above the waste panels to the southern site boundary (see CRA-2004 Figure TFIELD- 58) and an increase in travel time, relative to the CCA model (Figure 8-1). Another factor, however that also contributed to the increase in travel times between the CCA and CRA is a decrease in the hydraulic gradient along the off-site

pathway. The Agency will require that DOE continue to refine and test their conceptual models.

8.2.3 Modification of T Fields for Mining Scenarios

As with the CCA, two categories of mining-impacted transmissivity fields are modeled; one with mining outside the LWB only, and the other with regions both inside and outside the LWB mined (partial- and full-mining scenarios, respectively). Flow modeling is performed starting with 100 stochastically calibrated T fields from McKenna and Hart 2003b. Each T field is modeled to reflect the effects of mining by multiplying the transmissivity value in cells that lie within designated mining zones by a random factor between 1 and 1000. A forward steady-state flow simulation is run for each new T field under each mining scenario (full and partial) across three replicates of mining factors, resulting in 600 simulations (there are 100 calibrated T fields). Particle tracking is performed on the modeled flow fields to determine the flow path and groundwater travel time from a point above the center of the WIPP disposal panels to the LWB. Cumulative probability distribution functions (CDF) are produced for each mining scenario and compared to the undisturbed scenario generated from Task 4 of AP-088, as well as to the full- and partial-mining scenarios from the 1996 CCA and the 2004 CRA (Lowry 2003). The CDFs describe the probability of a conservative tracer reaching the LWB at a given time. In addition to comparing travel times, particle tracking directions are also examined to determine the effect on the regional flow direction in the WIPP area due to mining. The flow fields generated from the mining scenarios are then refined and passed to Task 6 of AP-100 that performs radionuclide transport modeling in the Culebra.

For PA purposes, the DOE assumes that all economically extractable potash is mined outside of the WIPP LWB during the 100 years after closure of the WIPP repository when active institutional control of the site is maintained. Following that 100-year period, the DOE further assumes there is a one in 100 probability that the potash within the LWB will be mined during any given century. Therefore, all PA calculations of transport of radionuclides released to the Culebra through inadvertent human intrusion of the repository assume that all potash outside the LWB has already been mined (the "partial-mining" scenario) by the time the intrusion occurs. The "full-mining" scenario is invoked when the sampled time of human intrusion is coincident with or later than the sampled time of mining within the LWB. Under both scenarios, the hydraulic conductivity (or T) of the Culebra is assumed to be increased by a random factor between one and 1,000 in the areas affected by mining. The process by which the calibrated Culebra T fields were modified to account for the effects of mining, and the characteristics of the resulting modified T fields, are discussed below.

Determination of Potential Mining Areas

For the CRA, DOE based their assumptions with respect to potentially mined areas on BLM maps (1993) that show current potash mines and economically recoverable resources (reserves) in the known potash lease area around the WIPP site. These are the areas where subsidence might occur in the future. Although the BLM maps show all reserves, DOE assumed that there was a one-quarter to one-half mile (402 to 805 m) exclusion zone around oil and gas wells for the purposes of assigning potentially mined areas. As will be discussed in the next section the Agency did not agree with this assumption and it was changed for the PABC.

Because the potash mining horizon is located in the Salado Formation, below the Culebra, the areas in the Culebra that might be disturbed by the mining activities are larger than shown on the maps due to angle-of-draw effects associated with subsidence. The rationale for determining the extent of these effects is described in Wallace (1996) with the final conclusion stating that an additional 253-m (830-ft)-wide disturbed zone was to be added to the mining-impacted areas to approximate a 45-degree angle of draw. This assumption was approved by the EPA during the CCA review.

For the CRA T fields, a buffer of three cell widths (300 m [984 ft]) was manually digitized and added to the mining zones. DOE then compared this new delineation to the CCA model mining zones to make sure there were no significant differences outside of those that can be explained by different grids for the two model domains and the addition of new data (Figure 8-2). The most notable difference between the two versions is that the area of potential future mining along the northeastern boundary of the LWB is no longer directly connected to the northern boundary of the model domain, which would be expected to decrease flow to the WIPP site.

As was done for the CCA, DOE assumed that mining impacts would not significantly change the boundary conditions used in T field calibration. Potash mining has already occurred along the northern boundary of the model domain, and the western model boundary is in Nash Draw where subsidence and fracturing of the Culebra are already incorporated in the model.

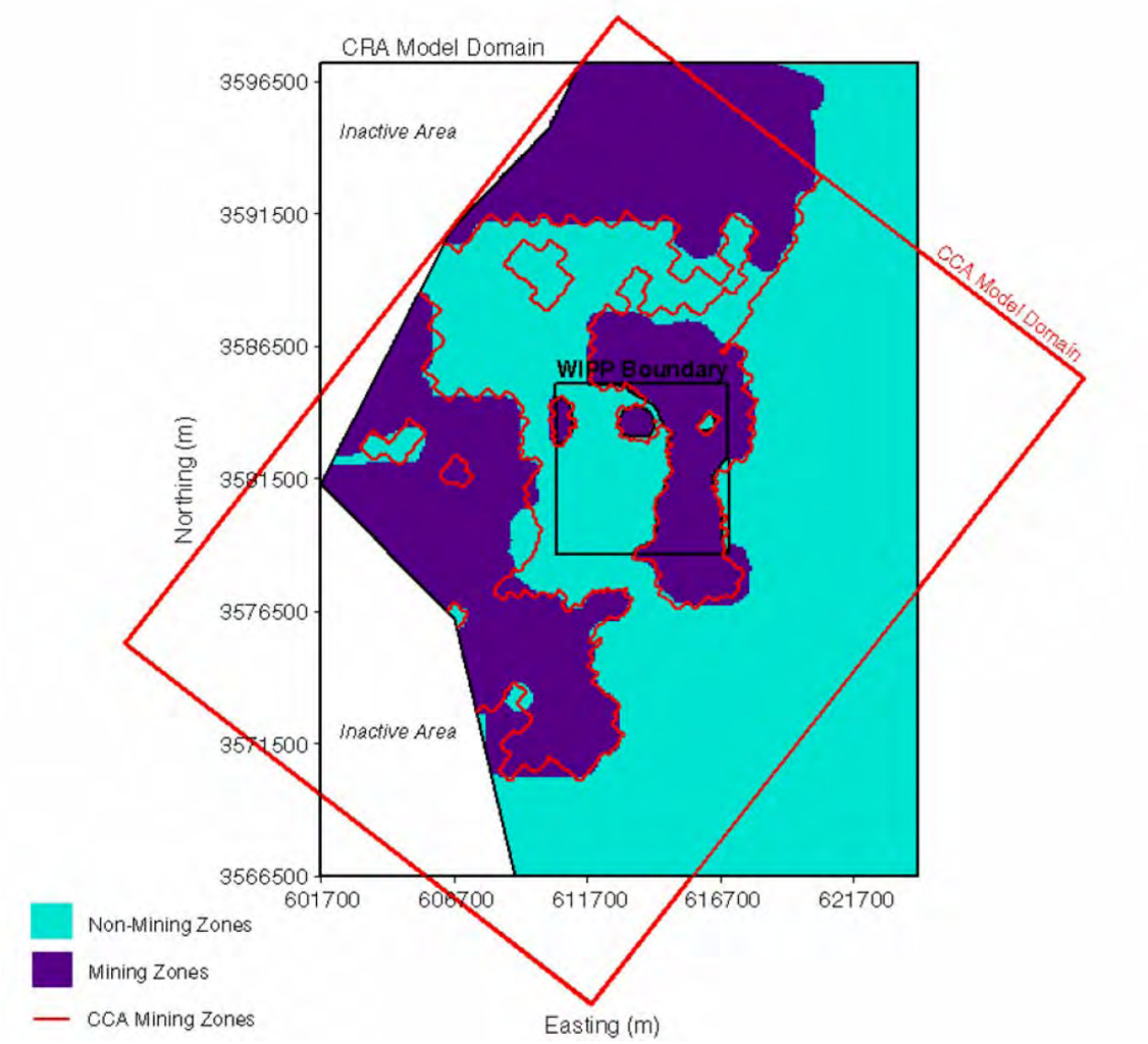

Figure 8-2. Comparison of CRA and CCA Areas Affected by Mining
(Source: DOE 2004b, Appendix PA, Attachment TFIELD)

Figures 8-3 and 8-4 compare the CDFs of travel time for all three replicates of the partial- and full-mining cases, respectively, to the Replicate 1 results from the CCA T fields (Wallace 1996). These plots show, first, that all three CRA replicates provided very similar results and, second, that the new travel times are consistently longer than the CCA travel times. DOE believes that the primary reason for this difference is probably the absence in the CRA T fields of the direct, high-T connection between the WIPP site and the northern model boundary that was present in the CCA T fields and that provided a source of water to the Culebra within the LWB.

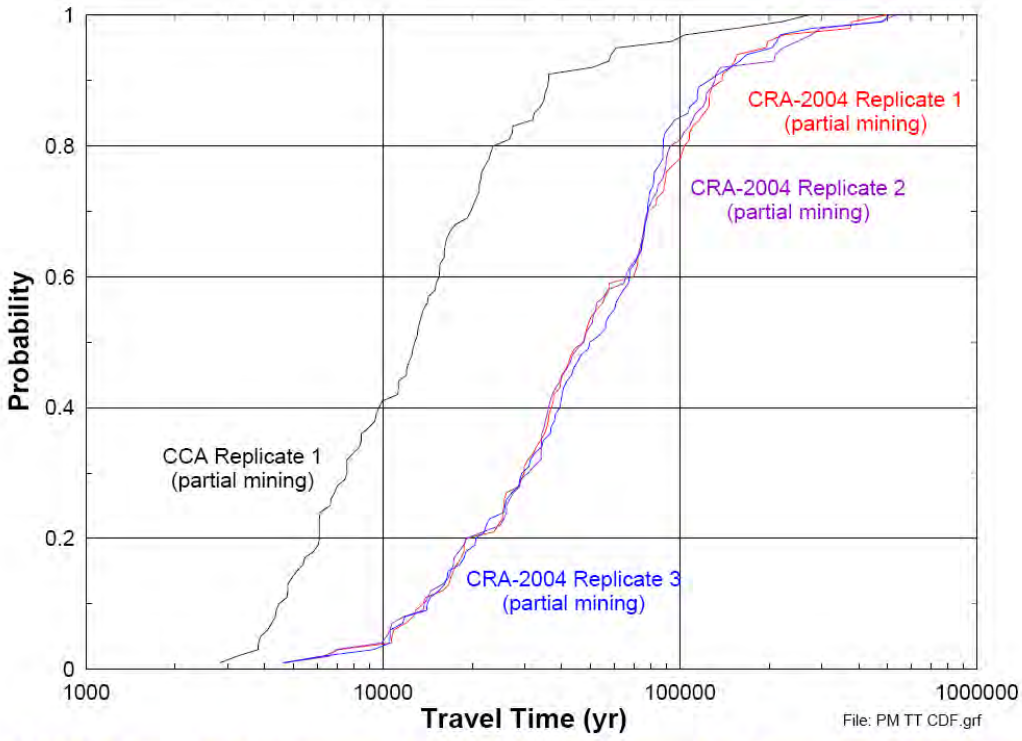

Figure 8-3. CDFs of Partial-Mining Travel Times for Three CRA Replicates and One CCA Replicate
(Source: DOE 2004b, Appendix PA, Attachment TFIELD)

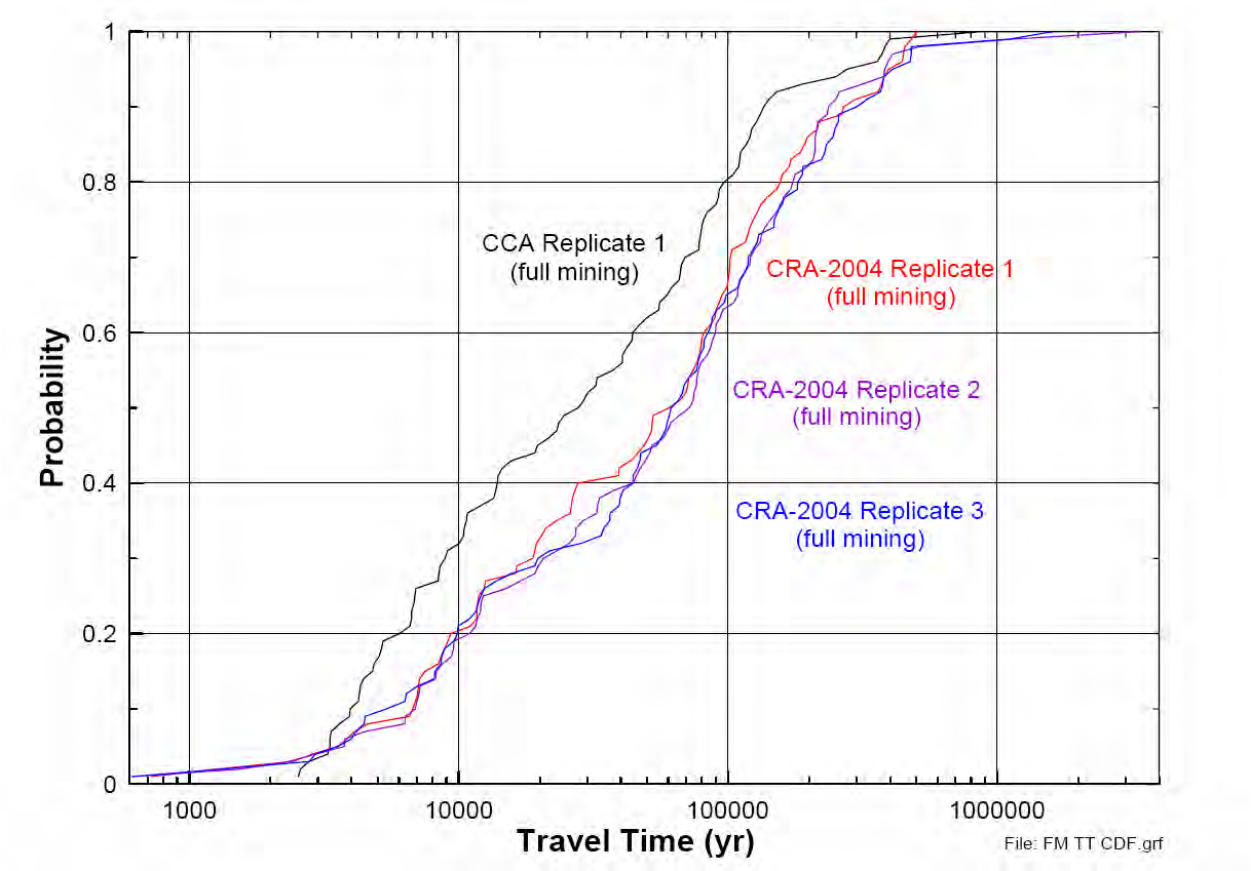

Figure 8-4. CDFs of Full-Mining Travel Times for Three CRA Replicates and One CCA Replicate
(Source: DOE 2004b, Appendix PA, Attachment TFIELD)

Changes in T Fields for PABC

During the review of the CRA, the Agency did not approve of one aspect of DOE's approach to account for the potential effect of potash mining on Culebra T fields. Specifically, as noted in EPA Completeness Letter No. 4, the Agency states: "In section TFIELD-9.1 paragraph 2 of Attachment TFIELD the CRA states: "The current version of the map differs from the one used for the CCA calculations in that several areas north of the LWB have been ruled out as potential mining areas in the updated version due to recent oil and gas drilling in those areas." EPA does not agree with this approach" (Cotsworth 2004c, Docket A-98-49, Item II-B3-78).

The Agency disagreed with the use of a 1-mile-radius exclusion zone around existing oil and gas wells for potash resources outside the LWB and directed DOE to update the transmissivity fields to better represent the mining areas around the WIPP Site (Docket A-98-49, Item II-B3-80). In response, DOE redefined the potash mining areas in the PABC to consist of all mined and un-mined potash resources including where they fall within 1-mile exclusion zones around oil and gas wells. Based upon the new mining areas, the mining modifications to the Culebra T fields

and the Culebra flow fields were re-calculated in Lowry 2004 and the results are summarized below.

The model domains of the CCA grid, CRA grid, and the CRA-revised (i.e., PABC) grid for both the full- and partial-mining scenarios are shown in Figures 8-5 and 8-6, respectively. Results show that for both the full- and partial-mining scenarios, the median particle travel times of 75,774 and 129,202 years are 4.14 and 7.06 times longer than for the non-mining scenario (18,289 years). The increase in transmissivity due to mining increases the relative flow rate through the mining zones, with a corresponding decrease in flow through the non-mining zones. This decrease in flow through the non-mining zones produces longer travel times for the mining scenarios. Comparing the full-mining scenarios of the PABC analysis to the CCA and CRA calculations, the median travel times are approximately 2.53 and 1.14 times longer, respectively. For the partial mining case, the median travel time for the PABC is 9.33 times greater than the median for the CCA, and 2.67 times greater than the CRA. DOE attributes this increase in the travel time over the CRA to the higher percentage of area deemed as mining zone. DOE points out that unlike the CRA, a negative correlation was found in the PABC analysis between the travel times and the random mining factor (the higher the random mining factor, the longer the particle travel time). DOE believes this is also due to a higher percentage of mining zone area in the PABC analysis as compared to the CRA. With a higher percentage of mining area, the random mining factor has a larger influence on the regional flow regime. As the mining factor is increased, the flow through the non-mining areas is decreased, producing longer travel times and the negative correlation. However, additional analysis shows that most of the travel time variability is due to differences in the base T fields and not the random mining factor.

By eliminating the exclusion zone around the existing oil and gas wells the DOE has addressed the Agency's concern with respect to the mining scenario.

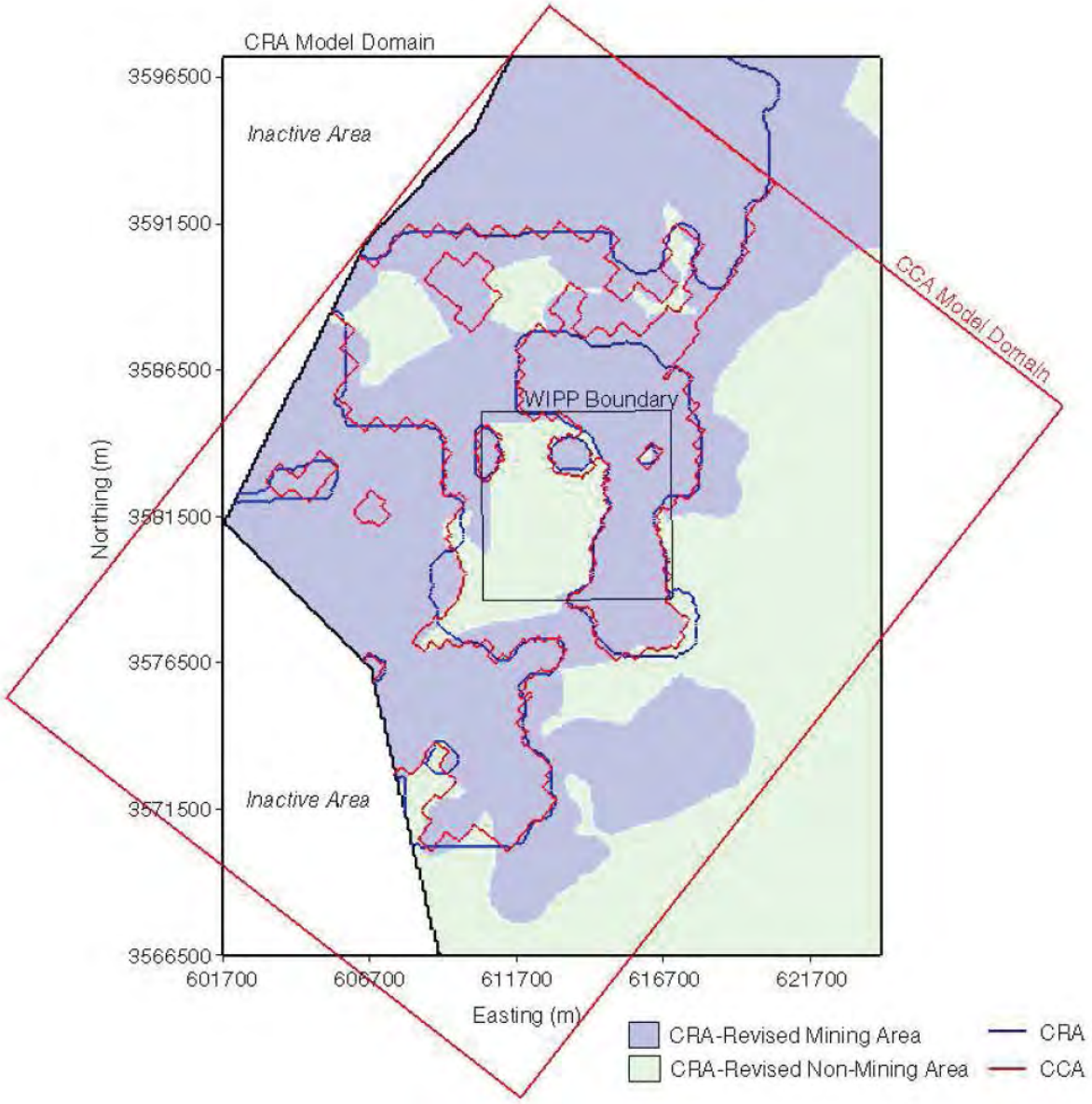

Figure 8-5. The CRA-Revised (PABC) Full Mining Zones Overlaid with the 1996 CCA (red) and CRA delineations (blue)
(Source: Lowry and Kanney 2005)

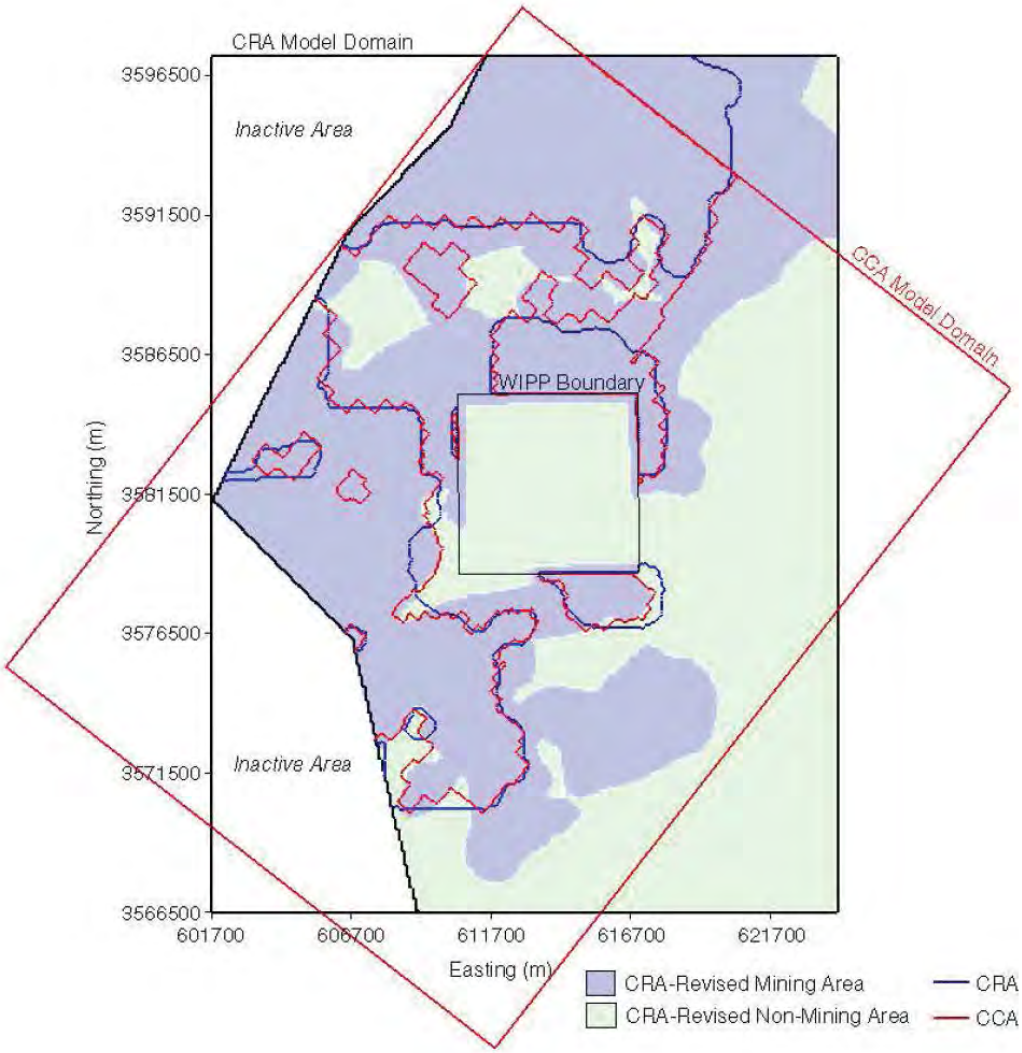

Figure 8-6. The CRA-Revised (PABC) Partial Mining Zones Overlaid with the 1996 CCA (red) and CRA Delineations (blue)
(Source: Lowry and Kanney 2005)

9.0 SALADO FLOW AND TRANSPORT

Flow in the Salado is computed by BRAGFLO (Stein 2003), which simulates brine and gas flow in and around the repository. BRAGFLO includes the effects of processes such as gas generation and creep closure. Outputs from the BRAGFLO simulations describe the conditions (pressure, brine saturation, porosity) and flow patterns (brine flow up an intrusion borehole and out anhydrite marker beds to the accessible environment) that are used by other software to predict radionuclide releases. Some of the specific processes included in the BRAGFLO calculations include:

- Brine and gas flow
- Creep closure of the waste-filled regions within the repository
- Gas generation due to corrosion of steel and degradation of biodegradable materials (cellulosics, plastics, and rubbers)
- Physical changes (e.g. permeability and porosity) in the modeling domain over time
- The consequences of rock fracturing due to high pressure

The overall transport and decay of radionuclides in the Salado is calculated using the computer code NUTS (NUclide Transport System). NUTS is a five-point finite difference code designed to model multi-dimensional, multi-component, and radioactive-contaminant transport in single-porosity, dual-porosity**,** and/or dual-permeability porous media, including parent daughter first-order decay. The key processes modeled with NUTS are advective transport, decay, precipitation, solubility limits, and interior sources, all in a continuous matrix. No dispersion is modeled. The initial condition for each run is to assume no contamination present within the model domain, with the exception of the source term in the waste panel area.

Any flow of brine up the shafts, borehole(s), and out the marker beds is calculated using BRAGFLO and these results are required prior to running NUTS. This input is the ASCII input file containing the grid specifications, initialization parameters, and material maps as well as the BRAGFLO post-processed binary file (CDB) that describes the flow-field. The CDB files are the source for brine fluxes at the cell interfaces, porosity, saturation, pressure, and the geometric information. In addition, NUTS uses a CDB file that contains the "effective solubilities," "lumped inventory" source terms created by PANEL (Garner and Leigh 2005), and atomic weights and half-lives of the modeled isotopes. NUTS also uses its own input file that contains the run parameters and the isotope decay data.

The mathematical formulations and model conceptualizations of both BRAGFLO and NUTS have been evaluated by EPA and found to be acceptable (EPA 1998b).

In the PAVT, the same single disposal system geometry was used in both the BRAGFLO and NUTs computational models (Docket: A-93-02, II-G-1, Volume XVII, Appendix BRAGFLO). Four different maps of material properties were assigned: one for undisturbed conditions; one for the E1 intrusion event, in which a borehole penetrates the panel and a Castile brine reservoir; one for the E2 intrusion event, in which a borehole penetrates the repository but not a Castile brine reservoir; and one for the E1E2 intrusion event, in which at least one E1 borehole and one other

borehole penetrate a disposal panel. The geometry and material maps used for each scenario were similar; each is a model for fluid flow and radionuclide transport calculations that represents the three-dimensional physical system in a two-dimensional plane that cuts vertically through the repository and surrounding strata. Side views of the vertical cross section and two of the material maps used in PAVT are presented in Figures 9-1 and 9-2 (DOE 1996b, Section 6).

9.1 MODIFICATIONS SINCE THE PAVT

9.1.1 Technical Baseline Migration

The Technical Baseline Migration (TBM) was an effort begun by DOE in 2001 to merge the CCA (DOE 1996b) and PAVT (SNL 1997) PA baselines, while at the same time implementing conceptual model changes being reviewed by the Salado Flow Peer Review in preparation for the CRA. The TBM analysis eventually consisted of a full PA calculation which implemented several changes from the PAVT. As part of this migration, a new BRAGFLO numerical grid (mesh) was developed and presented as Figure 9-3 and further described in Hansen et al. 2002. The most important changes with respect to the TBM BRAGFLO grid were the implementation of the Option D panel closure design, which was mandated by the EPA as a condition to their final rule, and the removal of an explicit representation of the shaft seal system in the grid. Additional grid refinements were implemented to increase numerical accuracy and computational efficiency and to reduce numerical dispersion in transport simulations that used the same grid as BRAGFLO.

In May 2002, the Salado Flow Peer Review panel met in Carlsbad to evaluate changes to conceptual models for the PA. These changes are detailed in a report by Hansen et al. 2002. To demonstrate the effects of these changes on BRAGFLO results, a set of PA calculations were conducted (referred to by DOE as The Technical Baseline Migration (TBM)). The peer review panel judged the changes to be "generally sound in their structure, reasonableness, and relationship to the original models;" however, the panel required that a total systems PA be run and complementary cumulative distribution functions (CCDFs) be generated before they would agree to the changes (Caporuscio et al. 2003). In response to this finding, DOE conducted a total system PA for the TBM and produced CCDFs (Dunagan 2003) that were presented to the Salado Flow Peer Review panel during their second and last meeting in Carlsbad in February 2003.

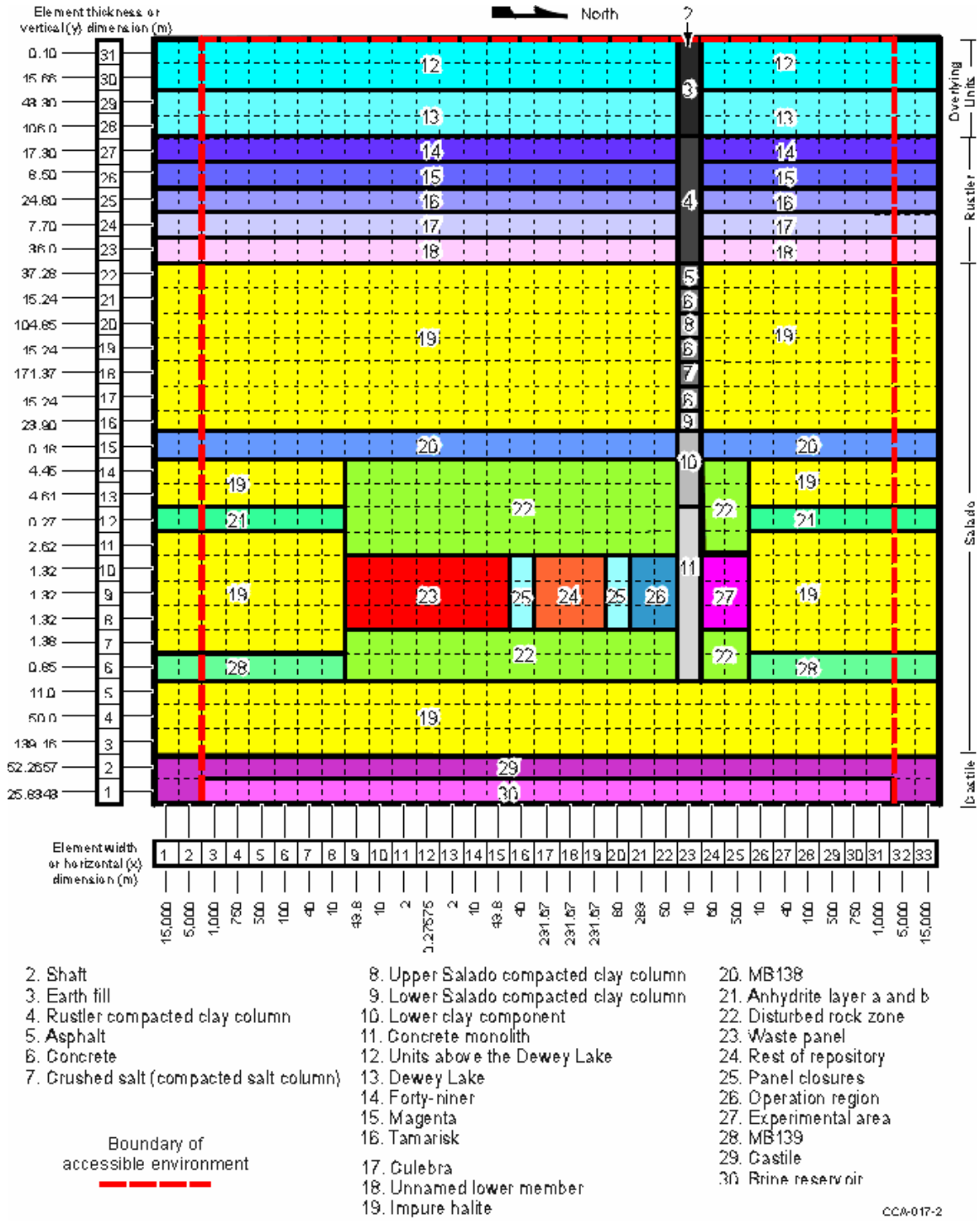

Figure 9-1. A Side View of the BRAGFLO\NUTS Elements and Material Regions Used for Simulation of Undisturbed Performance
(Source: DOE 1996b, Section 6)

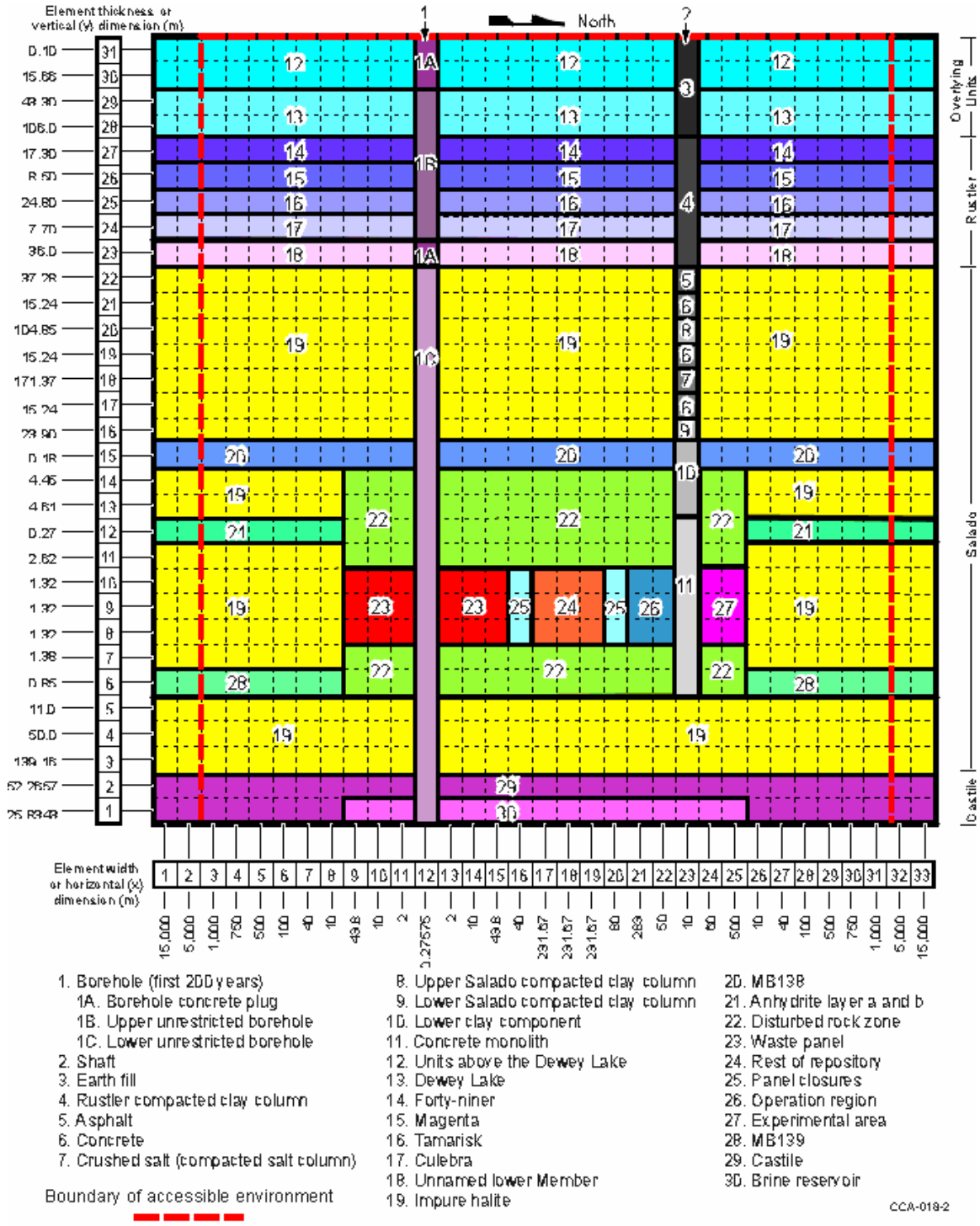

Figure 9-2. A Side View of the BRAGFLO\NUTS Elements and Material Regions Used to Simulate the E1 Event
(For E2 Event, the Borehole Extends Only Between the Surface and the Base of the Repository)
(Source: DOE 1996b, Section 6)

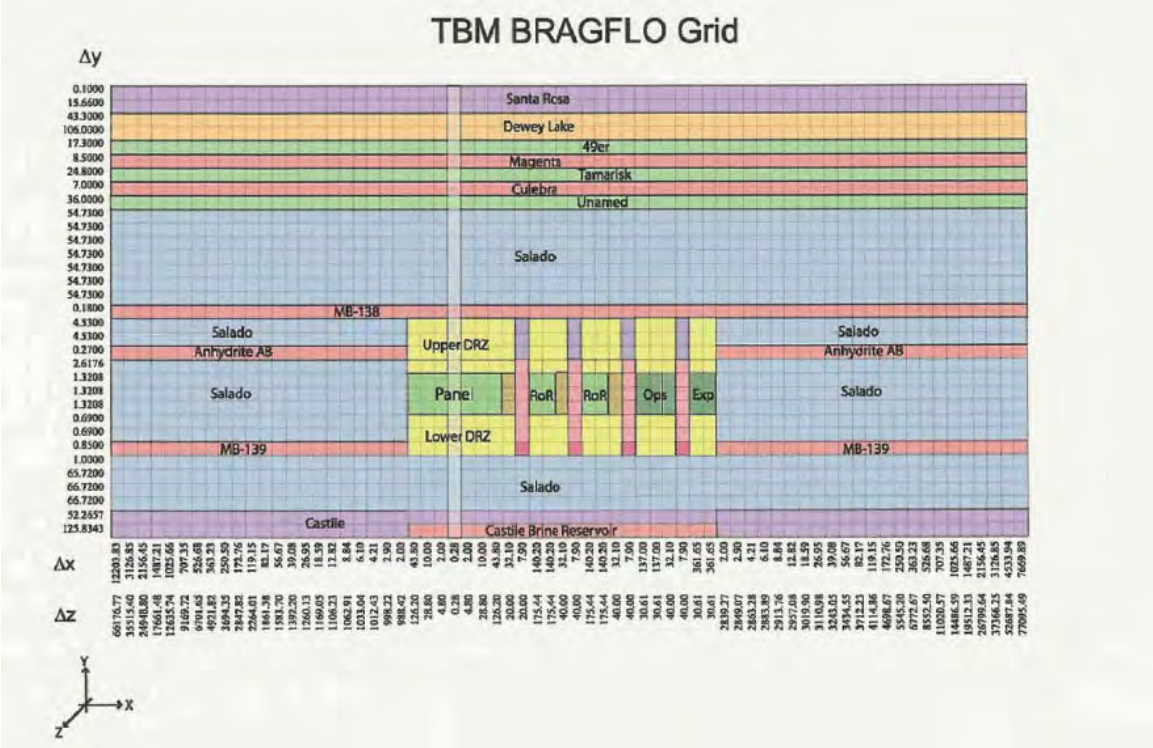

Figure 9-3. Technical Baseline Migration (TBM) Logical BRAGFLO Grid
(Source: Stein and Zelinski 2003c)

9.1.2 Compliance Recertification Application

After the initial meeting of the Salado Peer Review panel in May 2002, the DOE received two letters from the EPA (EPA 2002a, 2002b) with a list of topics that the Agency requested be considered in the PA calculations for the CRA. Additional issues and concerns were discussed in a series of technical exchange meetings. Two of the topics considered in these meetings relate specifically to assumptions made for the TBM BRAGFLO calculations; (1) the presence or absence of the shaft in the BRAGFLO model grid, and (2) the move of the repository horizon up approximately 2 m to Clay Seam G for panels 3, 4, 5, 6, and 9. These panels are located in the southern half of the waste disposal area. Both of these topics are further discussed below.

Simplified Shaft

DOE's TBM calculations did not include an explicit model of the shaft seal system in the BRAGFLO grid. DOE removed the shaft because, in all the previous TBM calculations, no significant flow occurred in this region and the shaft model required that nearly 1,000 separate parameters be defined. In subsequent discussions, EPA made it clear that the continued presence of the shaft in the grid was considered to be important. Therefore, DOE developed an approach for implementing a simplified shaft model with equivalent properties to the original detailed model. This work is described in AP-094 (James and Stein 2002) and in the associated analysis report (James and Stein 2003).

EPA has reviewed that work and finds that the simplifications (e.g., averaging of properties) do not significantly (or adversely) impact the results, and are therefore acceptable to the Agency.

Clay Seam "G"

The second issue relates to a request by DOE to EPA to raise the repository horizon in Panels 3, 4, 5, 6, and 9 so that the roof is at Clay Seam "G" (DOE 2000). EPA responded to the request in a letter (EPA 2000) in which EPA agreed with DOE that the effects to long-term performance would be minimal. At the time, DOE considered the change minor enough not to warrant a full-scale impact assessment. However, in a subsequent letter from EPA the Agency stated that "the conceptual model of the repository should reflect the change to raise the level of excavation to Clay Seam G. The conceptual change should be appropriately addressed in the modeling, if warranted" (EPA 2002a). In response to this letter, DOE began an effort to evaluate the effects, if any, on PA resulting from the move in the repository horizon. Specifically, DOE initiated two sets of analyses:

(1) The horizon change may influence the creep-closure porosity surface calculated by the code SANTOS and used by BRAGFLO. The SANTOS calculations are being repeated with the new horizon to test whether the response surface will change significantly. This work is described in AP-093 (Park 2002).

(2) The thickness of upper and lower Disturbed Rock Zone (DRZ) represented in the BRAGFLO grid may change due to the horizon change. This change may affect flow pathways around the Option D panel closures as well as the total pore volume represented in the DRZ above and below the waste rooms. A new BRAGFLO grid was developed to include these changes and two sets of BRAGFLO simulations were run to test whether these changes significantly affect WIPP PA (Stein and Zelinski 2003b).

DOE summarizes the results of BRAGFLO and a limited set of CCDFGF calculations which were presented to the Salado Flow Peer Review panel during the February 2003 meetings in Stein and Zelinski 2003b. For these meetings, DOE ran several analyses to test whether modifications and corrections made in the TBM conceptual models significantly affected BRAGFLO and other PA results. These modifications include the addition of the simplified shaft, allowing fracturing in the upper DRZ, and correcting minor errors found in the TBM. Additional discussion pertaining to these modifications is presented below.

CRA Model Grid

The CRA grid described below is essentially the TBM grid with the following changes:

(1) The simplified shaft model was included in the grid.

(2) Double-wide panel closures used in the north end.

(3) Modifications to allow fracture flow "around" the Option D panel closures both above and below the closure concrete through the DRZ and marker beds were made.

(4) A minor error relating to the volume of the rest of the repository regions in the TBM grid (Stein 2002) was corrected.

The grid used for NUTS in the CRA calculations is the same as the grid used for the BRAGFLO calculations (Figure 9-3). The extent of the modeling domain is 46,630 m in the horizontal (x) direction by 940 m in the vertical (y) direction, which is the same as for the PAVT calculations. The domain is discretized into 68 × 33 (x,y) non-uniform grid cells with higher resolution in the repository area and lower resolution towards the edges of the modeling domain. The grid is more refined and includes a more detailed representation of the panel closures and waste regions than was used for the PAVT calculations. The changes made to the grid were accepted by the Salado Flow Peer Review panel in February 2003 (Caporuscio et al. 2003). A full description of the grid can be found in Stein and Zelinski 2003c.

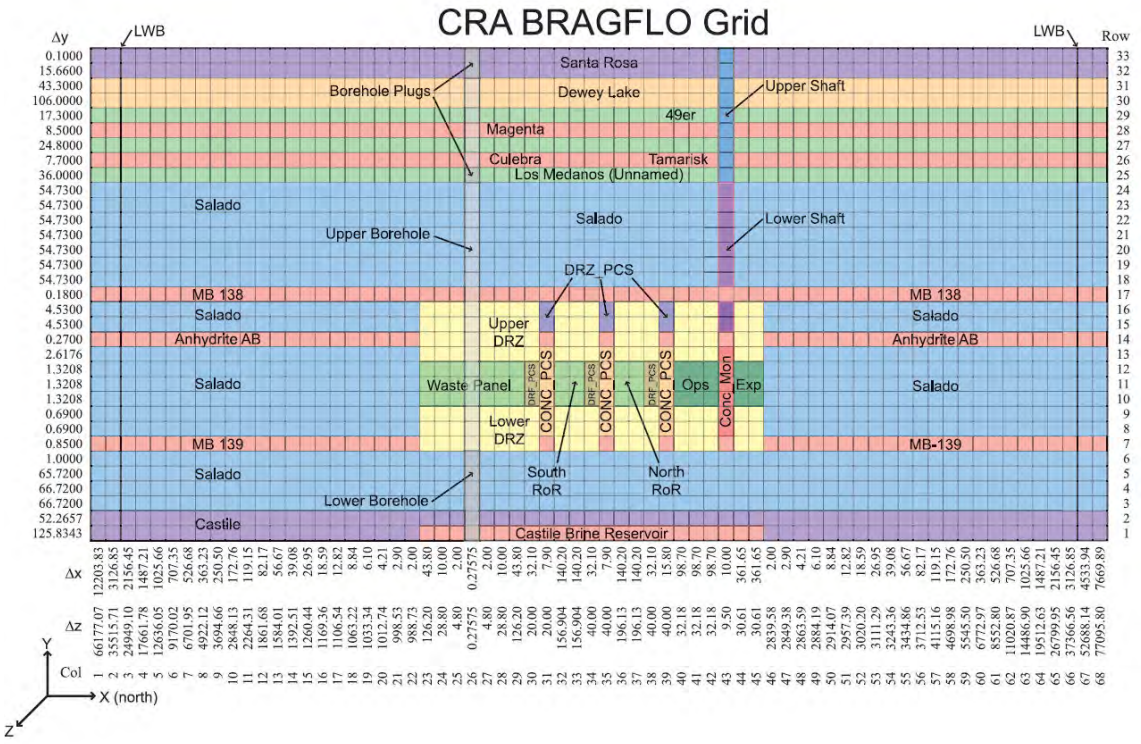

Figure 9-4. CRA and PABC Logical BRAGFLO Grid
(Source: Stein and Zelinski 2003c)

Simplified Shaft Seal

A shaft seal model is included in the CRA grid, but it is implemented in a simpler fashion than that used for the PAVT. A detailed description of the model and its parameters is discussed in AP-094 (James and Stein 2002) and the resulting analysis report (James and Stein 2003). The new approach does not alter the conceptual model of the shaft seal components as described previously in SNL 1996. Rather, it conservatively represents the behavior of seal components in the repository system model. Specifically, the original 11 separate material layers that defined the shaft model for the PAVT were reduced to two layers each with properties equivalent to the

composite effect of the original materials combined in series. Additionally, the six time intervals that were used to represent the evolution of the shaft seal materials over time are reduced to two intervals.

The modeling results presented by Stein and Zelinski 2003b with the simplified shaft seal do show differences in pressures and brine saturations when compared to the PAVT results. However, the differences are only slight and considered by the Agency not to be significant. Although brine flow up the shaft decreased with the simplified shaft conceptualization, the releases to the Culebra will not be significantly affected because (1) the amount of brine entering the Culebra from an intrusion borehole far exceeds any brine contributions from the shaft, and (2) such small volumes of brine are unlikely to have ever contacted waste which is hundreds of meters below the Culebra. Therefore, the Agency accepts the Salado Flow Peer Review Panel's conclusions and a simplified version of the shaft seal model can be adopted for PA.

Double Wide Panel Closure Concrete in North End of Repository

In the TBM grid, an Option D panel closure was included between the operations area and the experimental area. In the CRA grid, the bottom of the simplified shaft that is represented by the material CONC_MON replaced this panel closure. This material is the same that was used for the bottom of the original shaft model implemented in the PAVT calculations. To account for this panel closure that is immediately south of the shaft, the dimensions of the concrete portion of the panel closure located between the northern rest of repository and the operations area was doubled (7.9 m × 2 = 15.8 m). This ensures that gas produced in the waste regions must effectively travel though the same number of panel closures to reach the experimental area as was modeled in the TBM. This is an important part of the revised conceptual model of repository geometry that was presented to the Salado Flow Peer Review panel. The Agency believes this depiction is more realistic that that used in the PAVT and accepts this new configuration.

Implementation of the Conceptual Model of DRZ Fracture in the TBM

In the TBM implementation of the conceptual model of DRZ fracture, the permeability and porosity in the DRZ were represented as they were for the PAVT. However, DOE did not believe that fracturing should be allowed in the DRZ above the repository and therefore did not apply the fracturing model to this region of the grid. The upper DRZ was allowed to fracture in the PAVT in order to provide a gas path in the case of unrealistically high repository pressures. The PAVT analysis did not find unrealistic pressures in the repository; hence DOE determined that the upper DRZ fracturing was not necessary for the TBM analysis since a fracture path was available in the lower DRZ. The argument DOE made for allowing the lower DRZ to fracture was as follows. There is only a 1.4 m section of Salado halite between the repository floor and Marker Bed (MB) 139. As rooms close, the floor heaves and fractures, and in the presence of higher gas pressures, fractures are not expected to heal thereby maintaining a hydraulic connection to MB 139. For this reason, fracturing was allowed only in the DRZ below the repository in the TBM. The Agency accepts DOE's arguments and fracturing in the DRZ above the repository does not need to be considered in PA.

Revision to the TBM Conceptual Model of DRZ Fracture. The proposed move of the repository horizon up 2.4 meters to Clay Seam G led to a re-evaluation of hydrofracture studies conducted in the WIPP underground in salt (Wawersik and Stone 1989) and required that the assumptions about allowing (or not allowing) fracturing in the grid elements representing the DRZ be modified from the conceptual model presented for the TBM (Hansen et al. 2002). Specifically, given the results of the hydrofracture studies (Wawersik and Stone 1989), and considering the variable permeability assigned to the DRZ, it is not justified to allow fracturing to occur in both the upper and lower DRZ. The move to Clay Seam G clarified the need for this change but even in the half of the repository that is not raised, DOE believes that the modification is still appropriate.

Figure 9-5 (Stein and Zelinski 2003c) compares the raised and unraised repository configurations in relation to the surrounding stratigraphy. In particular, in the raised half of the repository, the distance through the lower DRZ from the repository floor downward to MB 139 increases from 1.4 m to approximately 3.8 m. This change means that fracturing associated with floor heave will likely be reduced in this part of the repository.

The raised waste rooms have ready access to the Anhydrite "B" layer which will now be excavated to define the ceilings for the raised waste rooms. Anhydrite "B" is a thin ($\simeq$6 cm-thick), layer that is present directly above Clay Seam G. In the event of high repository pressures, DOE believes it is just as likely that a fracture pathway might form (1) parallel to the roof of the repository via Anhydrite "B," (2) vertically through the 2 m-thick DRZ to Anhydrite "A," or (3) perhaps all the way to MB 138 or, 3.8 m into the floor to MB 139.

The results of hydraulic fracturing tests performed in WIPP salt, from excavated rooms (Wawersik and Stone 1989), indicate that the pressures at which hydraulic fracturing is initiated fall in a similar range as for hydrofracture tests done in anhydrite Marker Beds 139 and 140 (Wawersik et al. 1997). Fracture initiation pressures for the anhydrite tests ranged from 7.36 to 12.46 MPa with an average initiation pressure of 10.5 MPa. For comparison, the fracture initiation pressures for the salt tests ranged from 4.14 to 17.24 MPa with an average initiation pressure of 11.98 MPa (Wawersik and Stone 1989). One important difference in the fracture behavior of intact salt is that because it is so impermeable, fractures in WIPP salt will tend to stop at more permeable anhydrite marker beds and change direction, moving along the bed rather than fracturing across beds (Wawersik et al. 1997). These data indicate that fractures in both materials will typically initiate at pressures below lithostatic, and thus repository pressures significantly above lithostatic are unjustified and unexpected.

Because the data support the application of the fracture model to intact salt as well as to the Marker Beds, DOE allows fracturing in both the upper and lower DRZ in the CRA analysis. Even in the parts of the repository that are not being raised to Clay Seam G, DOE notes that the test results support implementing the fracture model to both the upper and lower DRZ, considering the inherent uncertainty in exactly how the system will behave under possible near-lithostatic stresses. The important process that the fracture model simulates is the bleed off of very high pressures. Whether these pressures will bleed off through the upper or lower DRZ is not known, and therefore DOE allows it to go in either direction and lets the model determine which way is more favorable under the specific conditions in each vector. DOE also believes

that the parameters used by the BRAGFLO fracture model and applied to the Marker Bed materials and the DRZ are justified, because they do not allow repository pressures to significantly exceed lithostatic pressure.

The Agency believes that the processes should be modeled as realistically as reasonably practicable. Since the rock will fracture once lithostatic pressures are exceeded, the DRZ should be allowed to fracture. Furthermore, the pressure distribution within the repository should be relatively uniform at both the top and the bottom. Therefore, DOE's conceptualization that both the upper and lower DRZ's can fracture is appropriate.

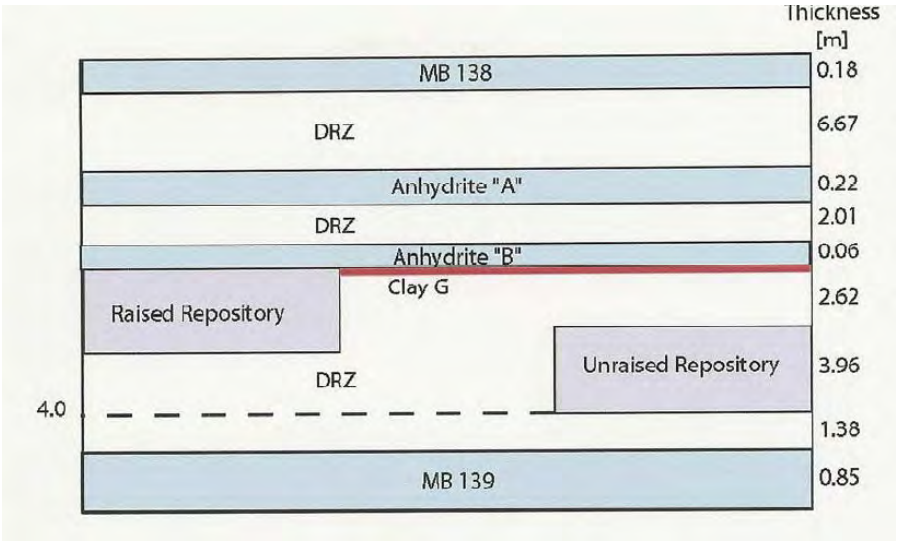

Figure 9-5. Schematic of the Stratigraphy Surrounding the Raised and Unraised Sections of the Repository
(Not to scale)
(Source: Stein and Zelinski 2003c)

Interaction between DRZ and Option D Pane1 closures. In the CRA grid, DOE represents regions where the Option D panel closures and the shaft intersect a Marker Bed as isolated blocks of marker bed material. DOE believes this representation is warranted for two reasons.

First, the marker bed material has a very similar permeability distribution (10^{-21} to $10^{-17.1}$ m^2) as the concrete portion of the Option D panel ($10^{-20.699}$ to $10^{-17.}$ m^2), and thus assigning this material as anhydrite marker bed in the model has essentially the same effect as referring to it as concrete, as long as pressures are below the facture initiation pressure.

Second, in the case of high pressures (near lithostatic) it is expected that fracturing may occur in the anhydrite marker beds and flow could go "around" the pane closures out of the 2-D plane considered in the model grid. In this case the flow would be through the marker bed material that is already allowed to fracture. Therefore, DOE believes that assigning these isolated cells as anhydrite marker bed materials is appropriate.

The Agency agrees with DOE's rationale for the assignment of Option D parameters within the grid.

Minor Repository Volume Error Corrected

DOE identified a minor error in the dimensions of the TF3M grid during the CRA calculations and documented by Stein in a memo to M.K. Knowles (Stein 2002). Fixing this error required adjusting the delta Z dimensions of the rest of repository blocks. This was done for the CRA grid.

Computational Models

BRAGFLO

Since the CCA PA, the BRAGFLO code has undergone a series of revisions. Versions 4.00 and 4.01 of BRAGFLO were used in the WIPP CCA. BRAGFLO 4.00 was used to calculate Salado flow; BRAGFLO 4.01 was used to calculate direct brine releases. These codes were validated on a DEC Alpha 2100 with the OpenVMS 6.1 operating system by demonstrating that the results of each test case met the acceptance criteria defined in the RD/VVPs (EPA 2004e).

BRAGFLO 4.10 was created to combine the capabilities of both BRAGFLO 4.00 and BRAGFLO 4.01 into a single code version. No new functionality was added. BRAGFLO 4.10 was validated on a DEC Alpha 2100 with OpenVMS 6.1 by demonstrating that the results of each test case met the acceptance criteria defined in the RD/VVP. Several changes were made to BRAGFLO 4.10 during its revision to BRAGFLO 5.0. This included removing a number of parameter assignments from embedded data to input data; moving the porosity surface from embedded data to input data; and changing the input-output format.

In June 2003, the EPA completed a report documenting the Agency's approval with respect to the migration and verification of BRAGFLO 4.10 (EPA 2003b) on those operating systems. For the CCA, the DOE modified BRAGFLO 4.10 to produce BRAGFLO 5.0 to allow the user to input information that was previously included in the BRAGFLO executable file. Beginning with BRAGFLO 5.0, the user will provide various constants and molecular weights as well as information defining the porosity surface, which comes from the SANTOS software. Changes from BRAGFLO 4.10 to BRAGFLO 5.0 involve input/output issues.

In January 2003, two new hardware systems were added to conduct performance assessments for the WIPP; a Compaq ES45 and a Compaq Alpha 8400, both running OpenVMS 7.3-1. EPA concluded that BRAGFLO 4.10 and BRAGFLO 5.0 meet the EPA acceptance criteria (EPA 2004e).

NUTS

For the PAVT, the DOE used NUTS for isothermal transport in the rock matrix. Consequently, the validation test demonstrated a subset of the capabilities of the NUTS code. Since the PAVT, the NUTS code has undergone a series of revisions. NUTS Version 2.02 was used in the PAVT.

During the PAVT, an error was found in NUTS 2.02; correction of this error resulted in NUTS Version 2.03. NUTS Version 2.05 was developed from NUTS 2.03 by adding the capability to calculate solubility limits with an implicit precipitation model. NUTS Version 2.05 was used for CRA and PABC.

EPA concluded that NUTS 2.05A met the specified EPA acceptance criteria (EPA 2004e).

SANTOS

Several steps must be completed before the BRAGFLO analysis can begin. Creep closure calculations (SANTOS) must be complete and an ASCII input file created that contains information about the porosity surface(s) to be used in the BRAGFLO calculation. The ASCII file used for the PABC is identical to those used for the PAVT and CRA calculations.

In 2005, the Agency reviewed SANTOS and concluded that although the accuracy of the SANTOS calculations may be limited, the SANTOS model is capable of reproducing the fundamental aspects of the conceptual model including simulation of the large-scale halite deformation and waste compaction accompanying room closure (EPA 2005f). EPA further concluded that the approximations of room closure and waste compaction developed by the SANTOS model are adequate for use in WIPP PA.

9.1.3 Modifications Since the CRA

Kanney and Leigh 2005 describe the transport calculations that are part of the "Salado Flow and Transport Calculations for the PABC." Specifically, that document covers the calculations to determine the mobilization and subsequent migration of radioisotopes throughout the repository, the shaft system, the Salado formation, and possible human intrusion boreholes. EPA required that DOE revise the CRA analysis and present results before EPA would judge the CRA to be complete (Cotsworth 2005). EPA noted a number of technical changes and corrections to the CRA that it deemed necessary.

Additionally, the EPA stated that a number of modeling assumptions used in the CRA have not been sufficiently justified and that alternative modeling assumptions must be used. The issues and changes mandated by the EPA for the PABC that affect the BRAGFLO\NUTS portion of WIPP PA can be found in Analysis Plan AP-122 (Kanney and Leigh 2005) and Cotsworth 2005, and include:

(1) Inventory information was updated (Crawford 2005).

(2) Parameters describing the bulk compressibility and residual gas saturation for the marker bed materials were changed to constants (Vugrin et al. 2005).

(3) Changes to the parameter describing the probability of microbial gas generation in the repository were made (Nemer 2005c).

(4) Methanogenesis is no longer assumed to be the primary microbial gas generation reaction (Nemer and Zelinski 2005).

(5) Microbial gas generation rates were revised to be consistent with long-term laboratory experimental results (Stein and Nemer 2005).

(6) The LHS software was revised (Vugrin 2004a).

For Items 1–5, Section 7 of this report compares the results of calculations for the PABC to results of earlier analyses, including the CRA and the PAVT. As mentioned above, significant changes to the BRAGFLO model include new significantly lower microbial gas generation rates and the removal of methanogenesis from the microbial-gas generation model. The new lower gas generation rates lead to a slower rate of pressurization of the repository, but the overall pressure at 10,000 years is not significantly different from the CRA. The effect of the removal of methanogenesis on BRAGFLO results is negligible.

DOE discovered two errors in the LHS software, Version 2.41 (Vugrin 2004a). These errors have been corrected, and a new version of the LHS software (Version 2.42) has been released (Vugrin 2005a). LHS Version 2.42 was used for the PABC. The first error in LHS Version 2.41 (Hansen 2004) affected the sampling of normal and lognormal distributions. The software is supposed to sample between the 1st and 99th quantiles, but due to the manner in which the sampling technique was implemented, it could return values outside of the specified sampling range. The second error in LHS Version 2.41 (Vugrin 2004a) affected the sampling of Student's t- and log Student's t-distributions. The software constrained sampled values to be within the range of data points supplied for the distribution by the PABC. The technique that the software employed for sampling allowed multiple vectors to have the same value for a parameter. Additionally, constraining the sampled values by the data points may unnecessarily restrict the sampling range. LHS Version 2.42 corrected this error by sampling all Student's t- and log Student's t-distributions between the 1st and 99th quantiles. Additionally, all vectors are ensured to have distinct values for Student's t- and log Student's t-distributions.

The Agency has reviewed the LHS code corrections and is satisfied that the errors have been properly addressed (EPA 2006b).

Computational Grid

The BRAGFLO\NUTS grid used for PABC calculations is the same as that used for the CRA (Stein and Zelinski 2003b). This grid is shown as a logical grid with dimensions in Figure 9-4. The grid incorporates the repository, the Castile brine reservoir, the Salado Formation, bedded units above the Salado, the shaft, panel seals, and an intrusion borehole, used for disturbed scenarios. The analysis report for the CRA (Stein and ZeIinski 2003a) provides a detailed explanation of all the stratagraphic and other materials used to represent the repository and surrounding units.

Initial and Boundary Conditions

BRAGFLO simulation of brine and gas flow in the vicinity of the WIPP site requires the assignment of initial conditions including brine pressure, brine saturation, and concentrations of iron and biodegradable material. These initial conditions are provided to BRAGFLO through various pre-processing steps during which values are extracted or sampled from the WIPP PA Parameter Database.

At the beginning of each BRAGFLO run (scenario-vector combination), the model simulates a short period of time representing disposal operations. This portion of the run is called the initialization period and lasts for 5 years (from t = -5 to 0 years), corresponding to the time a typical waste panel is expected to be open during disposal operations. For the PABC, an additional pressure increment is added to the atmospheric pressure initial conditions than was used in the PAVT and CRA. This increment of 26,714 Pa is intended to account for a short period of time with a higher microbial gas generation rate (Nemer et al. 2005). In the PAVT and CRA, the initial pressure was set to 1 atmosphere (101,325 Pa). The boundary conditions assigned for the BRAGFLO calculations are unchanged from the PAVT and CRA.

EPA accepts the change in initial conditions as appropriate for the revised microbial gas generation model.

10.0 DIRECT RELEASES

Direct releases are defined as solid and liquid materials removed from the repository and carried to the ground surface through intrusion boreholes at the time of drilling. Direct releases occur in WIPP PA through cuttings and cavings releases, direct brine releases (DBR), and spallings releases. These release modes and their PABC calculations were evaluated and compared with releases projected in the PAVT.

10.1 CUTTINGS AND CAVINGS CALCULATIONS

Cuttings and cavings are the solid materials removed from the repository and carried to the ground surface by drilling fluid during the process of drilling a borehole that intersects the repository. Cuttings are the materials removed directly by the drill bit, and cavings are the materials eroded from the borehole walls by shear stresses from the circulating drill fluid (Vugrin 2005g, Section 4.1). The CUTTINGS_S code is used in WIPP PA to calculate cuttings and cavings release volumes. Inputs to the CUTTING_S code include drilling characteristics such as bit size, rotational velocity and drill fluid properties, as well as waste shear strength. The radiological properties of the cuttings and cavings release volumes are calculated by the CCDFGF code (Vugrin 2005b, Section 2.1).

10.1.1 Modifications since the PAVT

Although the CUTTINGS_S code has been revised a number of times since the PAVT, the fundamental cuttings and cavings calculation approach approved by the Agency for the PAVT has not changed. CUTTINGS_S Version 5.04 was used in the PAVT. It was subsequently revised to Version 5.04A and then to Version 5.10 used in the CRA PA. Following the CRA PA, CUTTINGS_S was revised to Versions 6.00 and 6.01, and then to Version 6.02 used in the PABC calculations.

The revision from CUTTINGS_S Version 5.04 to Version 5.04A was made to remove linkages to SDBREAD_LIB and an INGRES database library, which were no longer used, and to relink with the libraries CAMDAT_LIB, CAMCON_LIB, and CAMSUPES_LIB. When making these changes, CUTTINGS_S Version 5.04A was structured to replicate CUTTINGS_S Version 5.04 as closely as possible (Gilkey 2000).

CUTTINGS_S Version 5.10 was used in the CRA-2004. The revision from CUTTINGS_S Version 5.04A to Version 5.10 was primarily made to add interface capability with the new DRSPALL model, identified in CUTTINGS_S Version 5.10 as spallings model 4. Additional discussion of the interface between the CUTTINGS_S and DRSPALL codes is presented in Section 10.3. Another change to CUTTINGS_S Version 5.10 corrected a problem found in earlier versions of CUTTINGS_S of reporting duplicate properties, resulting in two properties with the same name (Hansen 2003a, Section 9.0; Hansen 2003b).

The following four principal modifications were made in revising CUTTINGS_S Version 5.10, used for the CRA, to Version 6.00 (Gilkey 2004).

(1) Unnecessary functionality was removed from CUTTINGS_S Version 5.10 when developing CUTTINGS_S Version 6.00. This included unneeded functionality related to radionuclide release calculations, the calibration capability, the PreCuttings capability, and the early spall models 1 and 2. Unneeded global variables were removed as output, and unneeded input parameters were no longer processed.

(2) A new master control file was prepared for CUTTINGS_S Version 6.00 to process multiple intrusion scenarios, vectors, cavities (repository regions), and borehole intrusions in a single execution. The new master control file also identified the input and output files, which were defined previously as VMS logicals. These changes resulted in a significant increase in computational efficiency.

(3) A comprehensive text output file was produced for CUTTINGS_S Version 6.00 that eliminated the need for a SUMMARIZE code step between CUTTINGS_S and PRECCDFGF. This output file contains all the cuttings, cavings, and spallings information for all vector/time/scenario/location combinations and increased computational efficiency.

(4) Additional modifications were made in CUTTINGS_S Version 6.00 to make the code easier to read and maintain. The free-field reader was replaced with the standard CAMCON_LIB reader and subroutines were renamed.

CUTTINGS_S Version 6.01 was created for the primary purpose of changing the procedure for mapping the set of DRSPALL vectors to the set of PA vectors. This procedure was changed to accommodate direct, one-for-one, mapping when the number of vectors in the two sets are equal (Vugrin 2005e). See the discussion of spallings calculations in Section 10.3 for additional information.

CUTTINGS_S Version 6.02 was used for the PABC calculations and has all the modifications and capabilities of CUTTINGS_S Versions 6.00 and 6.01. CUTTINGS_S Version 6.02 was created for the primary purpose of correcting a potential error in calculating the radius at which the drill fluid flow becomes laminar. The code was changed such that the inner radius cannot be greater than the outer radius. This was accomplished by adding an IF statement to Subroutine DRILL in CUTTINGS_S Version 6.02 that assigns a value of RORIG to the outer radius (ROUTER) if the outer radius becomes less than the constant inner radius (RINNER). RORIG is equal to RINNER and is defined as the drill bit radius, which is the same as the original borehole radius. ROUTER is calculated iteratively as a function of waste shear strength and the drilling characteristics, and the final value of ROUTER is the radius of transition to laminar flow for the given realization (Vugrin 2005d and 2005f).

In addition to correcting the radius calculations, two hardcoded parameters, the drilling mud shear rate (DRILLMUD:SHEARRT) and drilling mud flow rate (DRILLMUD:MUDFLWRT), were relocated to the parameter database. This change locates these material properties in an appropriate place where they can be more readily identified and evaluated (Leigh et al. 2005a, Section 2.9).

The Agency considers the foregoing modifications to the CUTTINGS_S code to be appropriate. Validation of the CUTTINGS_S code is reviewed in EPA 2006b.

10.1.2 Calculation Results

The cuttings and cavings direct releases calculated for the PABC are presented in Section 5.5.1 of the *2004 Compliance Recertification Application Performance Assessment Baseline Calculation* (Leigh et al. 2005a). The CUTTINGS_S code calculates cuttings and cavings together and the combined results were presented by Leigh et al. 2005a (Tables 5-4 and 5-5), in terms of cuttings and cavings cross-section areas. All realizations had cuttings releases and about 90% of the realizations also had cavings releases (Vugrin 2005b, Section 5.0). For purposes of comparison with waste volumes released by spallings, the cuttings and cavings contact-handled (CH) waste volumes were calculated by the Agency by multiplying their cross-section areas by the initial repository height of 3.96 m (Leigh et al. 2005a, p. 96). The release volumes for CH waste in the CRA-2004 PABC ranged from 0.30 m^3 to 3.41 m^3 and averaged about 1.0 m^3. The release volumes for remote-handled (RH) waste are somewhat less because of the smaller height of an RH waste canister (0.509 m) (Dunagan 2004). Cuttings and cavings continue to be calculated with fundamentally the same conceptual and mathematical models used in the PAVT and release volumes have remained essentially the same (Dunagan 2004; Leigh et al. 2005a, Section 5.5.1).

Cuttings releases occur with every borehole penetration and combined cuttings and cavings releases are lowest when no cavings occur. In addition, cuttings release volumes depend only on the drill bit diameter and the initial repository height, neither of which is treated as an uncertain parameter. Cuttings releases are therefore the same in every realization and have the relatively small release volume of 0.30 m^3. The cavings volumes generally account for the bulk of the cuttings and cavings releases and are affected by two uncertain parameters: the shear strength of the waste and the drill string angular velocity. Lower shear strengths and higher angular velocities result in greater cavings releases (Leigh et al. 2005a, Section 7.3). These results are reasonable and appropriate, and are similar to the results obtained in earlier PA analyses.

Figure 10-1 illustrates the differences between projected cuttings and cavings radionuclide releases for the PAVT and PABC. Comparison of these projections shows that the contribution of mean cuttings and cavings to total mean radionuclide releases remains essentially unchanged. The increase in projected cuttings and cavings releases at low probabilities shown in the intermediate CRA results was due to the addition of low-volume, high-activity waste streams to the WIPP inventory after the PAVT was completed (Leigh et al. 2005a, Section 6.2 and Figure 6-15). The subsequent decrease in projected releases in the PABC resulted from reductions in the projected radionuclide inventory of a key small volume but high radioactivity Los Alamos waste stream, as explained in Sections 2.1 and 6.2 of Leigh et al. 2005a.

10.2 DIRECT BRINE RELEASE CALCULATIONS

Direct brine releases occur when contaminated brine originating in the repository is driven up an intrusion borehole to the ground surface by repository gas pressure. DBR occurs only when the gas pressure exceeds the estimated 8 MPa hydrostatic pressure of the drilling fluid and the brine saturation exceeds the residual saturation of the waste material (Leigh et al. 2005a, Section 3.7).

The BRAGFLO code is used in WIPP PA with a two-dimensional plan view grid that dips 1^{o} to the south to calculate DBR. Inputs to the BRAGFLO code for DBR calculations include the location of drilling penetration of the repository (either an up-dip, a middle, or a down-dip location is selected), and repository conditions at the time of penetration including gas/brine pressure and brine saturation. DBR volumes are calculated for 78 combinations of intrusion time, intrusion location, and repository conditions (Leigh et al. 2005a, Section 5.5.3). Volume-weighted averages of repository conditions (pressure, saturation, porosity, and crushed panel height) at the time of penetration are taken from the CUTTINGS_S code (Vugrin and Fox 2005, Section 2) and used to interpolate DBR volumes for a given realization from the 78 combinations calculated by BRAGFLO. This approach was found to provide sufficient accuracy and is the same as used in the PAVT. The radiological properties of the DBR volumes are calculated by the CCDFGF code (Vugrin 2005b, Section 2.3).

10.2.1 Modifications since the PAVT

BRAGFLO Version 4.10 was used for calculating DBR volumes for the PAVT, and BRAGFLO Version 5.00 was used for calculating DBR volumes for the CRA and the PABC. The following modifications were made between these two versions (Stein et al. 2005, Sections 3 and 4).

- An error in the well productivity index was corrected (the factor 2π was missing).
- The Agency-mandated Option D panel closure was implemented in the DBR grid and calculation.
- The extent of the DRZ into the repository walls was reduced to reduce brine flow around a panel closure following a borehole intrusion.
- The volume-averaged initial repository pressures and brine saturations were calculated based on three repository waste regions (the single waste panel, south rest-of-repository, and north rest-of-repository) instead of the four regions used in the PAVT, to conform with the revised 10,000-year BRAGFLO grid.
- The DRZ height was corrected from 43.6 m to 44.5 m to conserve the total brine volume in the DRZ surrounding the waste between the DBR grid and the 10,000-year BRAGFLO grid.
- A “middle” borehole location was added between the up-dip and down-dip locations to better account for the increased waste panel isolation provided by the Option D panel closures.
- Additional calculation sets were performed as a result of the new borehole location.

The Agency considers the foregoing modifications to the BRAGFLO code to be appropriate. Validation of BRAFGLO Version 5.00 was reviewed in EPA 2004e.

10.2.2 Calculation Results

Only a fraction of realizations result in direct brine flow to the ground surface because of the dependence of DBR on repository pressure and brine saturation. For example, in Replicate R1 of the PABC only 721 of the 7,800 DBR calculations (or about 10%) resulted in direct brine flow to the surface. In general, release volumes were low or zero when the pressure and brine saturation were both low, but release volumes were also low when brine saturation was high because of the reduced relative permeability to gas flow (Leigh et al. 2005a, Figure 5-53).

Figure 10-2 illustrates the differences between projected direct brine radionuclide releases for the PAVT and PABC. Comparison of these projections shows that the projected contribution of DBRs to total radionuclide releases has increased. The increase is most notable at probabilities less than about 0.002, where mean direct brine radionuclide releases have become the greatest contributors to total mean direct release in the PABC (see, for example, Leigh et al. 2005a, Figure 6-6). This is attributed primarily to changes in the PABC that increased actinide solubilities (Leigh et al. 2005a, Section 6.4). These changes included increased solubilities and revising the solubility uncertainty range (Leigh et al. 2005a, Sections 2.5 and 2.6). Given these changes, the calculated increase in DBR radionuclide releases is reasonable.

10.3 SPALLINGS CALCULATIONS

Spallings releases occur when solid waste is ejected through an intrusion borehole by repository gas pressures that exceed the estimated 8 MPa hydrostatic pressure of the drilling fluid (Vugrin 2005c, Section 2.0). The rapid release of highly pressurized repository gas during repository penetration by a borehole can cause localized mechanical failure and entrainment of solid waste as the gas moves into and through the borehole. The DRSPALL code is used in WIPP PA to calculate spallings release volumes. Inputs to the DRSPALL code include borehole characteristics such as length, diameter, and drilling rate; the repository gas pressure; and physical properties of the waste including permeability, porosity, tensile strength, and particle diameter after tensile failure. The DRSPALL code is used to calculate spallings release volumes for four values of repository gas pressure (10, 12, 14, and 14.8 MPa) for a single drilling intrusion (Leigh et al. 2005a, Section 5.5.2). The release volume for a given borehole intrusion in PA is then interpolated from these results by the CUTTINGS_S code using the repository gas pressure calculated by BRAGFLO at the time of intrusion. This volume is multiplied by the average repository activity and the fraction of the repository occupied by waste to estimate the spallings radionuclide release. The radiological properties of the spallings release volumes are calculated by the CCDFGF code (Vugrin 2005b, Section 2.2).

10.3.1 Modifications since the PAVT

DRSPALL is a new code that was developed to replace the original SPALLINGS code used as a basis for the range of spallings volumes sampled in the PAVT. DRSPALL Version 1.00 was used in the CRA (Vugrin 2005c, Section 2.0). The conceptual basis for the DRSPALL code was reviewed and approved by an independent peer panel (Yew and Teufel 2003; Yew 2004). Two additional sensitivity studies made at the Agency's request (EPA 2004a [Docket A-98-49, Item II-B3-72], Comments G-8-1 and G-8-2; see DOE responses in DOE 2004a

[Docket A-98-49, Item II-B2-35] and DOE 2004c [Docket A-98-49, Item II-B2-37]) also had positive outcomes.

DRSPALL includes the option to specify either a hemispherical or a cylindrical spallings cavity. A spherical geometry is nominally selected for WIPP PA because it better represents the shape of small cavities. However, in realizations that result in larger cavities, the cavity radius can exceed the height of the repository. In such situations, DRSPALL is restarted in the cylindrical mode with an initial radius specified to be the height of the repository to account for the cavity created when DRSPALL was run in the spherical mode. The volume of spalled material from the spherical run is added to the volume from the cylindrical run to compute the total spalled volume (Vugrin 2005c, Section 4.2.4). The Agency believes that this approach provides a reasonable approximation of the total spalled volume.

DRSPALL Version 1.10 was used for the PABC. This version contains the following four procedural changes to the original DRSPALL Version 1.00 (Vugrin 2005c, Section 3.0).

(1) Uncertain DRSPALL parameters were included in the same Latin hypercube sample as the uncertain parameters for the other WIPP performance assessment codes. This ensured that no spurious correlations existed among the uncertain parameters, because the WIPP Latin hypercube sampling code LHS enforces zero correlations between parameters unless a correlation is specified (Vugrin 2005g, Section 5).

(2) A complete set of three replicates consisting of 100 vectors each was calculated. This approach is consistent with the total number of PA vectors and eliminated the need in CRA PA to map a smaller set of 50 DRSPALL vectors to a larger set of 300 PA vectors.

(3) The utility code MERGESPALL was prepared and qualified for use in combination with the SUMMARIZE code to create the DRSPALL input file used in the CUTTINGS_S code to improve the traceability of the spallings calculations and run controls when both hemispherical and cylindrical cavity geometries are used in a realization (Vugrin 2005c, Section 4.2.5 and Appendix C). The Agency considers the use of this utility code to be appropriate.

(4) The parameter SPALLMOD:RNDSPALL used to map the 50 DRSPALL vectors to the 300 PA vectors in CRA was unnecessary and not used in PABC.

Additional errors that affected spallings calculations were corrected in the CCDFGF code. In CCDFGF Version 5.00, used in the CRA calculations, the spallings radionuclide release from a single borehole intrusion was erroneously calculated by multiplying the spall volume by the average repository activity without correcting for the fraction of the repository volume occupied by CH waste. Also, an error in the input control files for the SUMMARIZE code incorrectly listed the variable representing the spallings area instead of the variable representing the spallings volume. These errors were corrected and both corrections are incorporated in CCDFGF Version 5.02 used in the PABC calculations (Kirchner and Vugrin 2004; Vugrin 2004b and 2005a). In considering the approval of the DRSPALL conceptual model by an independent peer review panel, the positive outcomes of two additional sensitivity studies

requested by the Agency, and the successful validations, the Agency concludes that the DRSPALL code is appropriate for use in WIPP PA.

The Agency considers the foregoing modifications to the DRSPALL and CCDFGF codes to be appropriate. Validation of these codes is reviewed in EPA 2006b.

10.3.2 Calculation Results

Spallings release volumes were calculated for the PAVT using a model that had not been approved but was adequately demonstrated to conservatively overestimate spallings releases (DOE 2004b, Appendix PA, Attachment MASS, Section MASS-16.1.3). The new DRSPALL model has been accepted by an independent peer panel and by the Agency; it predicts lower releases—relative to the PAVT model—as illustrated by Figure 10-3. This reduction was in part due to the new model, but was also in part due to reduced long-term microbial gas generation rates and consequent lower repository pressures (Leigh et al. 2005a). The spallings release volumes calculated for the PABC are presented in Section 5.5.2 of Leigh et al. 2005a. As expected, mean spall volumes increased with increasing repository gas pressure and amounted to 0.172 m^3 at 12 MPa, 0.665 m^3 at 14 MPa, and 0.978 m^3 at 14.8 MPa (Leigh et al. 2005a, Table 5-6). Maximum spallings releases ranged from 7.71 m^3 at 12 MPa to 14.5 m^3 at 14.8 MPa (Leigh et al. 2005a, Table 5-6). No spallings releases occurred at a repository gas pressure of 10 MPa.

The waste permeability, waste porosity, waste tensile strength, and waste particle diameter after tensile failure are treated as uncertain parameters in the DRSPALL model. The largest spall volumes occurred when the waste permeability was low. This is because the lower permeability leads to increased resistance to gas flow through the waste, resulting in greater tensile stresses and tensile failures. Smaller particle diameters also led to larger spall volumes because the smaller particles could be transported more easily by the escaping repository gas. These results are reasonable and consistent with the spallings conceptual model.

Although spallings releases in a given borehole intrusion could exceed 10 m^3 and could therefore be larger than the largest cuttings and cavings release of 3.41 m^3, the frequency of spallings release in the PABC was low because of its dependency on repository gas pressure. Approximately two-thirds of all vectors did not experience any spallings (Vugrin 2005b, Section 5.0) and spallings were therefore not large contributors to total releases.

10.4 PAVT AND PABC DIRECT RELEASE COMPARISONS

A comparison of projected direct radionuclide releases for the PAVT and PABC at the Agency's regulatory limits at 0.1 and 0.001 probabilities is presented in Table 10-1. Given that the direct release models have been found to be reasonable and appropriate for WIPP performance assessment, the Agency concludes that the modeling results presented in Table 10-1 are also reasonable and appropriate. Total releases modeled for the PABC are discussed and compared to both calculated PAVT releases and regulatory release limits in Section 11.0.

Table 10-1. Combined Mean PAVT and PABC Releases for all Replicates

Release Mechanism	Mean Release in EPA Units at Probability = 0.1		Mean Release in EPA Units at Probability = 0.001	
	PAVT	PABC	PAVT	PABC
Cuttings and Cavings	0.0732	0.0818	0.276	0.314
DBR	0.000300	0.000832	0.175	0.521
Spallings	0.0756	0.0000462	0.215	0.0509

Data from Vugrin 2005h, Table 1.

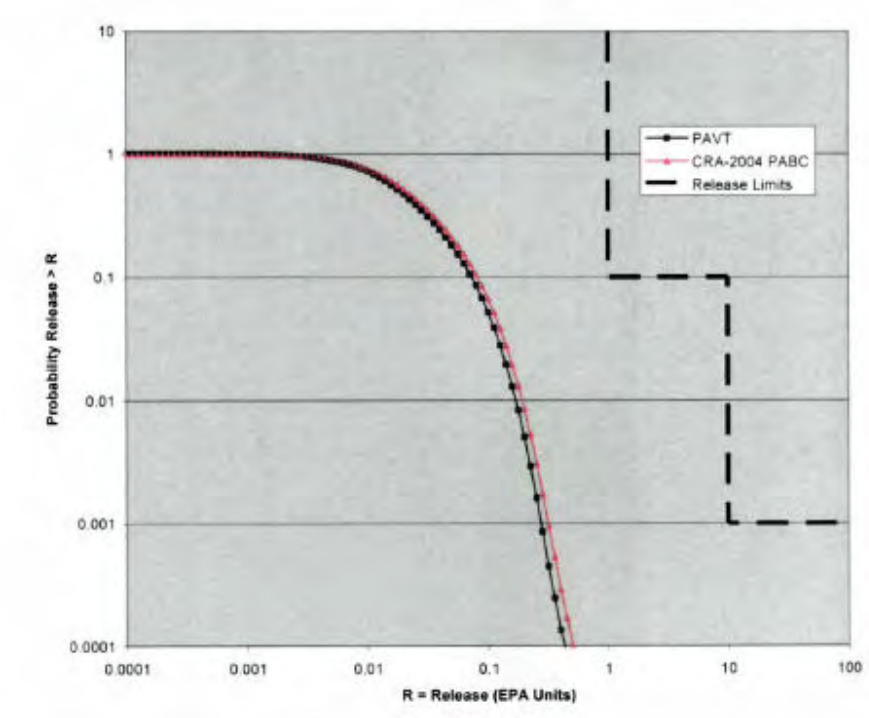

Figure 10-1. Combined Mean Cuttings and Cavings Release CCDFs for All PAVT and PABC Replicates
(Source: Vugrin 2005h, Figure 2)

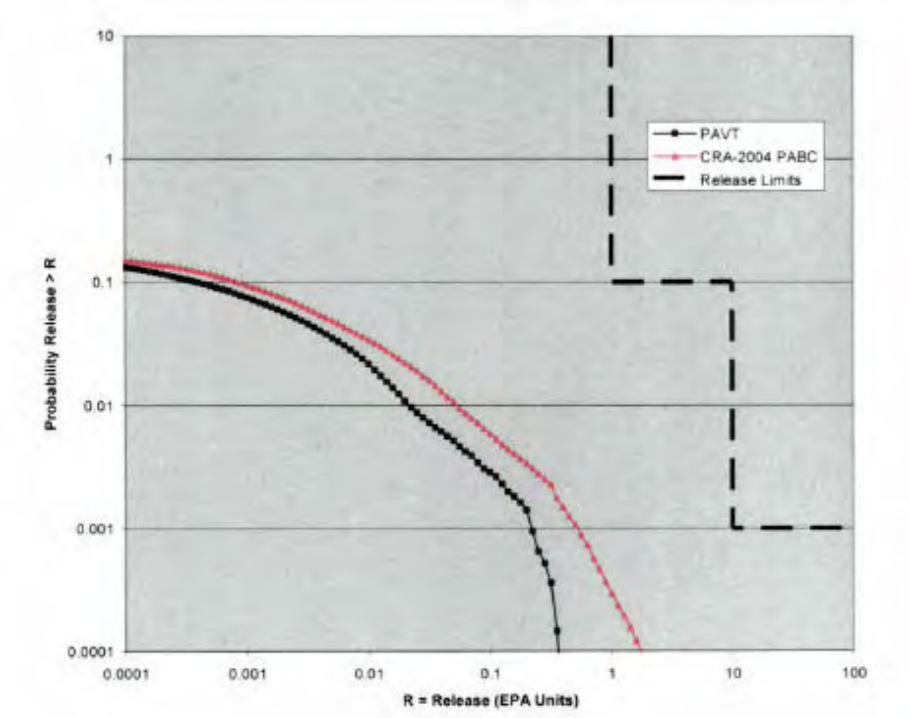

Figure 10-2. Combined Mean DBR CCDFs for All PAVT and PABC Replicates
(Source: Vugrin 2005h, Figure 4)

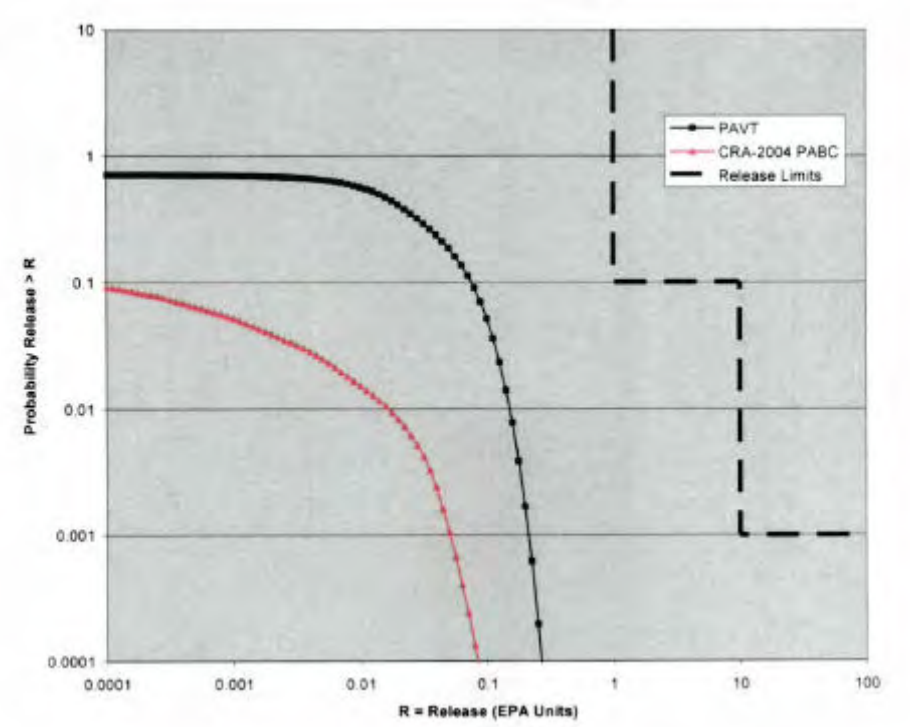

Figure 10-3. Combined Mean Spallings CCDFs for All PAVT and PABC Replicates
(Source: Vugrin 2005h, Figure 3)

11.0 RESULTS OF PABC PERFORMANCE ASSESSMENT CALCULATIONS

PABC performance assessment calculations were performed by the DOE to address the Agency's Containment Requirements (40 CFR 191.13), Individual Protection Requirements (40 CFR 191.15), and Groundwater Protection Requirements (40 CFR Part 191, Subpart C). In this section the performance assessment results are reviewed in the context of contributing release pathways and total releases. Undisturbed pathways (Section 11.1) are those that occur when there are no unlikely natural events or human intrusions into the repository and are used when addressing the Individual and Groundwater Protection Requirements. Human intrusion occurs if exploratory oil and gas boreholes disrupt the repository by intersecting the repository waste and creating new release pathways. These are called disturbed pathways (Section 11.2). Releases through both undisturbed and disturbed pathways are addressed in the Agency's Containment Requirements. The releases of the various radionuclides are normalized according to a procedure specified by the Agency (40 CFR Part 191, Appendix A). The normalized releases by undisturbed and disturbed pathways are then summed to project total releases for comparison with the Agency's Containment Requirements (Section 11.3). Upon completing the performance assessment calculations, the DOE performed a sensitivity analysis to determine which parameters have the greatest influence on the results (Section 11.4).

11.1 UNDISTURBED PATHWAYS

DOE has identified two credible pathways by which radionuclides could reach the accessible environment under undisturbed conditions (Leigh et al. 2005a, Section 4.1.3).

(1) Radionuclide transport may occur laterally, through anhydrite interbeds toward the subsurface boundary of the accessible environment in the Salado Formation.

(2) Radionuclide transport may occur through access drifts or anhydrite interbeds to the base of the WIPP shafts. In this case, if the pressure gradient between the waste panels and overlying strata is sufficient, contaminated brine may migrate up the shafts where they could be transported laterally away from the shafts, through permeable strata such as the Culebra, toward the subsurface boundary of the accessible environment.

The Agency concurs with this selection of pathways and notes that these pathways were also included in the Agency-mandated PAVT. These pathways are discussed in more detail in Sections 8 and 9. In both cases, brine flow is driven by high repository pressures.

11.1.1 Lateral Transport through Anhydrite Interbeds

Brine flow across the land withdrawal boundary under undisturbed conditions occurred in every replicate of the PAVT analysis. One vector in Replicate 1 of the PAVT analysis produced the relatively large brine flow across the land withdrawal boundary of 3,326 m^3; however, this flow was the result of an unusual combination of high interbed and DRZ permeabilities, a high repository pressure, and a low far-field pressure. Flows of this magnitude are improbable, as evidenced by maximum flows in Replicate 2 of 185 m^3 and in Replicate 3 of 130 m^3

(MacKinnon and Freeze 1997a, Section 1.1 and Table 2.1). Brine crossing the land withdrawal boundary is not necessarily contaminated with radionuclides because the brine may have been in storage in the interbeds at the start of the regulatory period and was never in contact with the waste. Radionuclide releases across the land withdrawal boundary in the PAVT were small (the maximum total integrated discharge was 4.84×10^{-10} EPA units), even considering the large brine flow in Replicate 1, and were thought by DOE to likely be artifacts of numerical dispersion (MacKinnon and Freeze 1997a, Section 3.1.1).

Small volumes of brine were also calculated in the PABC analysis to cross the land withdrawal boundary and enter the accessible environment by flowing through the anhydrite interbeds under undisturbed conditions. The maximum of any vector in Replicate 1, for example, was about 1,200 m^3 (Leigh et al. 2005a, Figure 4-17). Only one vector in the undisturbed PABC analysis was found to have the potential for the transport of radionuclides through the interbeds from the repository to the land withdrawal boundary. The maximum total integrated discharge across the land withdrawal boundary by this pathway in the undisturbed PABC analysis was 1.31×10^{-12} EPA units (Leigh et al. 2005a, Section 4.2.2). DOE again notes that this magnitude is smaller than the effective numerical precision of the transport calculations when numerical dispersion is considered (Leigh et al. 2005a, Section 4.2.2). The small undisturbed releases calculated through anhydrite interbeds in the PABC were therefore consistent with the small releases calculated in the PAVT.

11.1.2 Transport through Shafts

Small volumes of brine were projected in the undisturbed PABC analysis to flow up the sealed shafts to the Culebra dolomite. The maximum of any vector in Replicate 1, for example, was about 55 m^3, whereas typical volumes were less than 8 m^3 (Leigh et al. 2005a, Figure 4-16). Brine moving up the shaft and entering the Culebra is not necessarily contaminated with radionuclides because, as previously noted, it may not have been in contact with the waste. For the undisturbed repository, the brine volumes moving up the shaft were sufficiently small that no vectors showed radionuclide transport through the shafts to the Culebra (Leigh et al. 2005a, Section 4.2.1). Consequently, in the PABC analysis no radionuclides were calculated to be transported through the Culebra to the accessible environment under undisturbed conditions. Brine flow up the shaft in the PAVT analysis was also insignificant (MacKinnon and Freeze 1997a, Section 2.0).

11.1.3 Comparison with Individual Protection Standard

The Individual Protection Standard contained in 40 CFR 191.15 limits the maximum annual committed effective dose to 15 millirem. Undisturbed releases applicable to this standard can occur through the overlying Culebra dolomite via brine flow from the repository through the WIPP shafts or from lateral, subsurface brine migration to the accessible environment through anhydrite interbeds within the Salado repository host formation. In both the undisturbed PAVT and PABC analyses, brine flow up the shaft was insignificant and releases through the anhydrite interbeds were small and likely due to model limitations resulting from numerical dispersion. The Agency therefore considers the Individual Protection Standard to continue to be met.

11.1.4 Comparison with Groundwater Protection Standard

The Groundwater Protection Standard contained in 40 CFR 191.24(a)(1) states the following:

> *General. Disposal systems for waste and any associated radioactive material shall be designed to provide a reasonable expectation that 10,000 years of undisturbed performance after disposal shall not cause the levels of radioactivity in any underground source of drinking water, in the accessible environment, to exceed the limits specified in 40 CFR Part 141 as they exist on January 19, 1994.*

The National Primary Drinking Water Standards are specified by the Agency in 40 CFR 141. Both undisturbed release pathways considered in WIPP performance assessment have the potential to affect the groundwater. As stated above, in both the PAVT and PABC analyses, releases via the Culebra and anhydrite interbed pathways were not significant and the Agency therefore considers the Groundwater Protection Standard to continue to be met.

11.2 DISTURBED PATHWAYS

The DOE has identified six credible pathways by which radionuclides could reach the accessible environment under disturbed conditions (Leigh et al. 2005a, Section 5). These consist of the two pathways described above for the undisturbed repository plus the four additional pathways described below. The Agency concurs with this selection of pathways and notes that they were also included in the Agency-mandated PAVT. The four additional pathways consist of radionuclide releases via exploratory oil and gas boreholes that intersect repository waste. The first three of these additional pathways involve direct releases. These three pathways account for most calculated repository releases and are discussed in more detail in Section 10. The fourth pathway may occur because of releases of contaminated brine through a plugged borehole into the Culebra. These four pathways are characterized as follows:

(1) Radionuclides may be transported to the ground surface as borehole cuttings and cavings. These are the solid materials removed from the repository and carried to the ground surface by drilling fluid during the process of drilling a borehole that intersects repository waste. Cuttings are the waste materials removed directly by the drill bit, and cavings are the waste materials eroded from the borehole wall by shear stresses from the circulating drill fluid.

(2) Radionuclides may be transported to the ground surface when contaminated brine originating in the repository is driven up an intrusion borehole to the ground surface by repository gas pressures that exceed the estimated 8 MPa hydrostatic pressure of the drilling fluid. These are called direct brine releases (DBRs).

(3) Radionuclides may be transported to the ground surface when solid waste is ejected through an intrusion borehole by repository gas pressures that exceed the estimated 8 MPa hydrostatic pressure of the drilling fluid. These are called spallings releases.

(4) Radionuclides may be transported up to the Culebra dolomite through a degraded borehole seal and subsequently transported by moving groundwater through the Culebra to the subsurface boundary of the accessible environment.

The two drilling scenarios included in the PABC are the same as those in the PAVT. In the first scenario the borehole is assumed to pass through the repository and encounter a pressurized brine reservoir in the underlying Castile Formation. In this scenario, the borehole acts as a conduit connecting the brine reservoir with the repository and the repository with the ground surface. In the second scenario, the borehole is assumed to pass through the repository but does not encounter an underlying pressurized brine reservoir. In addition, the potential effects of climate change and mining for potash within the land withdrawal boundary on altering groundwater flow patterns in the Culebra are also considered.

11.2.1 Direct Releases

Direct radionuclide releases to the ground surface occur through cuttings and cavings, direct brine, and spallings releases. The calculated combined mean contributions of these release pathways to total releases are shown for the three replicates of the PAVT and PABC in Figures 11-1 and 11-2. These three release pathways account for nearly all calculated repository releases. Cuttings and cavings releases have changed little since the PAVT and continue to comprise the dominant release pathway at high probabilities. This is because contaminated drill cuttings are projected to be released to the ground surface in every intrusion borehole, and cavings releases are projected to occur in most intrusion boreholes. Calculated direct brine releases have increased significantly since the PAVT, particularly at low probabilities where they have become the dominant release pathway. This is primarily due to higher brine saturations resulting from lower microbial gas generation rates, and to changes in the PABC that increased actinide solubilities. Calculated spallings releases have decreased significantly since the PAVT at both high and low probabilities. This reduction was in part due to the new DRSPALL model, but was also in part due to reduced long-term microbial gas generation rates and consequent lower repository pressures. These models and their results are discussed in detail in Section 10.

11.2.2 Releases through the Culebra

The PABC results show that the volume of contaminated brine flowing through borehole plugs to the Culebra is typically calculated to be less than 10,000 m^3, but is occasionally calculated to range up to or exceed 100,000 m^3 (Leigh et al. 2005a, Figure 5-23). Maximum releases of brine to the Culebra in the PAVT analysis by disturbed pathways also exceeded 100,000 m^3 (MacKinnon and Freeze 1997a, Section 1.1). Computed subsurface radionuclide releases under disturbed conditions from the Culebra at the land withdrawal boundary during the 10,000-year regulatory time frame were small in both the PAVT and the PABC, primarily due to a combination of physical and chemical retardation during transport through the Culebra (DOE 2004b, Section 6.0.2.3.7). Most computed non-zero releases were vanishingly small and were attributed by DOE to numerical error inherent in transport calculations. Only ^{234}U species and its ^{230}Th decay product were transported to the land withdrawal boundary in any significant amount in both the PABC (Leigh et al. 2005a, Section 5.4.4) and in the PAVT (MacKinnon and Freeze 1997a, Section 1.1).

Releases through the Culebra were low probability events. In the PABC, normalized Culebra releases larger than 10^{-6} EPA units occurred only in Replicate 2 (Vugrin and Dunagan 2005, Section 4.5 and Figure 4.7). At the regulatory probability of $1x10^{-3}$, the release through the Culebra in Replicate 2 was about $1x10^{-4}$ EPA units. Because Culebra releases occurred in only one replicate, the combined mean release through the Culebra for all replicates, shown in Figure 11-2, was reduced to one-third of the Replicate 2 release due to the averaging process. The Culebra releases under disturbed conditions in the PABC were as much as four orders of magnitude smaller than typical direct releases. In the PAVT analysis, Culebra releases under disturbed conditions occurred in every replicate but were also small. At the regulatory probability of $1x10^{-3}$, the overall mean PAVT release from the Culebra was about $8x10^{-4}$ EPA units (MacKinnon and Freeze 1997a, Figure 7-5). At the regulatory probability of $1x10^{-1}$, Culebra releases in both the PAVT and PABC were less than 10^{-6} EPA units. The lower Culebra releases in the PABC were likely due to the reduced hydraulic gradient observed in late 2000 that was used when recalibrating the Culebra flow model (DOE 2004b, Appendix PA, Attachment MASS, Section MASS-15.1; Detwiler 2004g, Response to EPA Comment G-7). Disturbed releases through the Culebra were small in both the PABC and PAVT, and were not significant contributors to the total mean release in either analysis.

In addition, none of the 300 realizations in the PABC showed transport of radionuclides through the shaft to the Culebra under disturbed conditions (Leigh et al. 2005a, Section 5.4.2). Transport of radionuclides to the accessible environment through the shaft was also insignificant in the PAVT (MacKinnon and Freeze 1997a, Section 3.0).

11.2.3 Releases through Anhydrite Interbeds

None of the 300 realizations in the PABC resulted in transport of radionuclides through the anhydrite interbeds and across the land withdrawal boundary under disturbed conditions (Leigh et al. 2005a, Section 5.4.2). In the PAVT analysis the unusual Replicate 1 vector that produced a large brine flow across the land withdrawal boundary under undisturbed conditions (see Section 11.1.1) also produced brine flows greater than 2,000 m^3 across the land withdrawal boundary under the disturbed scenarios (MacKinnon and Freeze 1997a, Tables 2.2 through 2.6). Despite the greater brine flows across the land withdrawal boundary in the PAVT, transport of radionuclides to the accessible environment via the interbeds was insignificant (MacKinnon and Freeze 1997a, Section 3.0).

11.3 TOTAL NORMALIZED RELEASES

Total normalized releases are calculated by totaling the releases from each pathway and primarily consist of cuttings and cavings releases, DBRs, spallings releases, and releases from the Culebra. As previously noted, there were no releases from transport up the shaft in the PABC and no disturbed releases through the anhydrite interbeds. Undisturbed releases through the anhydrite interbeds in the PABC were as much as 11 orders of magnitude smaller than the typical disturbed releases, and were therefore not significant contributors to total normalized releases.

Combined mean normalized releases from the four primary release pathways and total combined mean normalized releases for the PAVT and PABC calculations are compared in Table 11-1 at the Agency's regulatory probabilities of 0.1 and 0.001. In addition, total combined mean normalized releases for the PAVT and PABC calculations are compared in Figure 11-3. The combined mean CCDF is computed as the arithmetic mean of the three mean CCDFs from each replicate. It is noted that the total releases are less than the sum of the component releases at the given probabilities. This is because the ranked percentiles generally correspond to different realizations for the individual release mechanisms, whereas the total releases represent the combination of all release mechanisms that occur in a given realization.

The increased releases at low probabilities in the PABC illustrated in Figure 11-3 reflect the increased DBRs and, as described in Section 10.2.2, are primarily due to higher brine saturations resulting from lower microbial gas generation rates, and to changes in the PABC that increased actinide solubilities. As can be seen from Table 11.1, for the PABC both the calculated mean releases and the upper 95% confidence levels on the mean have remained less than the regulatory limits at both 0.1 and 0.001 probabilities. Therefore, the Agency concludes that the WIPP continues to comply with the containment requirements of 40 CFR 191.13.

Table 11-1. Combined Mean PAVT and PABC Releases for All Replicates

Release Mechanism	Mean Release in EPA Units at Probability = 0.1		Mean Release in EPA Units at Probability = 0.001	
	PAVT	PABC	PAVT	PABC
Cuttings and Cavings	0.0732	0.0818	0.276	0.314
DBR	0.000300	0.000832	0.175	0.521
Spallings	0.0756	0.0000462	0.215	0.0509
Culebra	no releases	no releases	0.000724	0.00000139
Mean Total Releases	0.130	0.0877	0.382	0.601
Upper 95% Confidence Level	0.1373	0.0907	0.436	0.681
Regulatory Limits	1.00	1.00	10.0	10.0

Calculation results from Vugrin 2006, Table 1.
EPA confidence level requirement from 40 CFR 194.34(f).
EPA regulatory limits from 40 CFR 191.13(a).

11.4 SENSITIVITY ANALYSIS

Stepwise rank regression analyses were used by DOE to evaluate the sensitivity of the normalized releases to the sampled parameters. The results of these analyses for the PABC are presented in Leigh et al. 2005a (Section 7), and the results for the PAVT are presented in MacKinnon and Freeze 1997b (Section 6). These analyses compare the sampled input parameter values with the calculated release data to rank the relative importance of the parameters in their effect on releases. The calculated release is considered sensitive to a parameter if changes in the parameter value over its range of uncertainty result in large changes in the calculated release. The analysis results are limited to parameters that were treated as epistemic uncertainties in the performance assessment.

Because cuttings, cavings, direct brine, and spallings releases account for an overwhelming majority of the total releases, the calculated total releases are most sensitive to uncertainties in the parameters governing these release mechanisms. The calculated total releases were found to be most sensitive to the parameters listed in Table 11-2. Increasing sensitivity is indicated by increasing absolute values of the standardized rank regression coefficients (SRRCs) and high correlation coefficient (R^2) values. In both the PAVT and the PABC analyses, total normalized releases were most sensitive to uncertainty in waste shear strength (WTAUFAIL), which is a key parameter governing cavings volumes. The negative correlation found for WTAUFAIL in the analysis indicates increasing releases with decreasing shear strengths, and is expected. In the PAVT analysis, the six remaining parameters in Table 11-2 are all associated with spallings releases. BHPRM is the borehole permeability; VOLSPALL is the sampled released spallings volume; WMICDFLG is a flag for microbial degradation of cellulose; HALPOR is the halite porosity; DRZPRM is the DRZ permeability; and PBRINE is the probability that a drilling intrusion penetrates a Castile brine reservoir. VOLSPALL directly affects the size of a spallings release and the remaining parameters influence repository pressure.

In the PABC, direct brine releases supplant spallings as the second-most important contributor to total releases and even surpass cuttings and cavings at low probabilities (Figure 11-2). The second most important variable in the PABC analysis is WSOLVAR3, a solubility multiplier added to the PABC analysis to represent uncertainty in solubilities for all actinides in the +3 oxidation state. This parameter increased the radionuclide concentration in direct brine releases. The drill string angular velocity (DOMEGA), used in computing cavings releases, appears third.

Each of the remaining parameters in Table 11-2 for the PABC analysis explains less than 1% of the variability in the total releases and is therefore not particularly significant to total uncertainty. WFBETCEL is a scale factor used in defining the stoichiometric coefficient for microbial gas generation; BPINTPRS is the initial brine pore pressure in the Castile brine reservoir; PBRINE is the probability that a drilling intrusion penetrates a Castile brine reservoir; SHURGAS is the residual gas saturation in the upper shaft seal materials; and SHLPRM2 is the permeability of the lower shaft seal materials for the first 200 years after repository closure. Most of these parameters affect brine saturation and repository gas pressure, which have important roles in direct brine and spallings releases. The presence of the parameters SHURGAS and SHLPRM2 on this list is probably the result of statistical noise because no releases were calculated to occur through the shafts.

Table 11-2. Stepwise Rank Regression Analysis Results

Step[a]	Expected Normalized Release					
	PAVT			PABC		
	Parameter[b]	SRRC[c]	$R^{2(d)}$	Parameter[b]	SRRC[c]	$R^{2(d)}$
1	WTAUFAIL	-0.61	0.39	WTAUFAIL	-0.94	0.88
2	BHPRM	-0.40	0.56	WSOLVAR3	0.14	0.91
3	VOLSPALL	0.33	0.66	DOMEGA	0.10	0.92
4	WMICDFLG	0.27	0.74	WFBETCEL	-0.09	0.93
5	HALPOR	0.13	0.76	BPINTPRS	0.08	0.93
6	DRZPRM	0.12	0.78	PBRINE	0.07	0.94
7	PBRINE	0.12	0.79	SHURGAS	-0.06	0.94
8	- -	- -	- -	SHLPRM2	0.06	0.95

PAVT results from MacKinnon and Freeze 1997b, Table 6.1.1
PABC results from Leigh et al. 2005a, Table 7-2

(a) Steps in stepwise regression analysis
(b) Parameters listed in order of selection in regression analysis
(c) Standardized Rank Regression Coefficient in final regression model
(d) Cumulative R^2 value with entry of each variable into regression model

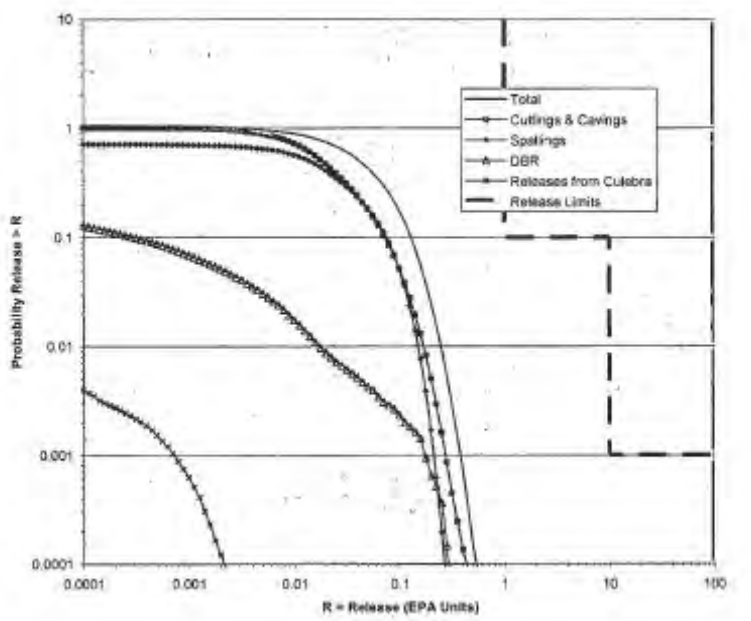

Figure 11-1. Combined Mean CCDFs for Components of Total Normalized Releases for All PAVT Replicates
(Source: Vugrin 2006, Figure 1)

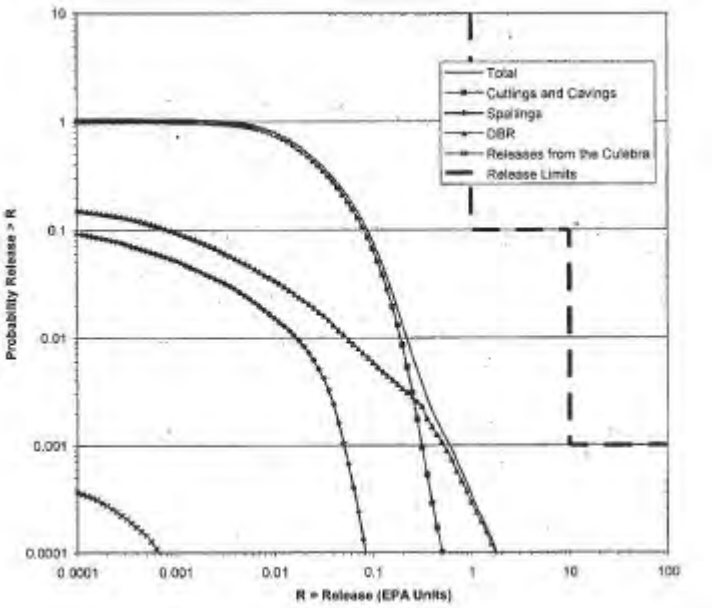

Figure 11-2. Combined Mean CCDFs for Components of Total Normalized Releases for All PABC Replicates
(Source: Vugrin 2006, Figure 2)

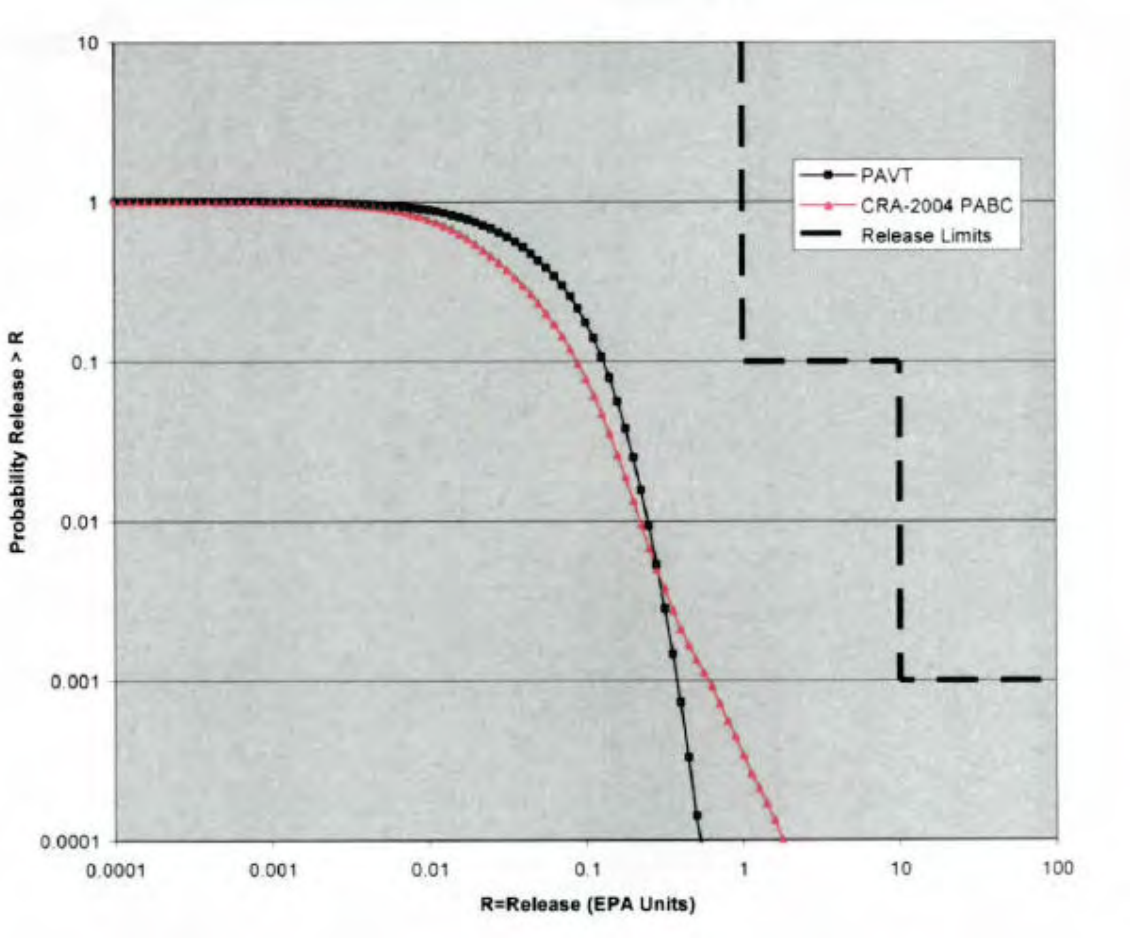

Figure 11-3. Combined Total Mean Normalized Release CCDFs for All PAVT and PABC Replicates
(Source: Vugrin 2005h, Figure 1)

12.0 SUMMARY AND CONCLUSIONS

In its March 4, 2005 letter (Docket A-98-49, Item II-B3-80), EPA advised DOE that a revised PA was required for recertification, replacing the PA included in the March 26, 2004 Compliance Recertification Application submitted by DOE. EPA's review as to the whether the requested changes were appropriately implemented in the revised performance assessment (the PABC) is summarized below.

Actinide Solubilities

EPA stated that the solubility of U(+VI) needed to be changed to a fixed value of 1×10^{-3} M because of experimental data that became available since the CCA. In addition, EPA required that new solubility uncertainty ranges, based on the FMT database and currently available experimental solubility data, be incorporated into the PABC. DOE made additional changes to the calculation of the +III, +IV, and +V actinide solubilities based on revised thermodynamic data for the +IV actinides, a different Salado brine formulation, and revised concentrations of organic ligands. The organic ligands concentration changes were the result of corrections of the masses of organic ligands and the minimum estimated brine volume required for a release from the repository. These changes were properly implemented as discussed in Section 7.

Methanogenesis

Based on the inventories of nitrate and sulfate in the waste, DOE assumed in the CRA PA that these constituents would be quickly consumed during microbial degradation of CPR in the waste, and that methanogenesis would therefore be the dominant microbial degradation reaction. However, adequate sulfate anions are likely to be available in the anhydite interbeds and will insure that methanogenesis does not occur regardless of the quantity of sulfate in the waste. Because DOE had not conclusively demonstrated that methanogenesis would be the dominant pathway for microbial degradation reactions, the model required revision. As discussed in Section 6, this pathway was eliminated by DOE in the PABC and only denitrification and sulfate reduction reactions were included in the microbial gas generation model. Based on revised PABC inventory values, 4% of the microbial gas generation is from denitrification and 96% is from sulfate reduction. These reactions will produce one mole of carbon dioxide for each mole of CPR carbon consumed by microbial degradation. As described in Section 6, DOE has adequately revised the microbial gas generation reactions and evaluated the effects on PA.

Packaging Materials

Packaging materials associated with emplacement of waste within the repository can affect the amounts of gas generated by microbial degradation reactions. These materials were not included in the CRA PA, but as required by EPA they were included in the PABC. As discussed in Section 3, cellulosics and plastics associated with emplacement materials were added to the CPR inventory.

Ten-Drum Overpack

DOE assumed in the CRA that one ten-drum overpack (TDOP) would occupy the same space as three seven-packs of 55-gallon drums. Based on a site inspection, EPA determined that one TDOP would occupy the space of only two seven-packs, creating the possibility that one seven-pack could be placed on top of a TDOP. EPA required that the revised PA inventory reflect this EPA finding. DOE addressed this issue in the PABC Inventory Report (Leigh et al. 2005b) noting that the cuttings/caving model assumes that each intrusion encounters a stack of waste with an initial height of 3.96 m. It is immaterial whether this height is achieved with a stack of three seven-packs or one TDOP and one seven-pack. Based on the acceptability of this explanation, no change was required in the PABC to reflect EPA's finding.

Culebra Transmissivity Fields

Two new computer codes, MODFLOW-2000 and PEST, have replaced SECOFL2D and GRASP-INV for the PABC. The Agency finds that these codes provide a significant enhancement in predicting groundwater flow and constructing Culebra transmissivity fields. Since the CCA, the DOE has continued to investigate the transmissivity of the Culebra. Although uncertainties remain, the introduction of a geologically-based conceptual model provides an improved means to predict the spatial variability of the Culebra. EPA required that the revised PA include updated transmissivity fields in the Culebra to better represent potash mining areas around the WIPP site. As discussed in Section 8, for the PABC, the potash mining areas were redefined to consist of all mined and unmined potash resources even if they fall within a one-half mile diameter exclusion zone around oil and gas wells. Transmissivity fields were modified based on this assumption and Culebra flow and transport were recalculated for the PABC.

Microbial Degradation

EPA required that the probability of microbial degradation be set at 100% rather than 50% as was done for the CRA. In addition, EPA permitted DOE to alter the rates of microbial gas generation from those used in the CRA as long as the changed rates of gas production were supported by appropriate data. As discussed in Section 6, the probability of microbial degradation of CPR materials was set at 100% as required. It was assumed, based on the available experimental data, that there would be a 75% probability of microbial degradation only of cellulosics, with a 25% probability that all CPR materials would be degraded. Also, as described in that section, the microbial gas generation rates were modified to reflect rates observed in long-term experiments. The Agency's review indicated that these changes are reasonably consistent with the available data and were correctly implemented in the PABC.

Inventory

Both DOE and EPA identified errors in the CRA inventory and changes made since the CRA inventory was developed that could impact PA. Consequently, EPA directed DOE to include revised and updated information in the revised PA. As discussed in Section 3, these changes were made for the PABC.

Computer Codes

DOE was required to correct several errors in computer codes used in the CRA. In addition, the number of realizations obtained during calculation of spallings releases was specified to be 300, consistent with the number of realizations from other models and codes. Changes to these codes affecting direct releases are documented in Section 9. A full set of 300 realizations was run with the spallings code (DRSPALL) as required.

Parameters

Many of the modifications required for the PABC, as outlined above, necessitated changes to parameters used in modeling performance assessment. As described in Section 5, EPA validated all parameters changes made from the CRA to the PABC.

12.1 CONCLUSION

Based on the information presented here, EPA is satisfied that the revised performance assessment (PABC) contains all of changes requested by the Agency. These changes are transparent, traceable against prior PAs, consistent with EPA direction, and have been properly implemented. The PABC results described in Section 11 show that the WIPP continues to comply with the containment requirements of 40 CFR 191.13.

13.0 REFERENCES

Al Mahamid, I., C.F. Novak, K.A. Becraft, S.A. Carpenter, and N. Hakem. 1998. Solubility of Np(V) in K-Cl-CO_3 and Na-K-Cl-CO_3 Solutions to High Concentrations: Measurements and Thermodynamic Model Predictions. *Radiochimica Acta* 81:93-101.

Altmaier, M., V. Neck, and T. Fanghänel. 2004. Solubility and Colloid Formation of Th(IV) in Concentrated NaCl and $MgCl_2$ Solution. *Radiochimica Acta* 92:537-543.

Beauheim, R.L. 2002a. *Analysis Plan for the Evaluation of the Effects of Head Changes on Calibration of Culebra Transmissivity Fields, AP-088, Revision 1*. ERMS 524785. Carlsbad, New Mexico: Sandia National Laboratories, WIPP Records Center.

Beauheim, R.L. 2002b. *Routine Calculations Report In Support of Task 3 of AP-088, Calculation of Culebra Freshwater Heads in 1980, 1990, and 2000 for Use in T-Field Calibration*. ERMS 522580. Carlsbad, New Mexico: Sandia National Laboratories, WIPP Records Center.

Beauheim, R.L., and R.M. Holt. 1990. *Hydrogeology of the WIPP Site in Geological and Hydrological Studies of Evaporites in the Northern Delaware Basin for the Waste Isolation Pilot Plant (WIPP), New Mexico*. D. Powers, R. Holt, R.L. Beauheim, and N. Rempe, eds. GSA Field Trip #14 Guidebook. Dallas, TX: Dallas Geological Society. 131-179.

Beauheim, R.L., and G.J. Ruskauff. 1998. *Analysis of Hydraulic Tests of the Culebra and Magenta Dolomites and Dewey Lake Redbeds Conducted at the Waste Isolation Pilot Plant Site*. SAND98-0049. Albuquerque, New Mexico: Sandia National Laboratories.

Brush, L.H. 2004. *Implications of New (Post-CCA) Information for the Probability of Significant Microbial Activity in the WIPP*. Sandia National Laboratories, Albuquerque, New Mexico, ERMS 536205.

Brush, L.H. 2005. *Results of Calculations of Actinide Solubilities for the WIPP Performance Assessment Baseline Calculations*. Analysis Report, Sandia National Laboratories, Carlsbad, New Mexico, ERMS 539800.

Brush, L.H., J. Garner, and E. Vugrin. 2005. *PA Implementation of Uncertainties Associated with Calculated Actinide Solubilities.* Memorandum to Dave Kessel, February 2, 2005. Sandia National Laboratories, Carlsbad, New Mexico, ERMS 538537.

Brush, L.H., and Y. Xiong. 2003a. *Calculation of Actinide Solubilities for the WIPP Compliance Recertification Application, Analysis Plan AP-098, Rev 1*. Unpublished Analysis Plan, Sandia National Laboratories, Carlsbad, New Mexico, ERMS 527714.

Brush, L.H., and Y. Xiong. 2003b. *Calculation of Organic Ligand Concentrations for the WIPP Compliance Recertification Application and for Evaluating Assumptions of Homogeneity in WIPP PA.* Sandia National Laboratories, Carlsbad, New Mexico, ERMS 531488.

Brush, L.H., and Y. Xiong. 2004. *Sensitivities of the Solubilities of +III, +IV, and +V Actinides to the Concentrations of Organic Ligands in WIPP Brines.* Rev 0, Sandia National Laboratories, Carlsbad, New Mexico, ERMS 538203.

Brush, L.H., and Y. Xiong. 2005a. *Calculation of Actinide Solubilities for the WIPP Performance-Assessment Baseline Calculations*. Analysis Plan AP-120, Rev. 0. Sandia National Laboratories, Carlsbad, New Mexico, ERMS 539255.

Brush, L.H., and Y. Xiong. 2005b. *Calculation of Organic-Ligand Concentrations for the WIPP Performance-Assessment Baseline Calculations*. WIPP:1.4.2.2:PA:QA-L539371. Sandia National Laboratories, Carlsbad, New Mexico, ERMS 539635.

Bynum, R. V. 1996. *Analysis to Estimate the Uncertainty for Predicted Actinide Solubilities*, WBS 1.1.10.1.1, Rev. 0, effective date 9/3/96, WPO41374.

Caporuscio, F., J. Gibbons, and E. Oswald. 2003. *Waste Isolation Pilot Plant: Salado Flow Conceptual Models Peer Review Report*. Report prepared for the U.S. Department of Energy, Carlsbad Area Office, Office of Regulatory Compliance. ERMS 523783.

Choppin, G.R., A.H. Bond, M. Borkowski, M. Bronikowski, J.-F. Chen, S. Lis, J. Mizera, O.S. Pokrovsky, N.A. Wall, Y.X. Xia, and R.C. Moore. 2001. *Waste Isolation Pilot Plant Actinide Source Term Test Program: Solubility Studies and Development of Modeling Parameters.* Sandia National Laboratories, Albuquerque, New Mexico, April 2001, SAND99-0943.

Cotsworth, E. 2004a. EPA's CRA Completeness Comments, 1st set. U.S. Environmental Protection Agency, Washington, DC. ERMS 535554. Docket A-98-49, Item II-B3-72.

Cotsworth, E. 2004b. EPA's CRA Completeness Comments, 2nd set. U.S. Environmental Protection Agency, Washington, DC. ERMS 537187. Docket A-98-49, Item II-B3-73.

Cotsworth, E. 2004c. EPA's CRA Completeness Comments, 3rd set. U.S. Environmental Protection Agency, Washington, DC. ERMS 536771. Docket A-98-49, Item II-B3-74.

Cotsworth, E. 2004d. EPA's CRA Completeness Comments, 4th set. U.S. Environmental Protection Agency, Washington, DC. ERMS 540236. Docket A-98-49, Item II-B3-78.

Cotsworth, E. 2005. EPA Letter on Conducting the Performance Assessment Baseline Change (PABC) Verification Test. U.S. EPA, Office of Radiation and Indoor Air, Washington, DC. ERMS 538858. Docket A-98-49, Item II-B3-80.

Crawford, B. 2005. Waste Material Densities in TRU Waste Streams from TWBID Revision 2.1 Version 3.13, Data Version D.4.15. Los Alamos National Laboratory, Carlsbad, New Mexico. ERMS 539323.

Crawford, B.A., and C.D. Leigh. 2003. Estimate of Complexing Agents in TRU Waste for the Compliance Recertification Application. Los Alamos National Laboratory, Carlsbad, New Mexico, ERMS 531107.

Davies, P.B. 1989. Variable-Density Ground-Water Flow and Paleohydrology in the Waste Isolation Pilot Plant (WIPP) Region, Southeastern New Mexico. Open-File Report 88-490. Albuquerque, New Mexico: U.S. Geological Survey.

Detwiler, P. 2004a. Initial Response to Environmental Protection Agency (EPA) September 2, 2004, Letter on Compliance Recertification Application [DOE Letter #6]. U.S. Department of Energy, Carlsbad, New Mexico. ERMA 540239. Docket A-98-49, Item II-B2-39.

Detwiler, P. 2004b. MgO Emplacement [DOE Letter #5]. U.S. Department of Energy, Carlsbad, New Mexico. ERMS 540238. Docket A-98-49, Item II-B2-38.

Detwiler, P. 2004c. Partial Response to Environmental Protection Agency (EPA) May 20, 2004, Letter on CRA. U.S. Department of Energy, Carlsbad, New Mexico. ERMS 537372. Docket A-98-49, Item II-B2-35.

Detwiler, P. 2004d. Partial Response to Environmental Protection Agency (EPA) May 20, 2004, Letter on CRA, [1st response submittal to EPA]. U.S. Department of Energy, Carlsbad, New Mexico. ERMS 537430. Docket A-98-49, Item II-B2-34.

Detwiler, P. 2004e. Response to Environmental Protection Agency (EPA) July 12, 2004, Letter on CRA. U.S. Department of Energy, Carlsbad, New Mexico. ERMS 537369. Docket A-98-49, Item II-B2-36.

Detwiler, P. 2004f. Response to EPA May 20, 2004, Letter on CRA [DOE Letter #4]. U.S. Department of Energy, Carlsbad, New Mexico. ERMS 540237. Docket A-98-49, Item II-B2-37.

Detwiler, R.P. 2004g. *Letter from R.P. Detwiler (DOE) to E. Cotsworth (EPA) dated August 16, 2004.* U.S. Department of Energy, Carlsbad, New Mexico, EPA Docket A-98-49, Item II-B2-35.

DOE (U.S. Department of Energy). 1994. *Waste Isolation Pilot Plant Transuranic Waste Baseline Inventory Report, Revision 0*, DOE/CAO-94-1005, Carlsbad, New Mexico. Department of Energy Carlsbad Area Office. June 1994. ERMS 503921.

DOE (U.S. Department of Energy). 1995a. *Waste Isolation Pilot Plant Transuranic Waste Baseline Inventory Report, Revision 1*, DOE/CAO-94-1005, Carlsbad, New Mexico. Department of Energy Carlsbad Area Office. February, 1995. ERMS 243201.

DOE (U.S. Department of Energy). 1995b. *Transuranic Waste Baseline Inventory Report, Revision 2*, DOE/CAO-95-1121, Carlsbad, New Mexico. Department of Energy Carlsbad Area Office. December, 1995. ERMS 531643.

DOE (U.S. Department of Energy). 1996a. *Transuranic Waste Baseline Inventory Report, Revision 3*, DOE/CAO-95-1121, Carlsbad, New Mexico. Department of Energy Carlsbad Area Office. June 1996. ERMS 242330.

DOE (U.S. Department of Energy). 1996b. *Title 40 CFR Part 191 Compliance Certification Application for the Waste Isolation Pilot Plant*, DOE/CAO-1996-2184, October 1996, Carlsbad Field Office, Carlsbad, New Mexico.

DOE (U.S. Department of Energy). 2000. Letter from Dr. Triay to Mr. Marcinowski, dated June 26, 2000.

DOE (U.S. Department of Energy). 2004a. *Partial Response to Environmental Protection Agency (EPA) May 20, 2004 Letter on CRA, Enclosure 1.* Letter from R. Paul Detwiler, U.S. Department of Energy Carlsbad Field Office to Elizabeth Cotsworth, U.S. Environmental Protection Agency Office of Radiation and Indoor Air, Washington DC, August 16, 2004. Docket A-98-49, Item II-B2-35.

DOE (U.S. Department of Energy). 2004b. *Title 40 CFR 191 Parts B and C Compliance Recertification Application*, DOE/WIPP 2004-3231, Carlsbad Field Office, Carlsbad, New Mexico, March 2004. Docket A-98-49, Item II-B2-27

DOE (U.S. Department of Energy). 2004c. *Response to EPA May 20, 2004 Letter on CRA*. Letter from R.P. Detwiler, U.S. Department of Energy Carlsbad Field Office to E. Cotsworth, U.S. Environmental Protection Agency Office of Air and Radiation, Washington, DC, September 29, 2004. Docket A-98-49, Item II-B2-37.

DOE (U.S. Department of Energy). 2004d. *Partial Response to Environmental Protection Agency (EPA) September 2, 2004, Letter on Compliance Recertification Application*. Letter from R. Paul Detwiler, U.S. Department of Energy Carlsbad Field Office to Elizabeth Cotsworth, U.S. Environmental Protection Agency Office of Radiation and Indoor Air, Washington DC, December 23, 2004. Docket A-98-49, Item II-B2-40

DOE (U.S. Department of Energy). 2005. *Untitled Response to EPA Comments.* November 29, 2005, EPA Docket A-98-49, Item II-B2-56.

Dunagan, S. 2004. *Analysis Package for Cuttings and Cavings: Compliance Recertification Application, Revision 1.0.* Sandia National Laboratories, Carlsbad, New Mexico, ERMS 533541.

EPA (U.S. Environmental Protection Agency). 1998a. *Technical Support Document for Section 194.24: EPA's Evaluation of DOE's Actinide Source-Term*. Office of Radiation and Indoor Air, May 1998. Docket A-93-02, V-B-17.

EPA (U.S. Environmental Protection Agency). 1998b. *Technical Support Document for Section 194.23: Models and Computer Codes*. Office of Radiation and Indoor Air, May 1998. Docket A-93-02, V-B-6.

EPA (U.S. Environmental Protection Agency). 2000. Letter from Mr. Marcinowski to Dr Triay, dated August 11, 2000. Docket A-98-49, Item II-A3-24

EPA (U.S. Environmental Protection Agency). 2002a. Letter from Mr. Marcinowski to Dr. Triay, dated August 6, 2002. Docket A-98-49, Item II-B3-36

EPA (U.S. Environmental Protection Agency). 2002b Letter from Mr. Marcinowski to Dr. Triay, dated December 13, 2002. Docket A-98-49, II-B3-43

EPA (U.S. Environmental Protection Agency). 2003a. *Review of WIPP Performance Assessment Parameter Database Migration, Final Report, April, 2003.* Office of Air and Radiation, Washington, DC. Docket A-98-49, II-B3-51.

EPA (U.S. Environmental Protection Agency). 2003b. Review of WIPP Performance Assessment Computer Code Migration. Office of Radiation and Indoor Air. Washington, DC. June 10, 2003. Docket A-98-49, Item II-B3-70

EPA (U.S. Environmental Protection Agency). 2004a. *First Set of CRA Comments (with enclosure).* Letter from Elizabeth Cotsworth, U.S. Environmental Protection Agency Office of Radiation and Indoor Air, Washington DC, to R. Paul Detwiler, U.S. Department of Energy Carlsbad Field Office, May 20, 2004. Docket A-98-49, Item II-B3-72.

EPA (U.S. Environmental Protection Agency). 2004b. *CRA Completeness Comments - 3rd set - August 2004*, Letter (with enclosure) from Elizabeth Cotsworth, U.S. Environmental Protection Agency Office of Radiation and Indoor Air, Washington DC, to R. Paul Detwiler, U.S. Department of Energy Carlsbad Field Office, September 2, 2004. Docket A-98-49, Item II-B3-74.

EPA (U.S. Environmental Protection Agency). 2004c. Letter from Frank Marcinowski Office of Radiation and Indoor Air, Washington DC, to R. Paul Detwiler, U.S. Department of Energy Carlsbad Field Office, March 26, 2004. Docket A-98-49, Item II-B3-68.

EPA (U.S. Environmental Protection Agency). 2004d. *Technical Support Document for Section 194.23: Review of Changes to the WIPP Performance Assessment Parameters Since the Database Migration.* Office of Air and Radiation, Washington DC, March 2004, Docket A-98-49, Item II-B3-69.

EPA (U.S. Environmental Protection Agency). 2004e. *Technical Support Document for Section 194.22 and 23: Review of WIPP Recertification Performance Assessment Computer Codes – CRA Code Review.* Office of Air and Radiation, Washington DC, December 1, 2004. Docket A-98-49, Item II-B1-7.

EPA (U.S. Environmental Protection Agency). 2005a. *Performance Assessment Issues.* Letter from Elizabeth Cotsworth, U.S. Environmental Protection Agency Office of Radiation and Indoor Air, Washington DC, to Inés Triay, U.S. Department of Energy Carlsbad Field Office, March 4, 2005. Docket A-98-49, Item II-B3-80.

EPA (U.S. Environmental Protection Agency). 2005b. *Technical Support Document for Section 194.24, Evaluation of the Compliance Recertification Actinide Source Term and Culebra Dolomite Distribution Coefficient Values.* Draft Final, U.S. Environmental Protection Agency Office of Radiation and Indoor Air, Washington DC, July 2005. Docket A-98-49, Item II-B1-3.

EPA (U.S. Environmental Protection Agency). 2005c. *Technical Support Document for Sections 194.25, 194.32 And 194.33, Compliance Recertification Application Review of Features, Events And Processes*, Office of Air and Radiation, Washington DC. Docket A-98-49, Item II-B1-11.

EPA (U.S. Environmental Protection Agency). 2005d. *Preliminary Review Comments on Actinide Solubility Uncertainty Analysis.* E-mail to U.S. Department of Energy Carlsbad Field Office, EPA Docket A-98-49, Item II-B3-89.

EPA (U.S. Environmental Protection Agency). 2005e. *Technical Support Document for Section 194.23 Review of Changes to the WIPP Performance Assessment Parameters From the Compliance Recertification Application to Performance Assessment Baseline Calculation*, Office of Air and Radiation, Washington DC. Docket A-98-49, Item II-B1-6.

EPA (U.S. Environmental Protection Agency). 2005f. *Technical Support Document For 194.23: SANTOS Computer Code in WIPP Performance Assessment*. Office of Radiation and Indoor Air. Washington, DC. January 2005. Docket A-98-49, II-B1-17

EPA (U.S. Environmental Protection Agency). 2006a. *Technical Support Document for Section 194.24: Review of the Baseline Inventory Used in the Compliance Recertification Application and the Performance Assessment Baseline Calculation.* Washington DC. January 2006, Docket A-98-49, Item II-B1-9

EPA (U.S. Environmental Protection Agency). 2006b. *Technical Support Document for Section 194.23: Models and Computer Codes – PABC Code Changes Review.* January 2006. Docket A-98-49, Item II-B1-8.

Felmy, A.R., D. Rai, and M.J. Mason. 1991. The Solubility of Hydrous Thorium(IV) Oxide in Chloride Media: Development of an Aqueous Ion-Interaction Model. *Radiochimica Acta* 55:177-185.

Felmy, A. R., D. Rai, S. M. Sterner, M. J. Mason, N. J. Hess, and S. D Conradson. 1997. Thermodynamic Models of Highly Charged Aqueous Species: Solubility of Th(IV) Hydrous Oxide in Concentrated $NaHCO_3$ and Na_2CO_3 Solutions. *Journal of Solution Chemistry* 26:233-248.

Felmy, A.R., D. Rai, and R. Fulton. 1990. The Solubility of $AmOHCO_3$(c) and the Aqueous Thermodynamics of the System Na-Am-HCO_3-CO_3-OH-H_2O, *Radiochimica Acta* 50:193-204.

Felmy, A.R., D. Rai, J.A. Schramke, and J.L. Ryan. 1989. The Solubility of Plutonium Hydroxide in Dilute Solution and in High-Ionic-Strength Chloride Brines. *Radiochimica Acta* 48:29-35.

Francis A.J., J.B. Gillow, and M.R. Giles. 1997. *Microbial Gas Generation Under Expected Waste Isolation Pilot Plant Repository Conditions*. Sandia National Laboratories, Albuquerque, New Mexico, SAND96-2582.

Garner, J. W. and C. D. Leigh. 2005. *Analysis Package for PANEL, CRA-2004 Performance Assessment Baseline Calculation*. Revision 0, Sandia National Laboratories, Carlsbad, New Mexico, ERMS 540572.

Giambalvo, E.R. 2002a. *Recommended Parameter Values for Modeling An(IV) Solubility in WIPP Brines.* Memorandum to L.H. Brush, Sandia National Laboratories, July 26, 2002, ERMS 522986.

Giambalvo, E.R. 2002b. *Recommended Parameter Values for Modeling An(V) Solubility in WIPP Brines*. Memorandum to L.H. Brush, July 26, 2002, ERMS 522990.

Giambalvo, E.R. 2002c. *Recommended Parameter Values for Modeling Organic Ligands in WIPP Brines.* Memorandum to L.H. Brush, Sandia National Laboratories, July 25, 2002, ERMS 522981.

Giambalvo, E.R. 2003. *Release of FMT Database FMT_021120.CHEMDAT.* Memorandum to L.H. Brush, Sandia National Laboratories, March 10, 2003, ERMS 526372.

Giffaut, E. 1994. *Influence des Ions Chlorure sur la Chimie des Actinides*, Ph. D. Thesis, Université de Paris-Sud, Orsay, France, 259 pp.

Gilkey, A.P. 2000. *Change Control Form for CUTTINGS_S Version 5.04A.* Sandia National Laboratories, Carlsbad, New Mexico, ERMS 515342.

Gilkey, A.P. 2004. *Change Control Form for CUTTING_S, Version 5.10.* Sandia National Laboratories, Carlsbad, New Mexico, ERMS 537036.

Gillow J.B., and A.J. Francis. 2002. Re-evaluation of Microbial Gas Generation Under Expected Waste Isolation Pilot Plant Conditions: Data Summary and Progress Report (July 14, 2001 - January 31, 2002), January 22, 2002. *Sandia National Laboratories Technical Baseline Reports, WBS 1.3.5.3, Compliance Monitoring; WBS 1.3.5.4, Repository Investigations, Milestone RI110, January 31, 2002.* Sandia National Laboratories, Carlsbad, New Mexico, ERMS 520467, pp. 2.1 - 1 to 2.1 - 26.

Gillow, J., and A.J. Francis. 2003. *Microbial Gas Generation Under Expected Waste Isolation Pilot Plant Repository Conditions*. Final Report, Revision 0, October 6 Draft, ERMS 532877.

Gitlin, B.C. 2005. Fifth Set of CRA Comments. U.S. Environmental Protection Agency, Washington, DC. ERMS 540240. Docket A-98-49, Item II-B3-79.

Harvill, 2004, *Summary Review of Transuranic Waste Baseline Inventory Waste Profile Forms Developed to Support the Compliance Recertification Application*, ERMS 534062, January 7, 2004.

Hansen, C.W. 2003a. *Requirements Document and Verification and Validation Plan for CUTTINGS_S Version 5.10.* Sandia National Laboratories, Carlsbad, New Mexico, ERMS 532335.

Hansen, C.W. 2003b. *Change Control Form for CUTTINGS _S Version 5.10.* Sandia National Laboratories, Carlsbad, New Mexico, ERMS 532337.

Hansen, C.W. 2004. Software Problem Report (SPR) Form 04-006 for LHS Version 2.41. Sandia National Laboratories, Carlsbad, New Mexico. ERMS 536209.

Hansen, C.W., C. Leigh, D. Lord and J.S. Stein 2002. BRAGFLO Results for the Technical Baseline Migration. Sandia National Laboratories, Carlsbad, New Mexico. ERMS 523209.

Holt, R.M. 1997. Conceptual Model for Transport Processes in the Culebra Dolomite Member, Rustler Formation. SAND97-0194. Albuquerque, New Mexico: Sandia National Laboratories.

Holt, R.M., and D.W. Powers. 1988. Facies Variability and Post-Depositional Alteration Within the Rustler Formation in the Vicinity of the Waste Isolation Pilot Plant, Southeastern New Mexico. DOE/WIPP 88-004. Carlsbad, New Mexico: U.S. Department of Energy.

Holt, R.M., and L. Yarbrough. 2002. Analysis Report, Task 2 of AP-088, Estimating Base Transmissivity Fields. ERMS 523889. Carlsbad, New Mexico: Sandia National Laboratories, WIPP Records Center.

Holt, R.M., and L. Yarbrough. 2003a. Addendum to Analysis Report, Task 2 of AP-088, Estimating Base Transmissivity Fields. ERMS 527601. Carlsbad, New Mexico: Sandia National Laboratories, WIPP Records Center.

Holt, R.M., and L. Yarbrough. 2003b. Addendum 2 to Analysis Report, Task 2 of AP-088, Estimating Base Transmissivity Fields. ERMS 529416. Carlsbad, New Mexico: Sandia National Laboratories, WIPP Records Center.

James, S.J., and J. Stein. 2002. *Analysis Plan for the Development of a Simplified Shaft Seal Model for the WIPP Performance Assessment*. AP-094. Carlsbad, New Mexico: Sandia National Laboratories. ERMS 524958.

James, S.J., and J. Stein. 2003. *Analysis Plan for the Development of a Simplified Shaft Seal Model for the WIPP Performance Assessment Rev. 1*. Carlsbad, New Mexico: Sandia National Laboratories. ERMS 525203.

Kanney, J.F., and C.D. Leigh 2005. *Analysis Plan for Post CRA PA Baseline Calculation AP-122*. Sandia National Laboratories, Carlsbad, New Mexico. ERMS 539624.

Khalili, F.I., V. Symeopoulos, J.-F. Chen, and G.R. Choppin. 1994. Solubility of Nd in Brine. *Radiochimica Acta* 66/67:51-54.

Kirchner, T. B. and E. D. Vugrin. 2004. *Errors Affecting Spallings Releases.* Sandia National Laboratories, Carlsbad, New Mexico, ERMS 537852.

Kirkes, R. 2005a. *Baseline Features, Events and Processes List for the Waste Isolation Pilot Plant.* Revision 1, Sandia National Laboratories, Carlsbad, New Mexico, ERMS 539356.

Kirkes, R. 2005b. *Features, Events and Processes Assessment for the Performance Assessment Baseline Calculation*. Sandia National Laboratories, Carlsbad, New Mexico, ERMS 540366.

Kirkes, 2005c. *Performing FEPs Baseline Impact Assessments for Planned and Unplanned Changes*. Sandia National Laboratories Document SP 9-4, Revision 0, April 2005.

Larson, K. 1996. *Brine-Waste Contact Volumes for Scoping Analysis of Organic Ligand Concentration.* Albuquerque, New Mexico, WPO# 36044.

Lavenue, A.M. 1996. Analysis of the Generation of Transmissivity Fields for the Culebra Dolomite. ERMS 240517. Carlsbad, New Mexico: Sandia National Laboratories, WIPP Records Center.

Leigh and Crawford, 2004. Inventory Reassessment Summary for the CRA-2004 TRU Waste Inventory, ERMS 534059.

Leigh, C.D. 2003. *New Estimates of the Total Masses of Complexing Agents in the WIPP Inventory for Use in the 2003 WIPP Performance Assessment*. Memorandum to L.H. Brush, Sandia National Laboratories, September 3, 2003, ERMS 531319.

Leigh, C.D. 2005. Organic Ligand Masses TRU Waste Streams from TWBID Revision 2.1 Version 3.13 Data Version D4.15, Revision 1. Memorandum to L.H. Brush, Sandia National Laboratories, April 18, 2005, ERMS 539550.

Leigh, C.D. and J.R. Trone 2005a. *Calculation of the Waste Unit Factor for the Performance Assessment Baseline Calculation, Revision 0.* Sandia National Laboratories, Carlsbad, New Mexico. ERMS 539613.

Leigh, C., J. Kanney, L. Brush, J. Garner, R. Kirkes, T. Lowry, M. Nemer, J. Stein, E. Vugrin, S. Wagner, and T. Kirchner. 2005a. *2004 Compliance Recertification Application Performance Assessment Baseline Calculation.* Sandia National Laboratories, Carlsbad, New Mexico, ERMS 541521.

Leigh, C.D., J.R. Trone and B. Fox. 2005b. *TRU Waste Inventory for the 2004 Compliance Recertification Application Performance Assessment Baseline Calculation*. Sandia National Laboratories, Carlsbad, New Mexico. ERMS 541118.

Leigh, C. and B. Fox 2005c. *Unit Conversion and Date Transfer for Decay to 2033 Using ORIGEN Version 2.2: Post-CRA Assessment Baseline Calculation, Revision 0.* ERMS 539329, Sandia National Laboratories, Carlsbad, New Mexico.

Lowry, T.S. 2003. Analysis Report, Task 5 of AP-088, Evaluation of Mining Scenarios. ERMS 531138. Carlsbad, New Mexico: Sandia National Laboratories, WIPP Records Center.

Lowry, T. S. 2004. Analysis Report for Inclusion of Omitted Areas in Mining Transmissivity Calculations in Response to EPA Comment G-11. ERMS 538218, Sandia National Laboratories, Carlsbad, New Mexico.

Lowry, T.S. 2005. Analysis Package for Salado Transport Calculations: CRA-2004 PA Baseline Calculation, Rev. 0. Sandia National Laboratories, Carlsbad, New Mexico. ERMS 541084.

Lowry, T.S., and J.F. Kanney 2005. Analysis Report for the CRA-2004 PABC Culebra Flow and Transport Calculations. EMRS 541508. Sandia National Laboratories, Carlsbad, New Mexico.

MacKinnon, R, and G. Freeze 1997a. *Supplemental Summary of EPA-Mandated Performance Assessment Verification Test (all Replicates) and Comparison with the Compliance Certification Application Calculations.* Sandia National Laboratories, Carlsbad, New Mexico, ERMS 414880.

MacKinnon, R, and G. Freeze 1997b. *Summary of Uncertainty and Sensitivity Analysis Results for the EPA-Mandated Performance Assessment Verification Test.* Sandia National Laboratories, Carlsbad, New Mexico, ERMS 420669.

McKenna, S.A., and D.B. Hart. 2003a. Analysis Report, Task 3 of AP-088, Conditioning of Base T Fields to Steady-State Heads. ERMS 529633. Carlsbad, New Mexico: Sandia National Laboratories, WIPP Records Center.

McKenna, S.A., and D.B. Hart. 2003b. Analysis Report, Task 4 of AP-088, Conditioning of Base T Fields to Transient Heads. ERMS 531124. Carlsbad, New Mexico: Sandia National Laboratories, WIPP Records Center.

Molecke, M.A. 1983. *A Comparison of Brines Relevant to Nuclear Waste Experimentation.* SAND83-0516, Sandia National Laboratories, Albuquerque, New Mexico.

Nancollas, G.H. and G.L. Gardner. 1974. Kinetics of Crystal Growth of Calcium Oxalate Monohydrate. *Journal of Crystal Growth* 21:267-276.

NEA (Nuclear Energy Agency). 2003. *Chemical Thermodynamics 5. Update on the Chemical Thermodynamics of Uranium, Neptunium, Plutonium, Americium, and Technetium.* Eds. Mompean, F.J., M. Illemassene, C. Domenech-Orti, and K. Ben Said. Organisation for Economic Co-operation and Development, Elsevier, Amsterdam.

Neck, V., J. I. Kim, and B. Kanellakopulos. 1994a. *Thermodynamisches Verhalten von Neptunium(V) in konzentrierten NaCl- und Na-ClO_4-Lösungen*, Kernforschungszentrum Karlsruhe, Report KfK 5301.

Neck, V., W. Runde, J. I. Kim, and B. Kanellakopulos. 1994b. Solid-liquid equilibrium reactions of neptunium(V) in carbonate solution at different ionic strength. *Radiochimica Acta* 65:29-37.

Neck, V., T. Fanghänel, G. Rudolph, and J.I. Kim. 1995a. Thermodynamics of neptunium(V) in concentrated salt solutions: Chloride Complexation and Ion Exchange (Pitzer) Parameters for the NpO_2^+ Ion. *Radiochimica Acta* 69:39-47.

Neck, V., W. Runde, and J.I. Kim. 1995b. Solid-Liquid Equilibria of Neptunium(V) in Carbonate Solutions of Different Ionic Strengths: II. Stability of the solid phases. *Journal of Alloys and Compounds* 225:295-302.

Neck, V., and J.I. Kim. 2001. Solubility and Hydrolysis of Tetravalent Actinides. *Radiochimica Acta* 89:1-16.

Neck, V., R. Müller, M. Bouby, M. Altmaier, J. Rothe, M.A. Denecke, and J.I. Kim. 2002. Solubility of Amorphous Th(IV) Hydroxide- Application of LIBD to Determine the Solubility Product and EXAFS for Aqueous Speciation. *Radiochimica Acta* 90:485-494.

Nemer, M. 2005a. *Parameter Data Entry Form, GRATMICH*. Sandia National Laboratories, Carlsbad, New Mexico. April 21, 2005, ERMS 539566.

Nemer, M. 2005b. *Parameter Data Entry Form, GRATMICI*. Sandia National Laboratories, Carlsbad, New Mexico. April 21, 2005, ERMS 539567.

Nemer, M. 2005c. *Updated Value of WAS_AREA:PROBDEG*. Sandia National Laboratories, Carlsbad, New Mexico. Memorandum to D.S. Kessel, April 20, 2005, ERMS 539441.

Nemer, M., and J. Stein. 2005. *Analysis Package for BRAGFLO: 2004 Compliance Recertification Application Performance Assessment Baseline Calculation.* Sandia National Laboratories, Carlsbad, New Mexico, ERMS 540527.

Nemer, M., J. Stein, and W. Zelinski. 2005. *Analysis Report for BRAGFLO Preliminary Modeling Results with New Gas Generation Rates Based Upon Recent Experimental Results.* Sandia National Laboratories, Carlsbad, New Mexico, ERMS 539437.

Nemer, M., and W. Zelinski. 2005. *Analysis Report for BRAGFLO Modeling Results with Removal of Methanogenesis from the Microbial-Gas-Generation Model.* Sandia National Laboratories, Carlsbad, New Mexico, ERMS 538748.

Novak, C.F., I. Al Mahamid, K.A. Becraft, S.A. Carpenter, N. Hakem, and T. Prussin. 1997. Measurement and Thermodynamic Modeling of Np(V) Solubility in Aqueous K_2CO_3 Solutions to High Concentrations. *Journal of Solution Chemistry* 26:681-697.

Novak, C.F., H. Nitsche, H.B. Silber, K. Roberts, P.C. Toretto, T. Prussin, K. Becraft, S.A. Carpenter, D.E. Hobart, and I. Al Mahamid. 1996. Neptunium(V) and Neptunium(VI) Solubilities in Synthetic Brines of Interest to the Waste Isolation Pilot Plant (WIPP). *Radiochimica Acta* 74:31-36.

Nowak, E.J. 2005. *Recommended Change in the FMT Thermodynamic Data Base.* Memorandum to L.H. Brush, April 1, Sandia National Laboratories, Carlsbad, New Mexico, ERMS 539227.

Park, B.Y. 2002. *Analysis Plan for Structural Evaluation of WIPP Disposal Room Raised to Clay Seam G*. AP-093. Carlsbad, New Mexico: Sandia National Laboratories.

Patterson, R. 2005. Hanford Tank and K-Basin Wastes [DOE Letter #9: Response to CRA Comments]. U.S. Department of Energy, Carlsbad, New Mexico. ERMS 540241. Docket A-98-49, Item II-B2-47.

Piper, L. 2004. Partial Response to Environmental Protection Agency (EPA) September 2, 2004, Letter on Compliance Recertification Application [DOE Letter #7: Response to CRA Comments]. U.S. Department of Energy, Carlsbad, New Mexico. ERMS 540242. Docket A-98-49, Item II-B2-40.

Plyasunov, A., T. Fanghänel, and I. Grenthe. 1998. Estimation of the Pitzer Equation Parameters for Aqueous Complexes. A Case Study for Uranium at 298.15 K and 1 atm. *Acta Chemica Scandinavica* 52:250-260.

Powers, D.W. 2003. Addendum 2 to Analysis Report, Task 1 of AP-088, Construction of Geologic Contour Maps. ERMS 525199. Carlsbad, New Mexico: Sandia National Laboratories, WIPP Records Center.

Powers, D.W., and R.M. Holt. 1990. .Sedimentology of the Rustler Formation near the Waste Isolation Pilot Plant (WIPP) Site,. in Geological and Hydrological Studies of Evaporites in the Northern Delaware Basin for the Waste Isolation Pilot Plant (WIPP), New Mexico. D. Powers, R. Holt, R.L. Beauheim, and N. Rempe, eds. GSA Field Trip #14 Guidebook. Dallas, Texas: Dallas Geological Society. 79-106.

Powers, D.W., and R.M. Holt. 1995. Regional Geologic Processes Affecting Rustler Hydrogeology. ERMS 244173. Carlsbad, New Mexico: Sandia National Laboratories, WIPP Records Center.

Rai, D., A.R. Felmy, and R. Fulton, 1992. Solubility and ion activity product of $AmPO_4 \bullet xH_2O$ *Radiochimica Acta* 56:7-14.

Rai, D., A. R. Felmy, D. A. Moore, and M. J Mason. 1995. The Solubility of Th(IV) and U(IV) Hydrous Oxides in Concentrated $NaHCO_3$ and Na_2CO_3 Solutions. *Scientific Basis for Nuclear Waste Management.* Materials Research Society Symposium Proceedings Vol. 353, Materials Research Society.

Rai, D., Felmy, A. R., Sterner, S. M., Moore, D. A., Mason, M. J., Novak, C. F. 1997. The Solubility of Th(IV) and U(IV) Hydrous Oxides in Concentrated NaCl and $MgCl_2$ Solutions. *Radiochimica Acta* 79:239-247.

Rai, D., D.A. Moore, C.S. Oakes, and M. Yui. 2000. Thermodynamic Model for the Solubility of Thorium Dioxide in the Na^+-Cl^--OH^--H_2O system at 23ºC and 90ºC. *Radiochimica Acta* 88: 297-306.

Rai, D., A.R. Felmy, and M. Yui. 2003. Thermodynamic Model for the Solubility of $NdPO_4$(c) in the Aqueous Na+-H+-H_2PO_4-HPO_4^{2-}-OH^--Cl^--H_2O System. *Journal of Radioanalytical and Nuclear Chemistry* 256:37-43.

Ramsey, J.L., M.G. Wallace, and H-N. Jow. 1996. Analysis Package for the Culebra Flow and Transport Calculations (Task 3) of the Performance Assessment Calculations Supporting the Compliance Certification Application (CCA), AP-019. ERMS 240516. Carlsbad, New Mexico: Sandia National Laboratories, WIPP Records Center.

Rao, L., D. Rai., A.R. Felmy, and C.F. Novak. 1999. Solubility of $NaNd(CO_3)_2 \cdot 6H_2O(c)$ in Mixed Electrolyte ($Na\text{-}Cl\text{-}CO_3\text{-}HCO_3$) and Synthetic Brine Solutions. In *Actinide Speciation in High Ionic Strength Media: Experimental and Modeling Approaches to Predicting Actinide Speciation and Migration in the Subsurface*. Eds. D.T. Reed, S.B. Clark, and L. Rao. Proceedings of an American Chemical Society Symposium on Experimental and Modeling Studies of Actinide Speciation in Non-Ideal Systems, Held August 26-28, 1996, in Orlando, Florida. Kluwer Academic/Plenum Publishers, pages 153-169.

Rudeen, D.K. 2003. User.s Manual for DTRKMF Version 1.00. ERMS 523246. Carlsbad, New Mexico: Sandia National Laboratories, WIPP Records Center.

Runde, W., and J.I. Kim. 1995 *Untersuchungen der Übertragbarkeit von Labordaten natürliche Verhältnisse: Chemisches Verhalten von drei- und fünfwertigem Americium in salinen NaCl-Lösungen (Study of the Extrapolatability of Laboratory Data in Natural Conditions: Chemical Behavior of Trivalent and Pentavalent Americium in Saline NaCl Solutions).* RCM-01094, Institute for Radiochemistry, Technical University of Munich, Munich, FRG, ERMS 241862.

Runde, W., M. P. Neu, and D. L., Clark. 1996. Neptunium(V) Hydrolysis and Carbonate Complexation: Experimental and Predicted Neptunyl Solubility in Concentrated NaCl Using the Pitzer Approach. *Geochimica et Cosmochimica Acta* 60:2065-2073.

Ryan, J.L., and D. Rai. 1987. Thorium(IV) Hydrous Oxide Solubility. *Inorganic Chemistry* 26:4140-4142.

Silva, R.J. 1982. *The Solubilities of Crystalline Neodymium and Americium Trihydroxides.* LBL-15055, Lawrence Berkeley National Laboratory, Berkeley, California.

SNL (Sandia National Laboratories) 1987. *Interpretations of Single-Well Hydraulic Tests Conducted At and Near the Waste Isolation Pilot Plant (WIPP) Site, 1983–1987*. SAND87-0039. Albuquerque, New Mexico.

SNL (Sandia National Laboratories) 1992. A Modeling Approach to Address Spatial Variability within the Culebra Dolomite Transmissivity Field. SAND92-7306. Albuquerque, New Mexico.

SNL (Sandia National Laboratories) 1996. *Waste Isolation Pilot Plant Shaft Sealing System Compliance Submittal Design Report*. SAND96-1326. Albuquerque, New Mexico.

SNL (Sandia National Laboratories) 1997. Final, *Supplemental Summary of EPA-Mandated Performance Assessment Verification Test (All Replicates) and Comparison with the Compliance Certification Application Calculations*. ERMS 414879.

Stein, J.S. 2002. Minor difference found in TBM grid volumes. Memorandum to M.K. Knowles, May 20, 2002. Carlsbad, New Mexico: Sandia National Laboratories. ERMS 522357.

Stein, J.S. 2003. User's Manual for BRAGFLO Version 5.00, Document Version 5.00. Sandia National Laboratories, Carlsbad, New Mexico. ERMS 525702.

Stein, J. 2005. *Estimate of Volume of Brine in Repository That Leads to a Brine Release*. Memorandum to L.H. Brush, April 13, Sandia National Laboratories, Carlsbad, New Mexico, ERMS 539372.

Stein, J., and M. Nemer. 2005. *Analysis Plan for Updating the Microbial Degradation Rates for Performance Assessment.* AP-116, Sandia National Laboratories, Carlsbad, New Mexico, ERMS 538596.

Stein, J.S., M. B. Nemer and J. R. Trone 2005. *Analysis Package for Direct Brine Releases, Compliance Recertification Application, 2004 PABC, Revision 0.* Sandia National Laboratories, Carlsbad, New Mexico, ERMS 540633.

Stein, J.S. and W. Zelinski (2003a). *Analysis Plan for the Testing of a Proposed BRAGFLO Grid to be used for the Compliance Recertification Application Performance Calculations*. AP-106. Carlsbad, New Mexico: Sandia National Laboratories. ERMS 525236.

Stein, J.S., and W. Zelinski (2003b). *Analysis Package for BRAGFLO: Compliance Recertification Application*. Sandia National Laboratories, Carlsbad, New Mexico. ERMS 530163.

Stein, J.S. and W. Zelinski (2003c). *Analysis Report for: Testing of a Proposed BRAGFLO Grid to be used for the Compliance Recertification Application Performance Assessment Calculations*. Sandia National Laboratories, Carlsbad, New Mexico. ERMS 526868.

Streit, J., L.-C. Tran-Ho, and E. Königsberger. 1998. Solubility of the Three Calcium Oxalate Hydrates in Sodium Chloride Solutions and Urine-Like Liquors. *Monatshefte für Chemie* 129:1225-1236.

Tomažič, B. and G.H. Nancollas. 1979. The Kinetics of Dissolution of Calcium Oxalate Hydrates. *Journal of Crystal Growth* 46:355-361.

Torres, 2004. Email "Debris Nuclide Data" from Enrique Torres to Christi Leigh. BNFL Inc. February 25, 2004. ERMS 536313.

Triay, I.R. 2005. Partial Response to Environmental Protection Agency (EPA) September 2, 2004, Letter on Compliance Recertification Application [DOE Letter #8: Response to CRA Comments]. U.S. Department of Energy, Carlsbad Field Office, Carlsbad, New Mexico. ERMS 540243. Docket A-98-49, Item II-B2-41.

Vugrin, E.D. 2004a. Software Problem Report (SPR) 2004-09 for LHS Version 2.41. Sandia National Laboratories, Carlsbad, New Mexico. ERMS 538239.

Vugrin, E. D. 2004b. *Corrected CRA Figures.* Memo from Eric Vugrin to David Kessel, December 14, 2004. Sandia National Laboratories, Carlsbad, New Mexico, ERMS 538260.

Vugrin, E. D. 2005a. *Incorrect Units for Two Figures in "Corrected CRA Figures."* Memo from Eric Vugrin to David Kessel, January 18, 2005. Sandia National Laboratories, Carlsbad, New Mexico, ERMS 538466.

Vugrin, E. D. 2005b. *Analysis Package for CUTTINGS_S: CRA 2004 Performance Assessment Baseline Calculation.* Sandia National Laboratories, Carlsbad, New Mexico, ERMS 540468.

Vugrin, E. D. 2005c. *Analysis Package for DRSPALL: CRA 2004 Performance Assessment Baseline Calculation.* Sandia National Laboratories, Carlsbad, New Mexico, ERMS 540415.

Vugrin, E. D. 2005d. *Change Control Form for CUTTING_S, Version 6.01.* Sandia National Laboratories, Carlsbad, New Mexico, ERMS 540159.

Vugrin, E. D. 2005e. *Change Control Form for CUTTINGS_S, Version 6.00.* Sandia National Laboratories, Carlsbad, New Mexico, ERMS 539215.

Vugrin, E. D. 2005f. *Software Problem Report (SPR) 05-001 for CUTTINGS_S Version 6.01.* Sandia National Laboratories, Carlsbad, New Mexico, ERMS 540158.

Vugrin, E. D. 2005g. *User's Manual for CUTTINGS_S Version 6.00.* Sandia National Laboratories, Carlsbad, New Mexico, ERMS 537039.

Vugrin, E. D. 2005h. *A Comparison of PAVT and CRA-2004 PABC Mean CCDFs.* Sandia National Laboratories, Carlsbad, New Mexico, ERMS 542046.

Vugrin, E.D. 2005i. Change Control Form for LHS Version 2.41 to 2.42. Sandia National Laboratories, Carlsbad, New Mexico. ERMS 538375.

Vugrin, E.D. 2006. *CCA PAVT and CRA-2004 PABC CCDF Quantiles and Confidence Limits.* Sandia National Laboratories, Carlsbad, New Mexico, ERMS 542271.

Vugrin, E. D. and B. Fox. 2005. *Software Installation and Checkout and Regression Testing for CUTTINGS_S Version 6.02 on the ES40 and ES45, Revision 0.* Sandia National Laboratories, Carlsbad, New Mexico, ERMS 540155.

Vugrin, E., and S. Dunagan 2005. *Analysis Package for CCDFGF: CRA-2004 Performance Assessment Baseline Calculation.* Sandia National Laboratories, Carlsbad, New Mexico, ERMS 540771.

Vugrin, E., T. Kirchner, J. Stein and B. Zelinski. 2005. *Analysis Report for Modifying Parameter Distributions for S_MB139;COMP_RCK and S_MB139:SAT_RGAS.* Sandfia National Laboratories, Carlsbad, New Mexico. ERMS 539301.

Wagner, S.W. and G.R. Kirkes. 2003. *FEPs Reassessment for Recertification.* Sandia National Laboratories, Carslbad, New Mexico. ERMS 525161.

Wagner, S., Kirkes, R., and Martell, M.A. 2003. *Features, Events and Processes: Reassessment for Recertification Report*. Sandia National Laboratories, Carlsbad, New Mexico, ERMS 530184.

Wallace, M. 1996. Records Package for Screening Effort NS11: Subsidence Associated with Mining Inside or Outside the Controlled Area. ERMS 412918. Carlsbad, New Mexico: Sandia

National Laboratories, WIPP Records Center.

Wang, Y. and LH. Brush. 1996. *Estimates of Gas-Generation Parameters for the Long-Term WIPP Performance Assessment*. Unpublished memorandum to M.S. Tierney, Sandia National Laboratories, Albuquerque, New Mexico, January 26, 1996, WPO 31943.

Warren 2004- See Harvill 2004.

Wawersik, W.R., and C.M. Stone 1989. A Characterization of Pressure Records in Inelastic Rock Demonstrated by Hydraulic Fracturing Measurements in Salt. *International Journal of Rock Mechanics and Mining Sciences*. Vol. 26, No. 6, 613-627.

Wawersik, W.R., L.W. Carlson, J.A. Henfling, D.J. Borns, R.L. Beauheim, C.L. Howard, and R.M. Roberts 1997. *Hydraulic Fracturing Tests in Anhydrite Interbeds in the WIPP, Marker Beds 139 and 140*. SAND95-0596. Albuquerque, New Mexico: Sandia National Laboratories.

Xia, Y., A.R. Felmy, L. Rao, Z. Wang and N J. Hess. 2003. Thermodynamic Model for the Solubility of ThO_2(am) in the aqueous Na^+-H^+-OH^--NO_3^--H_2O-EDTA system. *Radiochimica Acta* 91:751-760.

Xiong, Y. 2004a. *A Correction of the Dimensionless Standard Chemical Potential of $NpO_2Ac(aq)$ in FMT_041116.CHEMDAT.* Memorandum to L.H. Brush, December 6, Sandia National Laboratories, Carlsbad, New Mexico, ERMS 538162.

Xiong, Y. 2004b. *A Correction of the Molecular Weight of Oxalate in FMT_0211120.CHEMDAT, and Incorporation of Calcium Oxalate Monohydrate (Whewellite) into CHEMDAT With Its Recommended Dimensionless Standard Chemical Potential Value.* Memorandum to L.H. Brush, June 8, Sandia National Laboratories, Carlsbad, New Mexico, ERMS 535813.

Xiong, Y. 2004c. *An Update on the Dimensionless Standard Chemical Potential of $NpO_2Ac(aq)$ in FMT CHEMDAT.* Memorandum to L.H. Brush, November 11, Sandia National Laboratories, Carlsbad, New Mexico, ERMS 537838.

Xiong, Y. 2004d. *Release of FMT_040628.CHEMDAT*. E-mail to J.J. Long, June 28, Sandia National Laboratories, Carlsbad, New Mexico, ERMS 536022.

Xiong, Y. 2005. *Release of FMT_050405.CHEMDAT.* Email to J.F. Kanney and J.J. Long, April 5, Sandia National Laboratories, Carlsbad, New Mexico, ERMS 539304.

Xiong, Y., E.J. Nowak, and L.H. Brush. 2004. *Updated Uncertainty Analysis of Actinide Solubilities for the Response to EPA Comment C-23-16.* Sandia National Laboratories, Carlsbad, New Mexico, ERMS 538219.

Xiong, Y., E.J. Nowak, and L.H. Brush. 2005. *Updated Uncertainty Analysis of Actinide Solubilities for the Response to EPA Comment C-23-16, Rev. 1 (Supercedes ERMS 538219)* Sandia National Laboratories, Carlsbad, New Mexico, ERMS 539595.

Yew, C., J. Hanson, and L. Teufel 2003. *Spallings Conceptual Model Peer Review Report*. Prepared by Time Solutions Corp., Albuquerque, New Mexico, for the U.S. Department of Energy, Carlsbad Area Office, Carlsbad, New Mexico, ERMS 532520.

Yew, C. 2004. *Spallings Conceptual Model Peer Review Report Revised Section 3.2.4, The Post Penetration Wellbore Flow.* Prepared by Time Solutions Corp., Albuquerque, New Mexico, for the U.S. Department of Energy, Carlsbad Area Office, Carlsbad, New Mexico, ERMS 541015.

APPENDIX A: VERIFICATION OF LONG-TERM MICROBIAL GAS GENERATION RATE CALCULATIONS

LIST OF TABLES

LIST OF FIGURES

Table A-1. Carbon Dioxide Generation Data from Experiments that were Anaerobic, Inundated, Inoculated, Nutrient-Amended, and with Excess Nitrate; Used by Nemer et al. 2005 to Calculate Maximum Inundated Long-Term Gas Generation Rate

Time (days)	µmoles CO_2 /g Cellulose	Standard Error	Source	Note
0	0.47	0.01	Nemer et al. 2005	
45	4.29	0.04	Nemer et al. 2005	
69	6.1	3.42	Nemer et al. 2005	Used in Wang and Brush 1996 maximum inundated rate calculation
104	19.7	6.6	Nemer et al. 2005	
132	25.8	6.4	Nemer et al. 2005	
164	45.4	8	Nemer et al. 2005	
200	61.4	8.2	Nemer et al. 2005	
228	56.2	13.6	Nemer et al. 2005	
264	92.8	8.6	Nemer et al. 2005	
297	76.4	8.8	Nemer et al. 2005	
356	129.2	13	Nemer et al. 2005	
411	162.6	13	Nemer et al. 2005	Used in Wang and Brush 1996 maximum inundated rate calculation
481	181	8	Nemer et al. 2005	
591	190	4	Nemer et al. 2005	
733	204	3	Nemer et al. 2005	
853	186	9	Nemer et al. 2005	
1,034	212	2	Nemer et al. 2005	
1,228	194	4	Nemer et al. 2005	
2,723	251	5	Nemer et al. 2005	
3,464	236	42	Nemer et al. 2005	Methane detected (Gillow and Francis 2003)
3,929	219	75	Gillow and Francis 2003	

Figure A-1. Carbon Dioxide Generation Data from Experiments that were Anaerobic, Inundated, Inoculated, Nutrient-Amended, and with Excess Nitrate

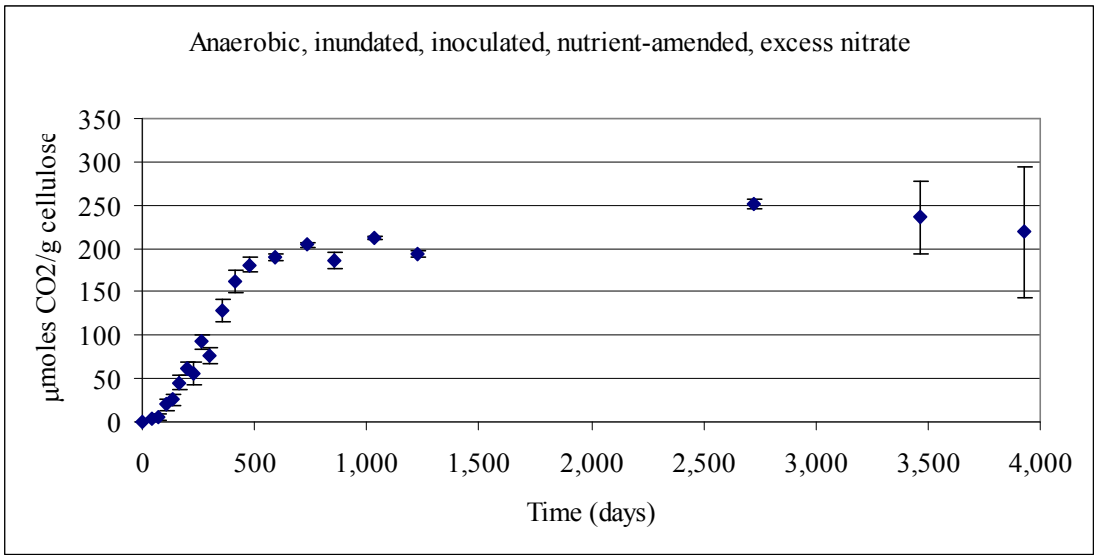

Table A-2. Microsoft® Excel Linear Regression Results for Anaerobic, Inundated, Inoculated, Nutrient-Amended, and with Excess Nitrate Data Used by Nemer et al. 2005 to Calculate Maximum Inundated Microbial Gas Generation Rate

SUMMARY OUTPUT: 481-day to 3,464-day data (range used by Nemer et al. 2005)

Regression Statistics	
Multiple R	0.88272681
R Square	0.77920663
Adjusted R Square	0.74240773
Standard Error	12.703604
Observations	8

ANOVA

	df	*SS*	*MS*	*F*	*Significance F*
Regression	1	3417.210672	3417.21067	21.1747289	0.003685817
Residual	6	968.2893278	161.381555		
Total	7	4385.5			

	Coefficients	*Standard Error*	*t Stat*	*P-value*	*Lower 95%*	*Upper 95%*
Intercept	178.77377	7.558777913	23.6511474	3.75E-07	160.2781073	197.269434
X Variable 1	0.02015034	0.004378985	4.60160069	0.00368582	0.00943535	0.03086533

Table A-3. Microsoft® Excel Linear Regression Results for Anaerobic, Inundated, Inoculated, Nutrient-Amended, and with Excess Nitrate Data Used by Nemer et al. 2005 with Additional 3,929-Day Data

SUMMARY OUTPUT: 481-day to 3,929-day data

Regression Statistics	
Multiple R	0.77995299
R Square	0.60832666
Adjusted R Square	0.55237333
Standard Error	15.9011604
Observations	9

ANOVA

	df	*SS*	*MS*	*F*	*Significance F*
Regression	1	2748.960583	2748.96058	10.8720359	0.013169958
Residual	7	1769.928306	252.846901		
Total	8	4518.888889			

	Coefficients	*Standard Error*	*t Stat*	*P-value*	*Lower 95%*	*Upper 95%*
Intercept	184.828023	8.829278924	20.9335355	1.4271E-07	163.9500963	205.70595
X Variable 1	0.01393641	0.004226641	3.29727704	0.01316996	0.003941988	0.02393082

Table A-4. Microsoft® Excel Linear Regression Results for Anaerobic, Inundated, Inoculated, Nutrient-Amended, and with Excess Nitrate Data Used by Nemer et al. 2005 without 3.464-Day Data Where Methanogenesis was Observed

SUMMARY OUTPUT: : 481-day to 2,723-day data

Regression Statistics	
Multiple R	0.91850188
R Square	0.8436457
Adjusted R Square	0.81237484
Standard Error	10.3228946
Observations	7

ANOVA

	df	*SS*	*MS*	*F*	*Significance F*
Regression	1	2874.903518	2874.90352	26.9786544	0.003484121
Residual	5	532.8107681	106.562154		
Total	6	3407.714286			

	Coefficients	*Standard Error*	*t Stat*	*P-value*	*Lower 95%*	*Upper 95%*
Intercept	171.244422	7.183270816	23.8393382	2.4192E-06	152.7792367	189.709608
X Variable 1	0.02869149	0.005523863	5.19409804	0.00348412	0.014491945	0.04289103

Table A-5. Carbon Dioxide Generation Data from Experiments that were Anaerobic, Inundated, Inoculated, Nutrient-Amended, and without Nitrate; Used by Nemer et al. 2005 to Calculate Minimum Inundated Long-Term Gas Generation Rate

Time (days)	μmoles CO_2/ g Cellulose	Standard Error	Source	Note
0	-0.06	0.01	Nemer et al. 2005	
45	3.79	0.04	Nemer et al. 2005	
69	-3.28	3.42	Nemer et al. 2005	
104	7.22	6.6	Nemer et al. 2005	
132	18.2	6.4	Nemer et al. 2005	
164	24.2	8	Nemer et al. 2005	
200	26	8.2	Nemer et al. 2005	
228	26.6	13.6	Nemer et al. 2005	
264	33.6	8.6	Nemer et al. 2005	
297	23.2	8.8	Nemer et al. 2005	
356	36.2	13	Nemer et al. 2005	
411	43.2	13	Nemer et al. 2005	
481	44.4	8	Nemer et al. 2005	
591	44.4	4	Nemer et al. 2005	
733	49.1	3	Nemer et al. 2005	
853	51.1	9	Nemer et al. 2005	
1,034	52	2	Nemer et al. 2005	
1,228	49.2	4	Nemer et al. 2005	
2,718	66.9	5	Nemer et al. 2005	Methane detected (Gillow and Francis 2003)
3,464	55.4	42	Nemer et al. 2005	Methane detected (Gillow and Francis 2003)
3,929	54.4	75	Gillow and Francis 2003	

Figure A-2. Carbon Dioxide Generation Data from Experiments that were Anaerobic, Inundated, Inoculated, Nutrient-Amended, and without Excess Nitrate

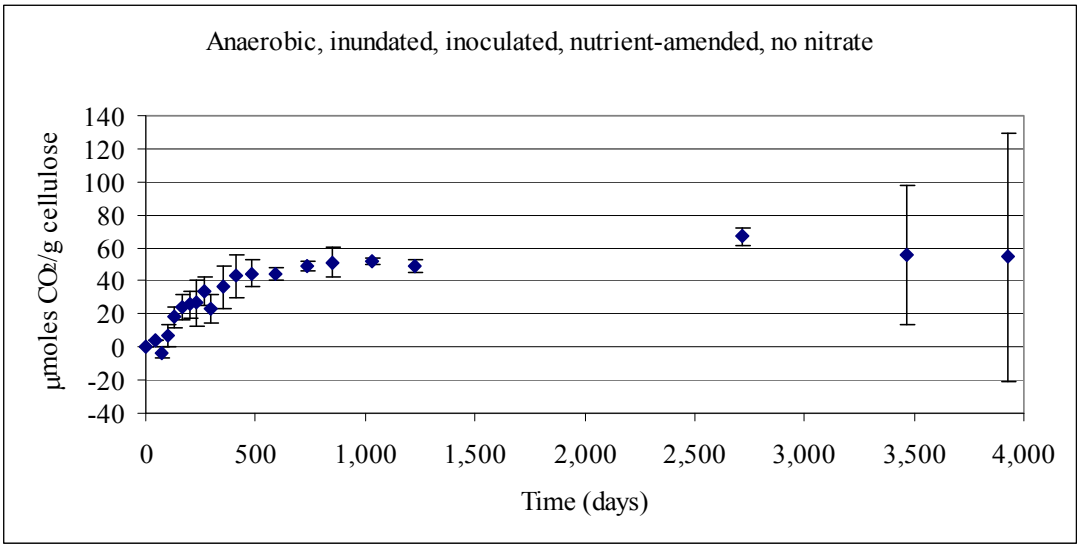

Table A-6. Microsoft® Excel Linear Regression Results for Anaerobic, Inundated, Inoculated, Nutrient-Amended, and without Excess Nitrate Data Used by Nemer et al. 2005 to Calculate Minimum Inundated Microbial Gas Generation Rate

SUMMARY OUTPUT: 411-day to 3,464-day data (range used by Nemer et al. 2005 for minimum inundated rate)

Regression Statistics	
Multiple R	0.79439405
R Square	0.63106191
Adjusted R Square	0.57835646
Standard Error	4.74274483
Observations	9

ANOVA

	df	*SS*	*MS*	*F*	*Significance F*
Regression	1	269.3246002	269.3246	11.9733728	0.010543908
Residual	7	157.4553998	22.4936285		
Total	8	426.78			

	Coefficients	*Standard Error*	*t Stat*	*P-value*	*Lower 95%*	*Upper 95%*
Intercept	43.7310009	2.545251266	17.1814082	5.5551E-07	37.712438	49.7495637
X Variable 1	0.00539573	0.001559343	3.46025618	0.01054391	0.001708466	0.00908299

Table A-7. Microsoft® Excel Linear Regression Results for Anaerobic, Inundated, Inoculated, Nutrient-Amended, and without Excess Nitrate Data Used by Nemer et al. 2005 with Additional 3,929-Day Data

SUMMARY OUTPUT: 411-day to 3,929-day data

Regression Statistics	
Multiple R	0.71194687
R Square	0.50686834
Adjusted R Square	0.44522689
Standard Error	5.20523206
Observations	10

ANOVA

	df	*SS*	*MS*	*F*	*Significance F*
Regression	1	222.7934738	222.793474	8.22284821	0.020907433
Residual	8	216.7555262	27.0944408		
Total	9	439.549			

	Coefficients	*Standard Error*	*t Stat*	*P-value*	*Lower 95%*	*Upper 95%*
Intercept	45.1686731	2.618967673	17.2467471	1.3003E-07	39.12932281	51.2080234
X Variable 1	0.00378275	0.001319158	2.86755091	0.02090743	0.000740769	0.00682474

Table A-8. Microsoft® Excel Linear Regression Results for Anaerobic, Inundated, Inoculated, Nutrient-Amended, and without Excess Nitrate Data Used by Nemer et al. 2005 without 2,718-Day and 3.464-Day Data Where Methanogenesis was Observed

SUMMARY OUTPUT: 411-day to 1,228-day data

Regression Statistics	
Multiple R	0.81798278
R Square	0.66909583
Adjusted R Square	0.602915
Standard Error	2.24645771
Observations	7

ANOVA

	df	*SS*	*MS*	*F*	*Significance F*
Regression	1	51.02142454	51.0214245	10.1101148	0.024548104
Residual	5	25.23286117	5.04657223		
Total	6	76.25428571			

	Coefficients	*Standard Error*	*t Stat*	*P-value*	*Lower 95%*	*Upper 95%*
Intercept	40.1680631	2.495242663	16.0978584	1.6853E-05	33.75383759	46.5822885
X Variable 1	0.0097962	0.003080915	3.17964067	0.0245481	0.001876459	0.01771595

Table A-9. Carbon Dioxide Generation Data from Experiments that were Anaerobic, Inundated, Inoculated, and Unamended with Nutrients or Nitrate

Time (days)	μmoles C/g Cellulose	Standard Error	Source	Note
0	2.11	0.04	Nemer et al. 2005	Used in Wang and Brush 1996 minimum inundated rate calculation
45	3.41	0.04	Nemer et al. 2005	
69	3.34	0.02	Nemer et al. 2005	
104	3.01	0.14	Nemer et al. 2005	
132	3.97	0.1	Nemer et al. 2005	
200	5.47	0.34	Nemer et al. 2005	
297	6.14	0.3	Nemer et al. 2005	
481	9.68	0.24	Nemer et al. 2005	
733	11.8	0.3	Nemer et al. 2005	
853	12.8	0.5	Nemer et al. 2005	
1,034	14	0.5	Nemer et al. 2005	Used in Wang and Brush 1996 minimum inundated rate calculation
1,228	13.9	1	Nemer et al. 2005	
2,723	24	1.7	Nemer et al. 2005	Methane detected (Gillow and Francis 2003 ERMS 532877)
3,464	26.1	2.2	Nemer et al. 2005	Methane detected (Gillow and Francis 2003 ERMS 532877)
3,929	27.4	5.8	Gillow and Francis 2003	

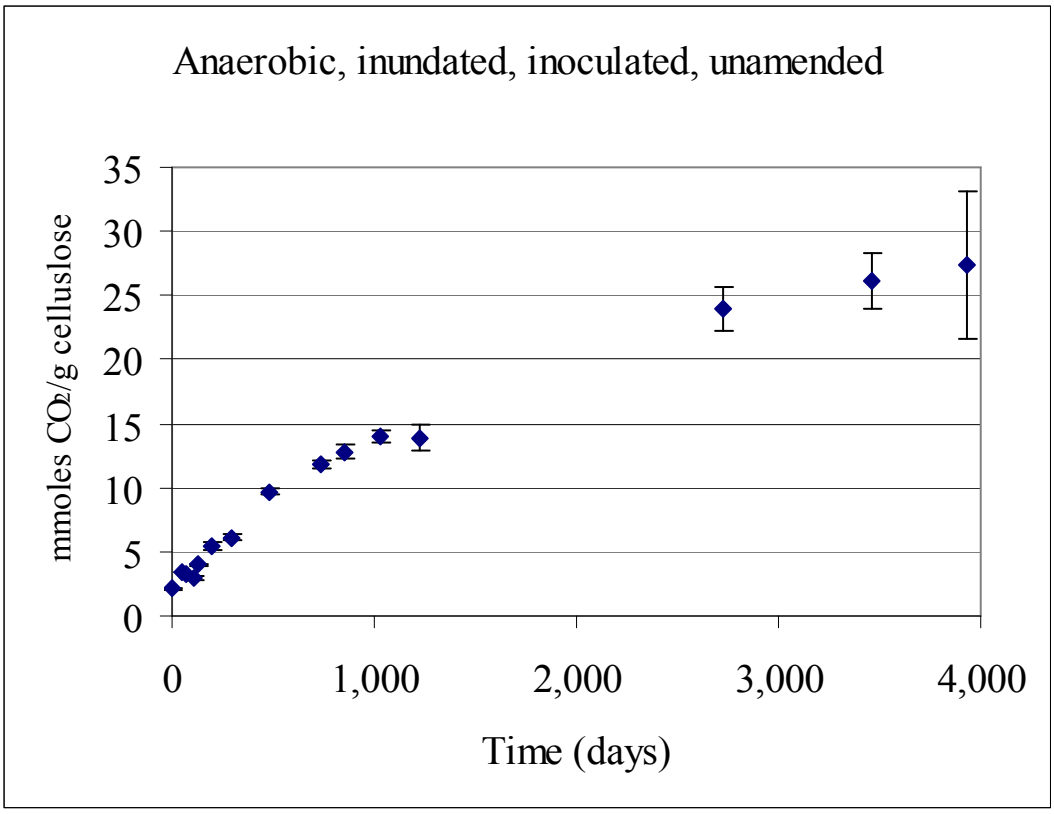

Figure A-3. Carbon Dioxide Generation Data from Experiments that were Anaerobic, Inundated, Inoculated, and Unamended with Nutrients or Nitrate

Table A-10. Microsoft® Excel Linear Regression Results for Anaerobic, Inundated, Inoculated, and Unamended Data

SUMMARY OUTPUT: 481-day to 3,464-day data evaluated by Nemer et al. 2005

Regression Statistics	
Multiple R	0.99297649
R Square	0.986002309
Adjusted R Square	0.983202771
Standard Error	0.823489825
Observations	7

ANOVA

	df	*SS*	*MS*	*F*	*Significance F*
Regression	1	238.8405225	238.8405225	352.2017725	7.91049E-06
Residual	5	3.390677463	0.678135493		
Total	6	242.2312			

	Coefficients	*Standard Error*	*t Stat*	*P-value*	*Lower 95%*	*Upper 95%*
Intercept	7.667393662	0.543977629	14.09505327	3.23467E-05	6.26905465	9.065732674
X Variable 1	0.005573245	0.00029697	18.76703952	7.91049E-06	0.00480986	0.00633663

Table A-11. Microsoft® Excel Linear Regression Results for Anaerobic, Inundated, Inoculated, and Unamended Data Evaluated by Nemer et al. 2005 with Additional 3,929-Day Data

SUMMARY OUTPUT: 481-day to 3,929-day data

Regression Statistics	
Multiple R	0.991736027
R Square	0.983540348
Adjusted R Square	0.980797073
Standard Error	0.987052755
Observations	8

ANOVA

	df	*SS*	*MS*	*F*	*Significance F*
Regression	1	349.3039612	349.3039612	358.5277541	1.4022E-06
Residual	6	5.845638847	0.974273141		
Total	7	355.1496			

	Coefficients	*Standard Error*	*t Stat*	*P-value*	*Lower 95%*	*Upper 95%*
Intercept	8.043068765	0.607556655	13.23838477	1.14789E-05	6.556431189	9.52970634
X Variable 1	0.005215331	0.000275436	18.93482913	1.4022E-06	0.004541363	0.005889298

Table A-12. Microsoft® Excel Linear Regression Results for Anaerobic, Inundated, Inoculated, and Unamended Data Evaluated by Nemer et al. 2005, without 2,723-Day and 3.464-Day Data Where Methanogenesis was Observed

SUMMARY OUTPUT: 481-day to 1,228-day data

Regression Statistics	
Multiple R	0.950435071
R Square	0.903326825
Adjusted R Square	0.871102433
Standard Error	0.64027817
Observations	5

ANOVA

	df	*SS*	*MS*	*F*	*Significance F*
Regression	1	11.4920516	11.4920516	28.03239329	0.013147407
Residual	3	1.229868404	0.409956135		
Total	4	12.72192			

	Coefficients	*Standard Error*	*t Stat*	*P-value*	*Lower 95%*	*Upper 95%*
Intercept	7.290347834	1.013179116	7.195517277	0.005532009	4.0659597	10.51473597
X Variable 1	0.005943234	0.001122517	5.294562616	0.013147407	0.002370886	0.009515583

Table A-13. Carbon Dioxide Generation Data from Experiments that were Unamended, Anaerobic, and Humid; Used by Nemer et al. 2005 to Calculate Maximum Long-Term Humid Gas Generation Rate

Time (days)	µmoles CO_2 /g Cellulose	Standard Error	Source	Note
6	7.7	0.12	Nemer et al. 2005	Used in Wang and Brush 1996 maximum humid rate calculation
100	20	3.8	Nemer et al. 2005	
140	28.5	7.1	Nemer et al. 2005	
415	72.6	24.4	Nemer et al. 2005	Used in Wang and Brush 1996 maximum humid rate calculation
2,156	155	36	Nemer et al. 2005	
2,616	135	28	Nemer et al. 2005	
2,945	115	20	Nemer et al. 2005	

Figure A-4. Unamended, Anaerobic, Humid Data Used by Nemer et al. 2005

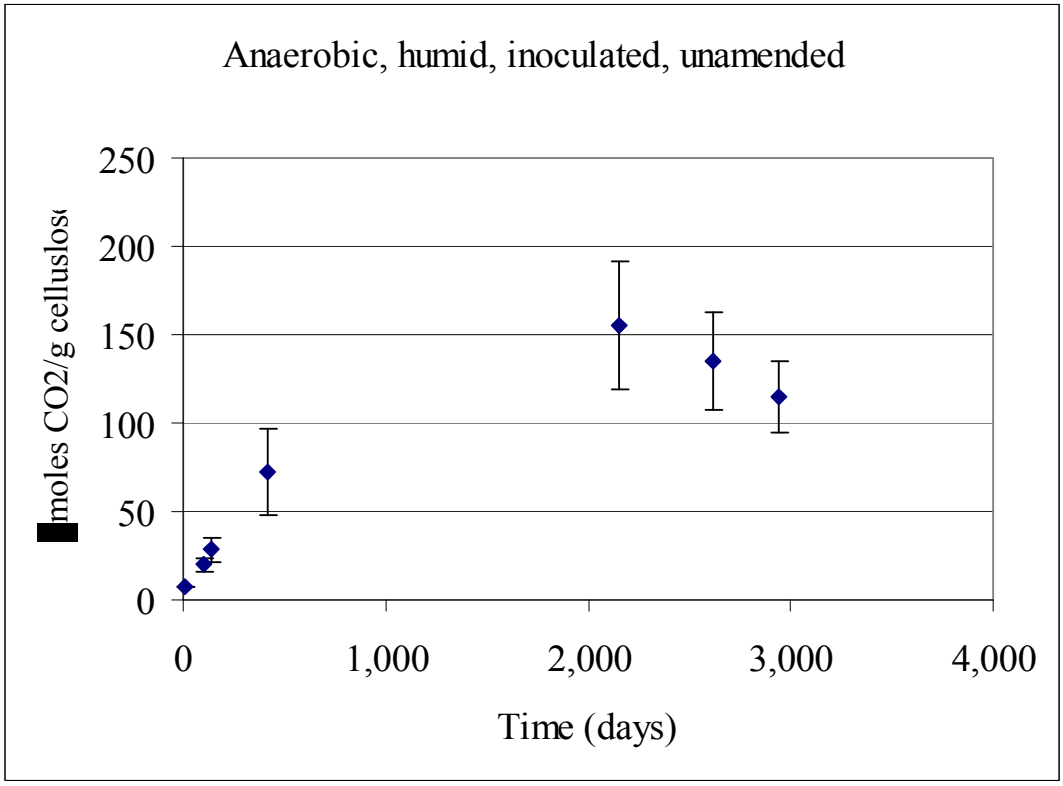

Table A-14. Microsoft® Excel Linear Regression Results for Unamended, Anaerobic, Humid Data Used by Nemer et al. 2005

SUMMARY OUTPUT: 415 to 2,945 day data (same range as Nemer et al. 2005)

Regression Statistics	
Multiple R	0.715985772
R Square	0.512635626
Adjusted R Square	0.268953439
Standard Error	30.10939578
Observations	4

ANOVA

	df	*SS*	*MS*	*F*	*Significance F*
Regression	1	1907.168571	1907.168571	2.103705781	0.284014228
Residual	2	1813.151429	906.5757144		
Total	3	3720.32			

	Coefficients	*Standard Error*	*t Stat*	*P-value*	*Lower 95%*	*Upper 95%*
Intercept	73.8831175	34.80619327	2.122700317	0.167783273	-75.87584497	223.64208
X Variable 1	0.022389022	0.015436279	1.450415727	0.284014228	-0.044027927	0.088805972

Table A-15. Amended, Anaerobic, Humid Gas Generation Rate Data

Time (Days)	μmoles CO_2 /g Cellulose	Standard Error	Source	Note
6	13.3	0.04	Gillow and Francis 2003	Used in Wang and Brush 1996 maximum inundated rate calculation
100	30.5	0.04	Gillow and Francis 2003	
140	32.77	0.02	Gillow and Francis 2003	
415	18.3	0.14	Gillow and Francis 2003	Used in Wang and Brush 1996 maximum inundated rate calculation
2156	9.85	0.1	Gillow and Francis 2003	
2616	26.79	0.34	Gillow and Francis 2003	
2945	21.92	0.3	Gillow and Francis 2003	

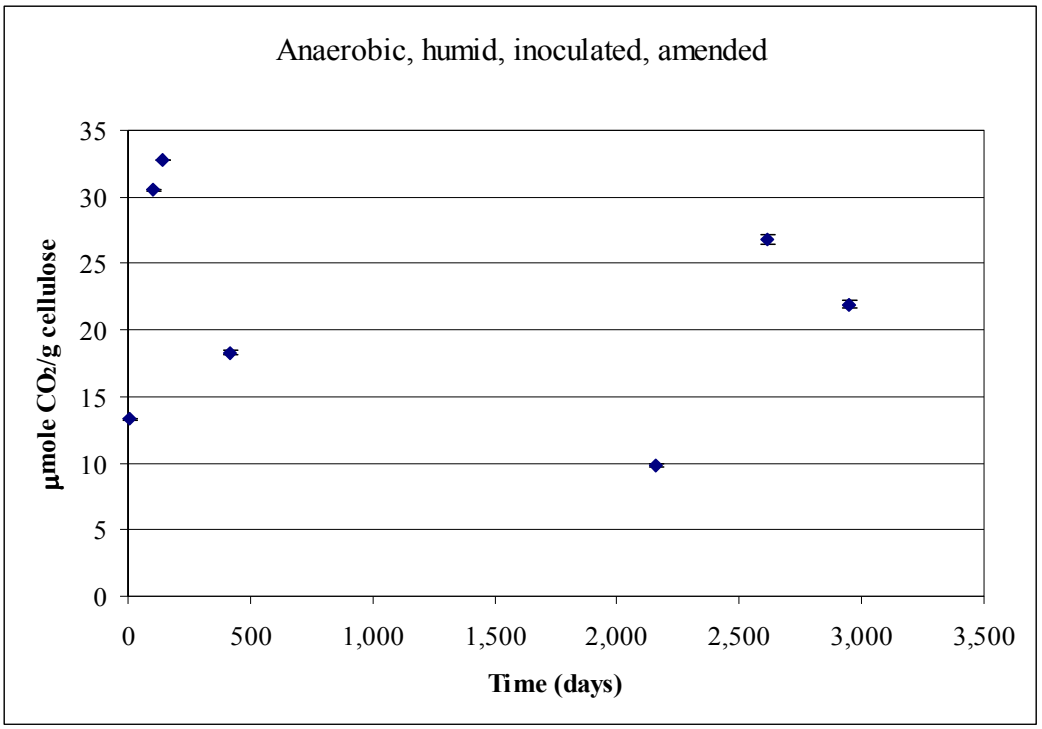

Figure A-5. Amended, Anaerobic, Humid Carbon Dioxide Generation Data

Table A-16. Microsoft® Excel Linear Regression Results for Amended, Anaerobic, Humid Carbon Dioxide Generation Data

SUMMARY OUTPUT: all data

Regression Statistics	
Multiple R	0.18286983
R Square	0.03344138
Adjusted R Square	-0.15987035
Standard Error	9.30766083
Observations	7

ANOVA

	df	*SS*	*MS*	*F*	*Significance F*
Regression	1	14.98673536	14.9867	0.17299	0.694715315
Residual	5	433.1627503	86.6326		
Total	6	448.1494857			

	Coefficients	*Standard Error*	*t Stat*	*P-value*	*Lower 95%*	*Upper 95%*
Intercept	23.3595183	4.937462078	4.73108	0.00519	10.66736801	36.0516687
X Variable 1	-0.00120394	0.002894628	-0.4159	0.69472	-0.00864482	0.00623693